Marine Geology 377 (2016) 7–39

Contents lists available at ScienceDirect

Marine Geology

journal homepage: www.elsevier.com/locate/margeo

Evolution of the gulf of Cadiz margin and southwest Portugal contourite depositional system: Tectonic, sedimentary and paleoceanographic implications from IODP expedition 339

F.J. Hernández-Molina [a,*], F.J. Sierro [b], E. Llave [c], C. Roque [d], D.A.V. Stow [e], T. Williams [f], J. Lofi [g], M. Van der Schee [b], A. Arnáiz [h], S. Ledesma [i], C. Rosales [h], F.J. Rodríguez-Tovar [j], E. Pardo-Igúzquiza [c], R.E. Brackenridge [k]

[a] Dept. Earth Sciences, Royal Holloway Univ. London, Egham, Surrey TW20 0EX, UK
[b] Dpto. de Geología, Univ. de Salamanca, Calle de los Caídos, 37008 Salamanca, Spain
[c] Instituto Geológico y Minero de España (IGME), Ríos Rosas, 23, 28003 Madrid, Spain
[d] Instituto Dom Luiz-IDL, Lisboa, Portugal
[e] IPE, Heriot-Watt Univ., Edinburgh EH14 4AS, Scotland, UK
[f] Lamont-Doherty Earth Observatory, Palisades, NY 10964, USA
[g] Géosciences Montpellier UMR 5243CC 060 — Bat. 22 Université de Montpellier 2 Place E. Bataillon, 34095 Montpellier Cedex 05, France
[h] REPSOL, Méndez Álvaro 44, Edif. Azul 2ª Planta, 28045 Madrid, Spain
[i] Gas Natural Fenosa, Avenida San Luis 77, 28033 Madrid, Spain
[j] Dpto. de Estratigrafía y Paleontología, Univ. Granada, 18002 Granada, Spain
[k] Shell International Exploration & Production B.V., Carel van Bylandtlaan 05.0B.03, 2596 HR The Hague, Netherlands

ARTICLE INFO

Article history:
Received 2 April 2015
Received in revised form 8 September 2015
Accepted 27 September 2015
Available online 9 October 2015

Keywords:
Neogene basins
IODP expedition 339
Contourites
Stratigraphy
Tectonic
Mediterranean outflow water

ABSTRACT

The contourite depositional system (CDS) along the southwestern Iberian Margin (SIM), within the Gulf of Cadiz and offshore areas of western Portugal bear the unmistakable signal of Mediterranean Outflow Water (MOW) exiting the Strait of Gibraltar. This locality records key information concerning the effects of tectonic activity on margin sedimentation, the effects of MOW dynamics on Atlantic circulation, and how these factors may have influenced global climate. Over the last four decades, numerous studies have been conducted on the late Miocene, Pliocene and Quaternary sedimentary stacking pattern of Neogene basins along the SIM for both academic and resources exploration purposes. However, understanding of the region rests primarily on basic seismic stratigraphy calibrated with limited data from only a few exploration wells. The Integrated Ocean Drilling Program (IODP) Expedition 339 recently drilled five sites in the Gulf of Cadiz and two sites on the western Iberian margin. The integration of core and borehole data with other geophysical databases leads us to propose a new stratigraphic framework. Interpretation of IODP Exp. 339 data along with that from industry sources and onshore outcrop analysis helps refine our understanding of the SIM's sedimentary evolution.

We identify significant changes in sedimentation style and dominant sedimentary processes, coupled with widespread depositional hiatuses along the SIM within the Cadiz, Sanlucar, Doñana, Algarve and Alentejo basins. Following the 4.5 Ma cessation of a previous phase of tectonic activity related to the Miocene–Pliocene boundary, tectonics continued to influence margin development, downslope sediment transport and CDS evolution. Sedimentary features indicate tectonic pulses of about 0.8–0.9 Ma duration with a pronounced overprint of ~2–2.5 Ma cycles. These more protracted cycles relate to the westward rollback of subducted lithosphere at the convergent Africa-Eurasia plate boundary as its previous NW–SE compressional regime shifted to a WNW–ESE direction. Two major compressional events affecting to the Neogene basins at 3.2–3 Ma and 2–2.3 Ma help constrain the three main stages of CDS evolution. The stages include: 1) the initial-drift stage (5.33–3.2 Ma) with a weak MOW, 2) a transitional-drift stage (3.2–2 Ma) and 3) a growth-drift stage (2 Ma-present time) with enhanced MOW circulation into the Atlantic and associated contourite development due to greater bottom-current velocity. Two minor Pleistocene discontinuities at 0.7–0.9 Ma and 0.3–0.6 Ma record the effects of renewed tectonic activity on basin evolution, appearing most prominently in the Doñana basin. Several discontinuities bounding major and minor units appear on seismic profiles. Quaternary records offer the clearest example of this, with major units of about 0.8–0.9 Ma and sub-units of 0.4–0.5 Ma. Sedimentation is controlled by a combination of tectonics, sediment supply, sea-level and climate. This research identifies time scales of tectonic

* Corresponding author.
E-mail address: javier.hermandez-molina@rhul.ac.uk (F.J. Hernández-Molina).

http://dx.doi.org/10.1016/j.margeo.2015.09.013

controls on deep-marine sedimentation, specifically over periods of 2.5–>0.4 Ma. Shorter-term climatic (orbital) mechanisms control sedimentation at time scales of ≤0.4 Ma. The role of bottom water circulation and associated processes in shaping the seafloor and controlling the sedimentary stacking pattern on continental margins has to be seriously reconsidered in future multidisciplinary studies. This is not only because of the common occurrence of sandy contourite deposits in deep water setting and their economic interest for hydrocarbon exploration, but principally because they archive the heartbeat of the interior Earth and therefore have important sedimentary and paleoceanographic implications.

1. Introduction

From the middle Miocene through the Quaternary, Earth has experienced major plate tectonic, climatic and oceanographic shifts that along with orbital variations, have contributed to the present day global climate and ocean dynamics (e.g., Knutz, 2008; Potter and Szatmari, 2009). Global climate transitioned from more uniform Pliocene climates to dynamic glacial/interglacial cycles during the Quaternary (Sarnthein et al., 2009). Plate tectonics influence climate over a wide range of timescales due to horizontal and vertical displacements of lithosphere, which control continental distribution, atmospheric and oceanic circulation, and the location of continental ice sheets (Hay, 1996). The transition from warm greenhouse conditions during the Late Cretaceous and early Cenozoic, to a world influenced by the Northern Hemisphere glaciations (NHG) in the last 2.6 My, occurred in tandem with distinct phases of plate-tectonic reconfiguration (Hay, 1996; Zachos et al., 2001). The most significant topographic and bathymetric modifications of Earth's surface were the opening and closing of oceanic gateways, which exerted a pervasive influence on global ocean circulation and climate (Wright and Miller, 1996; Potter and Szatmari, 2009). Surface uplift at plate boundaries, or due to magmatic underplating and mantle plumes appear to be strongly time-dependent (Rudge et al., 2008; Lovell, 2010) and act as a mechanism for sea-level variation on geological time scales (Whyte and Lovell, 1997; Jones et al., 2012). Limited

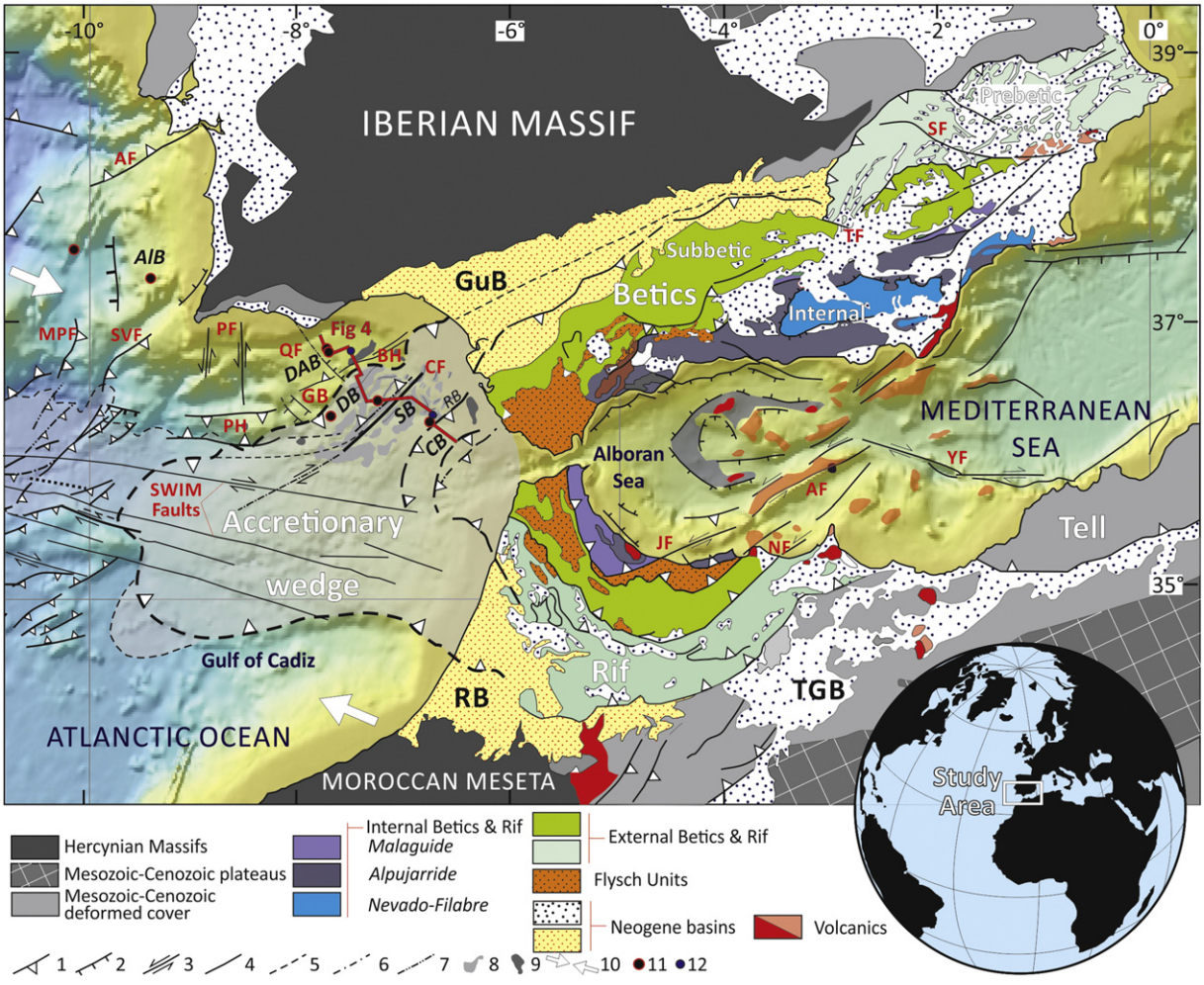

Fig. 1. Tectonic map showing principal structural units of the Betic–Rif Orogen and associated Neogene basins (originally from Iribarren et al., 2007 and Verges and Fernandez, 2012, also including Gulf of Cadiz tectonic features described by Terrinha et al., 2002; Medialdea et al., 2004, 2009; Fernández-Puga et al., 2007; Roque et al., 2012 and Duarte et al., 2013). SF, Socovos Fault (Betics); TF, Tiscar Fault (Betics); JF, Jehba Fault (Rif); NF, Nekor Fault (Rif); AF, Alboran Ridge Fault (Alboran); and YF, Yusuf Fault (Alboran). CF, Cadiz Fault; QF, Quarteira Fault; PH, Portimao High; BH, Basement High; SVF, San Vicent Fault; PF, Portimao Fault; MPF, Marquês de Pombal Fault; AF, Arrábida Fault. 1 = reverse and thrust faults; 2 = normal faults; 3 = strike slip faults; 4 = faults; 5 = contact below sediment; 6 = inferred/probable faults; 7 = blind faults; 8 = marly + salt diapirs (AUGC); 9 = Salt diapirs; 10: Nubia–Iberia plate convergence; 11 = Sites from IODP Exp. 339; 12 = 2 wells drilled by petroleum exploration companies. Legend for the sedimentary basins along the southern Iberian margin: DAB = Deep Algarve basin; AlB = Alentejo basin; CB = Cadiz basin; DB = Doñana basin; RB = Rota basin; SB = Sanlucar basin.

evidence of sedimentary pulses ranging from 1 to 10 Ma in duration (Rudge et al., 2008; Lovell, 2010) indicates that tectonics, climate and sea-level influence sedimentary stacking patterns on continental margins. More evidence concerning time-stratigraphic relationships between palaeoceanographic, environmental (climate and sea-level) and tectonic events is necessary to clarify specific cause-and-effect relationships among these factors, their relative importance, and specific time scales on which they operate (Hernández-Molina et al., 2014b).

The Gulf of Cadiz and offshore west Portugal (Fig. 1) along the southwestern Iberian margin (SIM), can help constrain some of these sedimentary pulses and their drivers. Previous research of these areas has primarily focused on the Mesozoic and Cenozoic history of the margin, especially the tectonic implications of convergence between the African and Eurasian plates in the middle and late Miocene (e.g., Maldonado et al., 1999; Gutscher et al., 2002; Alves et al., 2003; Gràcia et al., 2003; Terrinha et al., 2009; Medialdea et al., 2004; Iribarren et al., 2007; Zitellini et al., 2009; Duarte et al., 2011, 2013; Pereira et al., 2011; Vergés and Fernàndez, 2012 among others).

Several studies have described the evolution and stratigraphy of Pliocene and Quaternary offshore deposits (e.g., Faugères et al., 1985a, 1985b; Mougenot, 1988; Faugères et al., 1999; Maldonado et al., 1999; Llave et al., 2001, 2007a, 2011; Hernández-Molina et al., 2002, 2014a, 2014b; Marchès et al., 2010; Roque et al., 2012; Brackenridge et al., 2013). These studies identified various seismic units bound by regional discontinuities and interpreted them as significant changes in the stratigraphic stacking pattern of the slope. Age interpretations for these features, however, have been uncertain and controversial. Sediments from this region have only recently been sampled, and therefore the working model for the region's seismic stratigraphy was somewhat preliminary, having been calibrated with limited data from a few exploration wells drilled during the late seventies and early eighties. The stratigraphic model makes these basic assumptions about the study area: 1) sedimentation is continuous through time, although hiatuses may occur in the stratigraphic sequence, and 2) external processes such as glacio-eustatic changes and climate variation are primary factors controlling sedimentation. Integrated Ocean Drilling Program (IODP) Expedition 339 drilled six sites within the contourite depositional system (CDS) along the SIM, from November 2011 to January 2012 (Fig. 2). Expedition results have allowed us to identify hiatuses and other major shifts in the sedimentary record through the late Miocene, Pliocene and Quaternary. This expedition provided the opportunity to interpret events occurring around the Strait of Gibraltar in terms of their impacts on regional basin evolution, global ocean circulation and climate. The main objectives of this contribution are: a) to establish a more robust stratigraphic model for the SIM based on the integration of IODP Exp. 339 data with onshore geology and petroleum industry borehole, core, 2D and 3D seismic data. The correlation between the IODP Exp. 339 sites and the seismic profiles is here presented by first time; b) to interpret major changes in

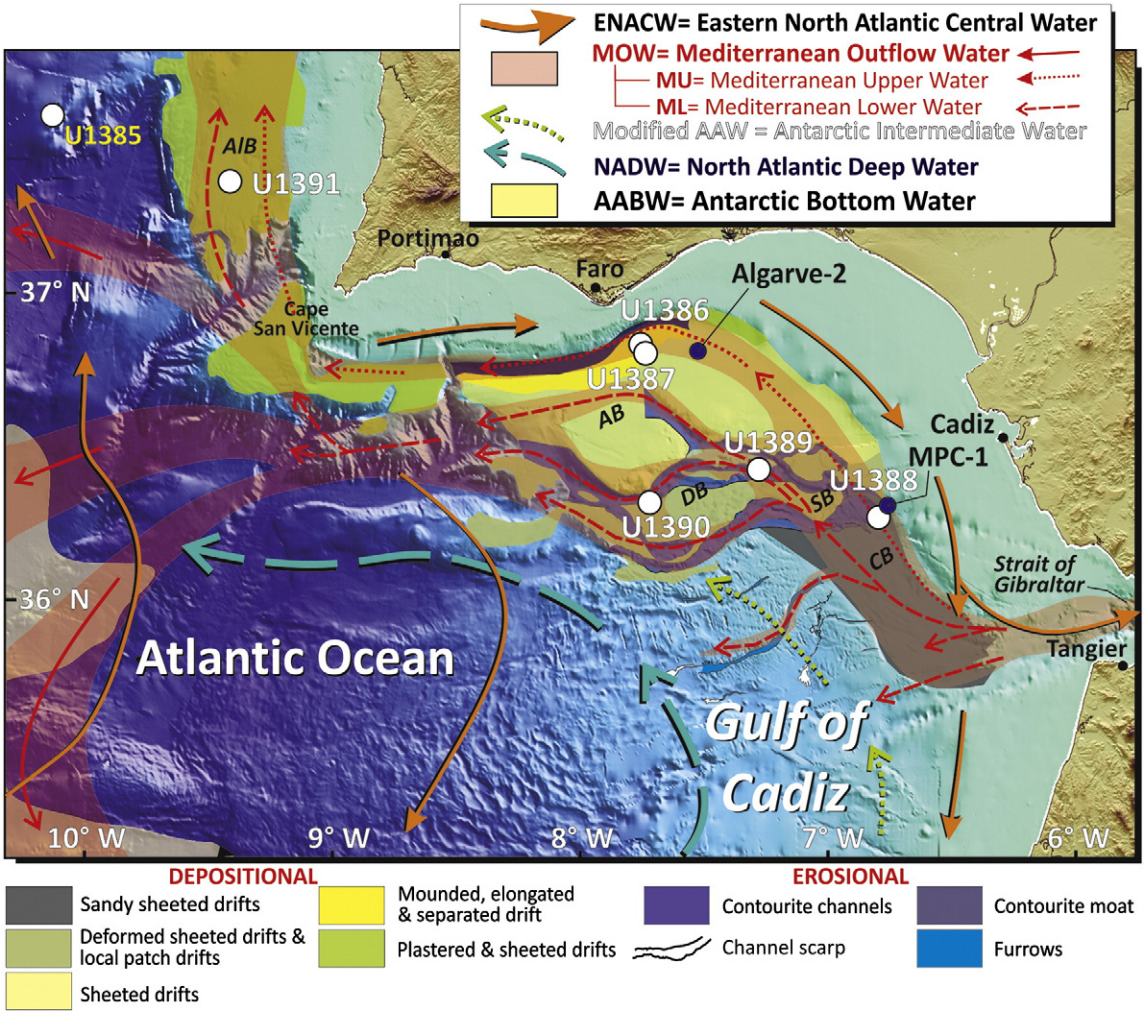

Fig. 2. Gulf of Cadiz showing the pathway of Mediterranean Outflow Water (MOW) after it exits Gibraltar Gateway, as well as the regional depositional and erosional features it generates along the mid-slope. IODP Exp. 339 sites shown as solid white circles and the two wells drilled by petroleum exploration companies are shown as blue circles. Bottom water masses and ocean currents are also shown. Legend for the sedimentary basins along the southern Iberian margin: AB = Algarve basin; AlB = Alentejo basin; CB = Cadiz basin; DB = Doñana basin; RB = Rota basin; SB = Sanlucar basin.

depositional style, sedimentation rates and margin evolution from the Pliocene through the Quaternary; and c) evaluate the broader tectonic, paleoceanographic and climatic implications of these events.

2. Geologic framework

The SIM is located near the Azores-Gibraltar Fracture Zone, a section of the convergent plate boundary between Eurasia (Iberia sub-plate) and Africa (Nubia sub-plate) (Fig. 1). The plates presently converge at a rate of ~4–5 mm/y in a WNW–ESE direction (Argus et al., 1989; Fernández-Ibánez et al., 2007). Counter-clockwise rotation along the margin is accommodated by a series of thrusts and dextral strike-slip faults, referred to as the SWIM faults (Fig. 1) (Zitellini et al., 2009) active since at least 1.8 Ma (Rosas et al., 2009; Duarte et al., 2011). Westward drift and collision of the Alboran Domain with the North African and south Iberian margins in the early to middle Miocene caused the formation of the Betic–Rif orogeny and the so-called Neogene basins, including the north Betic and south Riffian foredeeps. Westwards roll-back subduction of an oceanic lithosphere slab beneath the Gibraltar Arc and development of its accretionary wedge during the late Tortonian (Gutscher et al., 2002) caused radial emplacement of huge allochthonous masses evident as the "olistostrome unit" of the Guadalquivir basin (Iberian foreland), Rharb basin (North African foreland) and Gulf of Cadiz (Perconig, 1960–1962; Roberts, 1970; Flinch and Vail, 1998; Torelli et al., 1997; Maldonado et al., 1999; Terrinha et al., 2009). This unit, which marks the propagation of the Mediterranean Alpine collision belt into the Atlantic (Duarte et al., 2013), is specifically referred to as the allochthonous unit of the Gulf of Cadiz or AUGC (Medialdea et al., 2004). Structurally, the AUGC consists of a series of westwards imbricated thrusts cutting through an eastward-thickening package of sediments (up to ~2.75 km), which appear primarily as chaotic reflectors, numerous diffractions and hyperbolic reflections (Maldonado et al., 1999). Sediment includes Triassic, Cretaceous, Paleogene and Neogene units overlying Palaeozoic basement (Maldonado et al., 1999). Mud and salt diapirism affect Triassic salt units and uncompacted early to middle Miocene marls (Maestro et al., 2003).

The SIM divides into three major morpho-structural domains (Fig. 1) (Maldonado et al., 1999; Zitellini et al., 2009). These include: a) the Sudiberic paleomargin, which is part of the Iberian massif, b) Neogene basins, including the Guadalquivir and Rharb foreland basins and the Algarve basin, and c) the external front of the Betic–Rif collisional orogen, which represents the accretionary wedge or AUGC. Since the late Miocene, geodynamic evolution of the Neogene basins has been determined by oblique convergence between the Iberia and Nubian sub-plates (Zitellini et al., 2009; Duarte et al., 2011). This has been accommodated during distinct periods of crustal deformation and shortening phases, by fault reactivation, halokinesis and uplift of fault blocks (Maldonado et al., 1999; Gutscher et al., 2002; Alves et al., 2003; Gràcia et al., 2003; Maestro et al., 2003; Terrinha et al., 2003, 2009; García et al., 2009; Medialdea et al., 2004, 2009; Lopes et al., 2006; Fernández-Puga et al., 2007; Zitellini et al., 2009; Duarte et al., 2011; Pereira et al., 2011; Martínez-García et al., 2013). Latest Miocene to Pliocene deep and shallow marine deposits occur extensively within onshore basins (e.g., Martinez del Olmo et al., 1984; IGME, 1990, 1994; Sierro et al., 1991; Aguirre, 1995; Riaza and Martinez del Olmo, 1996; Ledesma, 2000), but are virtually absent onshore the Algarve basin (IGMP, 1998; Dias and Cabral, 1997), indicating that only the Guadalquivir, Rharb and the other basins around the Betic–Rif orogen were wider than their present expression (e.g., Michard et al., 2008; Salvany et al., 2011).

3. Oceanographic setting

The present-day circulation in the Gulf of Cadiz and along the western Portuguese margin is dominated by the exchange between the Atlantic and Mediterranean waters through the Strait of Gibraltar (Fig. 2). Upon exiting the Strait of Gibraltar, the Mediterranean Outflow Water (MOW) cascades downslope in a northwesterly direction, at an overflow rate of 0.67 ± 0.28 Sv. MOW consist of relatively warm and highly saline water (Serra et al., 2010; Rogerson et al., 2012) that settle into an intermediate contour current within the mid-slope region, between 400 and 1400 m water depth (Ochoa and Bray, 1991; Baringer and Price, 1999). The Strait of Gibraltar physically moderates Mediterranean–Atlantic water-mass exchange, contributing warm and highly saline MOW to the Atlantic Ocean at 300–1400 m water depth (Borenäs et al., 2002). MOW input enhances North Atlantic density and helps drive deep convection. Estimates suggest that without MOW, the Atlantic Meridional Overturning Circulation (AMOC) would be reduced by ~15% and North Atlantic sea surface temperatures would fall by up to 1 °C (Rogerson et al., 2012).

The MOW is a mixture of waters sourced from the Mediterranean Basin (Levantine Intermediate Water, LIW, and a small component of the West Mediterranean Deep Water, WMDW), a constricted basin under arid climate conditions that form warm, saline dense water averaging 13°C and 36.5‰ (Ambar and Howe, 1979; Bryden and Stommel, 1984; Bryden et al., 1994). The water mass accelerates through the narrow gateway of the Strait of Gibraltar, locally reaching velocities of up to 300 cm/s (Ambar and Howe, 1979; Mulder et al., 2003) and moves north-westwards along the mid-continental slope of the Gulf of Cadiz, beneath the Atlantic Inflow Water (AIW) and above the North Atlantic Deep Water (NADW). The AIW consists of North Atlantic Superficial Water (NASW; surface to a depth of approximately 100 m), and the Eastern North Atlantic Central Water (ENACW). It flows at depths between of 100 and 700 m and averages 12–16 °C and 34.7–36.25‰ TDS. In the Gulf of Cadiz, the Modified Antarctic Intermediate Water (AAIW), which averages ~10 °C, ~35.62‰ TDS and ~4.16 ml/l dissolved oxygen (Louarn and Morin, 2011), has been identified as circulating above the MOW (Hernández-Molina et al., 2014a). The underlying NADW is a cold (3–8 °C) and less saline (34.95–35.2‰) water mass that flows at depths >1500 m from the Greenland-Norwegian Sea region towards the south (Thorpe, 1975; Zenk, 1975; Gardner and Kidd, 1983; Ochoa and Bray, 1991; Baringer and Price, 1999; Serra et al., 2005). The MOW forms a 10 km (approximately) wide band as it accelerates through the Strait of Gibraltar, enters the Gulf of Cadiz at depths of 250–300 m and is then deflected to the west due to Coriolis effect (Ambar and Howe, 1979; Mulder et al., 2003). The MOW current velocity decreases immediately west of the Camarinal Sill within the Strait of Gibraltar, and continues to decline to 60–100 cm/s further to the northwest (Cherubin et al., 2000). From there onwards, its volume transport increases by a factor of three to four (Serra et al., 2010; Rogerson et al., 2012). Density-driven descent and mixing with overlying Atlantic waters result in decreasing salinity along the margin in a SE to NW direction (Baringer and Price, 1997). Eventually, the MOW reaches a neutral buoyancy and leaves the seabed at a depth of ~1400 m off Cape San Vicente, where it begins to raft above the NADW.

In the Gulf of Cadiz, the MOW pathway is influenced by the complex continental slope morphology and is locally enhanced where neotectonics have created diapiric ridges oblique to its flow direction (Fig. 2). These ridges are in part responsible for splitting the MOW into numerous distinctive cores, although vertical layering within the water core has also been proposed as a possible additional control (Millot, 2009; Copard et al., 2011). The main water cores consist of the Mediterranean Upper Core (MU) and the Mediterranean Lower Core (ML) (Madelain, 1970; Zenk, 1975; Ambar and Howe, 1979; Borenäs et al., 2002; Serra et al., 2005) (Fig. 2). The MU flows slope-parallel along southwestern Iberia at depths of 500–800 m with part of its flow captured by the Portimao Canyon at the Algarve margin (Marchès et al., 2007). Overall, the MU is warmer and less saline (13–14 °C and 35.7–37‰) relative to the ML (10.5–11.5 °C and 36.5–37.5‰), which follows a general northwestern trend between 800 and 1400 m water depth, with an average velocity of 20–30 cm/s (Llave et al., 2007a; García et al., 2009). The majority of the flow

concentrates west of 7° W (Madelain, 1970). At 7° W, a branch detaches from the southern part of the ML to veer off in a southwesterly direction. At 7° 20′ W, the ML divides into three distinct branches with a general northwest direction: the southern branch (SB), the principal branch (PB) and the intermediate branch (IB). Both Portimão Canyon and Cape St. Vincent act as a source of meddies (Serra et al., 2005, 2010; Ambar et al., 2008). After exiting the Gulf of Cadiz, the MOW includes three principal branches. The main branch flows to the north along the middle slope of the Portuguese Margin, the second to the west, and the third to the south reaching the Canary Islands, before veering west (Iorga and Lozier, 1999; Slater, 2003).

Following the opening of the Strait of Gibraltar in the latest Miocene (Duggen et al., 2003; Roveri et al., 2014), the MOW generated one of the world's most extensive and complex Contourite Depositional System (CDS; Fig. 2) along the SIM during the Pliocene and Quaternary (e.g., Faugères et al., 1985a, 1985b; Nelson et al., 1999; Llave et al., 2001, 2007a, 2011; Habgood et al., 2003; Hanquiez et al., 2007; Hernández-Molina et al., 2003, 2006, 2011, 2014a; Marchès et al., 2007, 2010; García et al., 2009; Roque et al., 2012). Large depositional and erosional features within the CDS are used to define five morphosedimentary sectors (detailed in Hernández-Molina et al., 2003 and Llave et al., 2007a, 2007b). In general, the drifts consist primarily of muddy, silty and sandy sediments of mixed terrigenous and biogenic composition (Gonthier et al., 1984). Sand and gravel are found in the large contourite channels (Nelson et al., 1993, 1999; Stow et al., 2013a), and across the many erosional features (Stow et al., 2013a; Hernández-Molina et al., 2014a). In the proximal sector close to the Strait of Gibraltar, an exceptionally thick (~815 m) sandy-sheeted drift occurs, with sand layers averaging thicknesses of 12–15 m (Nelson et al., 1993; Buitrago et al., 2001).

4. Methodology

This research has compiled and integrated extensive geophysical data and drill core records from late Miocene, Pliocene and Quaternary sediments. Results from the drillcore data acquired during IODP Exp. 339 aboard the R/V *JOIDES Resolution* have been correlated with petroleum industry drilling data from the margin (Fig. 3). Datasets were selected based on data coverage for the Pliocene and Pleistocene sections, which are not typically sampled by industry surveys.

IODP Exp. 339 aboard the R/V *JOIDES Resolution* drilled five sites in the Gulf of Cadiz and two sites off the west Iberian margin from 17 November 2011 to 17 January 2012 (Expedition 339 Scientists, 2012; Stow et al., 2013b; Hernández-Molina et al., 2013; Hodell et al., 2013). See details at http://iodp.tamu.edu/scienceops/expeditions/mediterranean_outflow.html. Six of the sites (U1386–U1391, Fig. 3) were specifically selected in order to study MOW-generated CDS.

Drilling activities employed all three of the vessel's standard coring systems, which include an advanced piston corer (APC), an extended core barrel (XCB), and a rotary core barrel (RCB). These allowed Exp. 339 to drill 19 holes (681 cores) in 46.1 days on site, with a penetration of 7857.4 m and 6301.6 m cored. In total, nearly 5.5 km of core were recovered, with an average recovery of 86.4% (Fig. 3). Stratigraphic correlation and specific age constraints were established onboard using: 1) lithostratigraphy, 2) biostratigraphy, 3) paleomagnetic data, 4) sediment core description, 5) geochemical analysis and 6) downhole measurements. Shipboard biostratigraphic dating was used to estimate regional correlations. Age data was essential for determining ages of key horizons (including several depositional hiatuses and stratigraphic boundaries) and sedimentary accumulation rates (for chronology details about the IODP sites, see Table S1 in Hernández-Molina et al., 2014b, and for the MPC-1 borehole, see Buitrago et al., 2001; Hernández-Molina et al., 2014a).

Preliminary onboard sedimentary facies description is reported in Stow et al. (2013b) and also integrated with seismo-acoustic and logging analysis in this work. We also report mineralogic and petrographic analysis of 32 samples of lower Pliocene sandstones from site U1387. Analysis, including SEM–EDS analyses, micro-x-ray fluorescence (micro-XRF), rare elements (REE) measurements and C and O stable isotope analysis was carried out by REPSOL (Caja et al., 2013).

Vertical seismic profiles (VSP) relating borehole depth to travel time in seismic reflection data (Fig. S1, in *Supplementary material*), have been critical for correlating IODP Exp. 399 results with regional multichannel seismic profiles. VSP were executed at sites U1386, U1387 and U1389. At sites U1390 and U1391 the depth to time conversion was based on the DSI sonic tool. Downhole logs were acquired with Schlumberger logging tools at five sites (U1386C, U1387C, U1389A, U1389E and U1391C, Fig. 3) following completion of coring operations. Log data was continuous with depth and measured in situ. Among the tools used during IODP Exp. 339, the Hostile Environment Natural Gamma Ray Sonde (HNGS) allowed us to continuously measure natural gamma radiation of sediment surrounding the open borehole. The HNGS signal primarily tracks clay content with high values generally identifying fine-grained deposits containing K-rich clay minerals that preferentially absorb U and Th. Low values reflect quartz and calcite, which are unlikely to contain such high concentrations of radioactive elements. The High-Resolution Laterolog Array (HRLA) performs five measurements of formation resistivity with increasing penetration into the formation. The logs can be interpreted in terms of the stratigraphy, lithology and geochemical composition of the formation sampled. IODP Exp. 339 results have been correlated to industry wells referred to as Algarve-2 and MPC-1. Algarve-2 data was provided by DGGE (Direcção Geral de Geologia e Energia-Portugal) through the DPEP (Divisão para a Pesquisa e Exploração de Petróleo). The MPC-1 well was drilled by Esso in 1982 (Buitrago et al., 2001; Hernández-Molina et al., 2014a). These two sites have been very useful for correlating seismic data, lithologies and log data at a regional scale.

In order to evaluate cyclic patterns in the sedimentary record and GR logs, we performed spectral analysis on HSGR logs from sites U1386C and U1387C, using the Lomb-Scargle periodogram method (Scargle, 1982), to tract the record of low- and high (orbital-scale) variations in the sediment properties during the last 2 Ma within the most depositional sector of the contourite depositional system. The age model for the last 2 Ma at these sites is based on results from Lofi et al., 2015. The Lomb-Scargle periodogram method is the best methodology of spectral estimation and is particularly useful when conducting cyclostratigraphic analysis with uneven sampling data, even when dealing with short time series or with a discontinuous sedimentary record (i.e., missing data, minor hiatuses, bioturbation, etc.) (Pardo-Igúzquiza and Rodríguez-Tovar, 2011, 2012; Rodrigo-Gámiz et al., 2014). To evaluate the significance of the registered spectral peaks, the Lomb-Scargle periodogram is integrated with the implemented achieved significance level using the permutation test (see Pardo-Igúzquiza and Rodríguez-Tovar, 2000, 2005, 2006, 2011, 2012 for a detailed description). A first cyclostratigraphic analysis has been conducted to evidence any possible cyclicity at the Milankovitch frequency band. Then, a second study focused on the lower frequency band, to evaluate the possibility of any cycles with periodicities longer than those corresponding to the short-term eccentricity cycle (≥100 ky). This has been achieved by reducing the periodogram smoothing in the low frequencies in order to increase the spectral resolution at those low frequencies.

We constructed a large regional seismic compilation using data collected by industry and on several national and international research projects (Fig. 3). Multichannel 2-D seismic reflection profiles (MCS) used were: 1) the PD00 Survey acquired by TGS–NOPEC, 2000 (TGS, 2005; acquisition data reported in George, 2011; Llave et al., 2011; Brackenridge et al., 2013), 2) BIO *Hespérides* HE-91-3 cruise (acquisition data details in Maldonado et al., 1999), 3) BIO *Hespérides* TASYO 2000 cruise (acquisition data information in Medialdea et al., 2004, 2009), 4) IAM survey and the CSIC-Institut Jaume Almera (http://geodb.ictja.csic.es) and 5) S81, P74 and GC_d surveys by Repsol and Gas Natural-

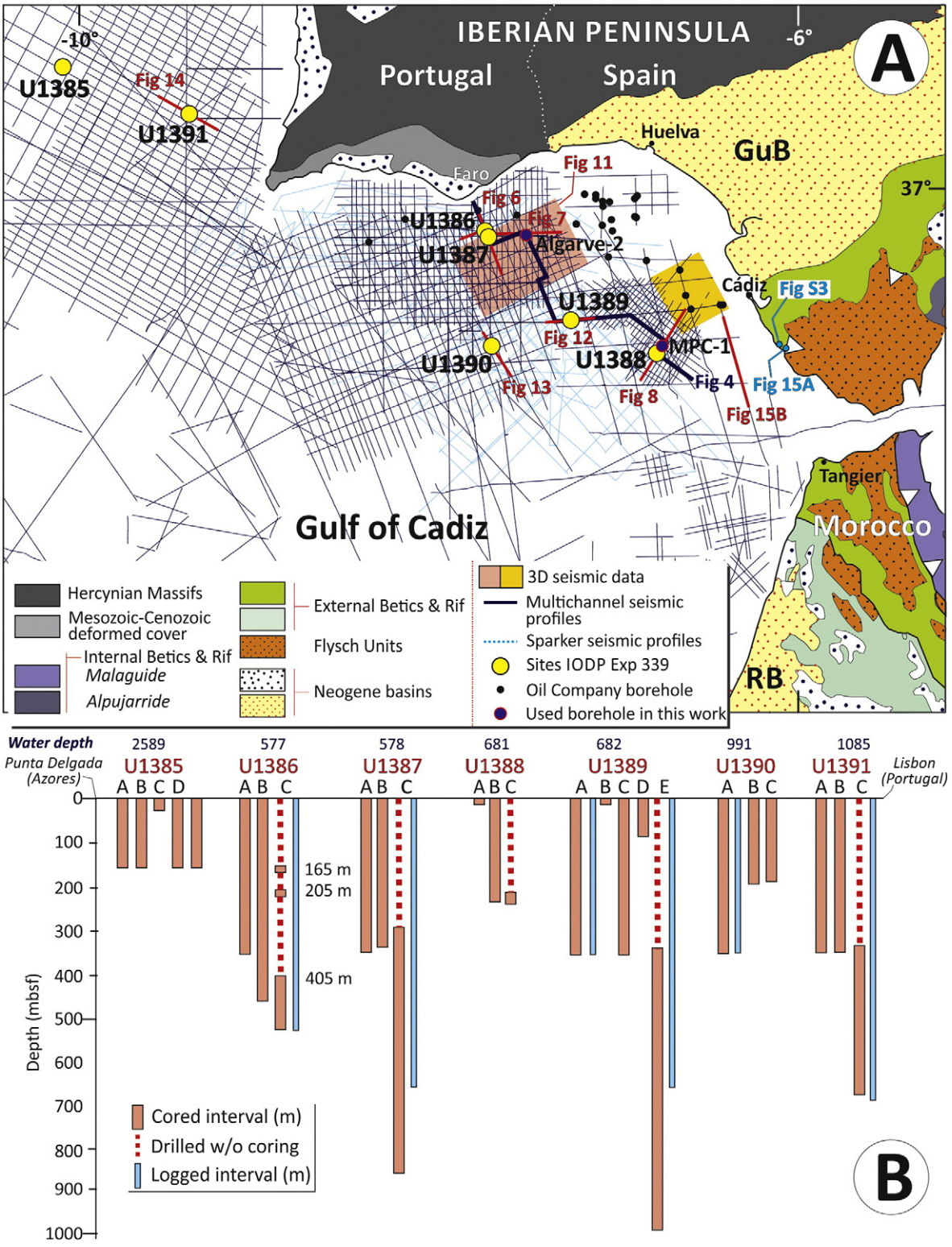

Fig. 3. A) Map locations of seismic profiles as well as sites drilled during IODP Exp. 339 and those sampled by previous drilling activity. Localities of outcrops reinterpreted by this study are also shown. B) Basic information on IODP Exp. 339 sites.

Fenosa. This study also incorporates additional MCS data from a 2012 3D seismic survey by Repsol, which covered Pliocene and Quaternary sediments, and included four amplitude anomaly maps. Several 2D seismic profiles of intermediate resolution were used for local analysis (Llave et al., 2001, 2006, 2007a, 2007b; Hernández-Molina et al., 2002, 2006). These were generated using Sparker 3000, 4000 and 7500 J sources and obtained during research cruises FADO 9711, ANASTASYA 9909 and ANASTASYA 2000/09. The seismic, core and borehole data have been interpreted using the commercially available software package, Kingdom Suite™, which processes chronostratigraphical, sedimentological and log data. Depth and thickness from seismic profiles are expressed in seconds Two-Way Travel-Time (TWTT).

Major stratigraphic features of offshore deposits have been correlated with onshore outcrops based on published literature records as well

Table 1
Table with the main units and sub-units described in the present work, including stratigraphic correlations interpreted by other authors.

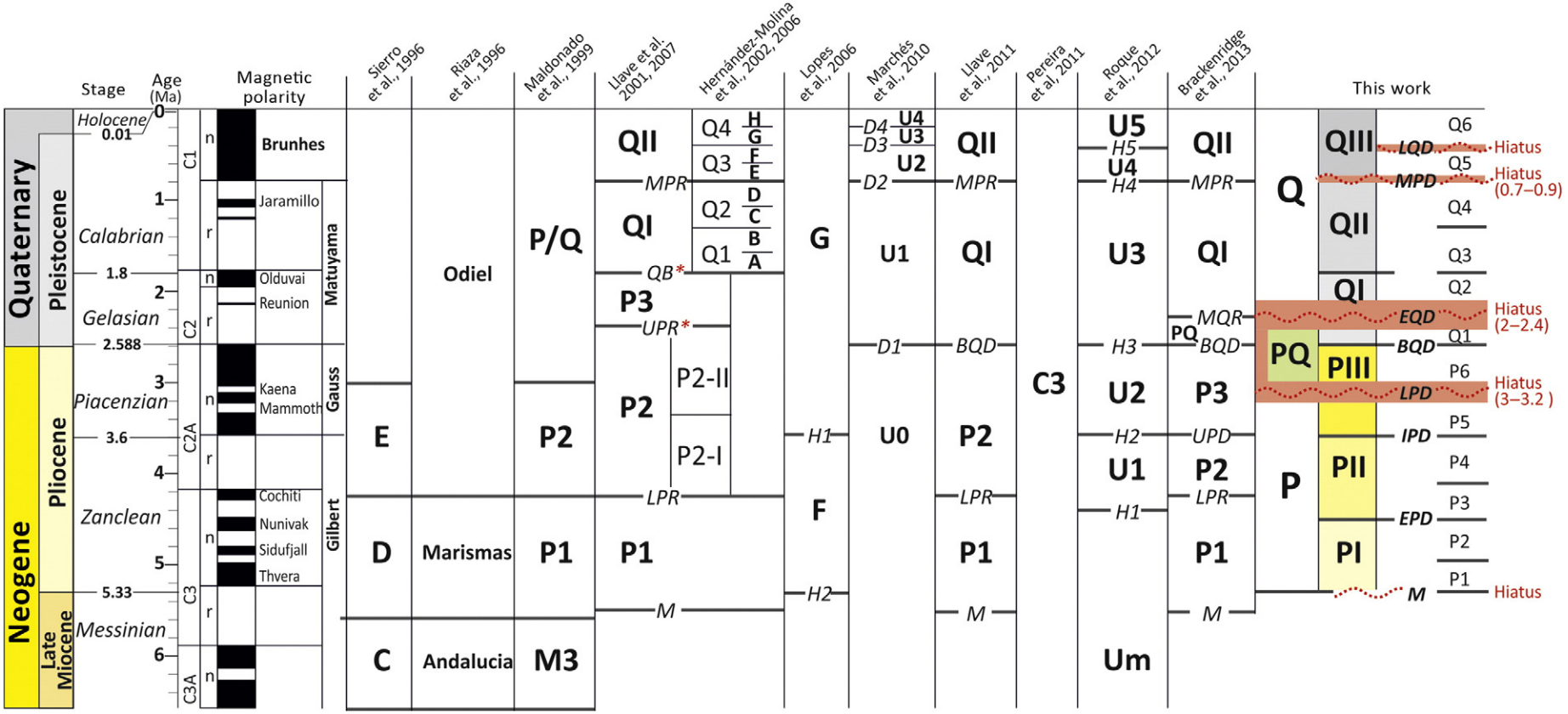

Data from Hernández-Molina et al., 2011.

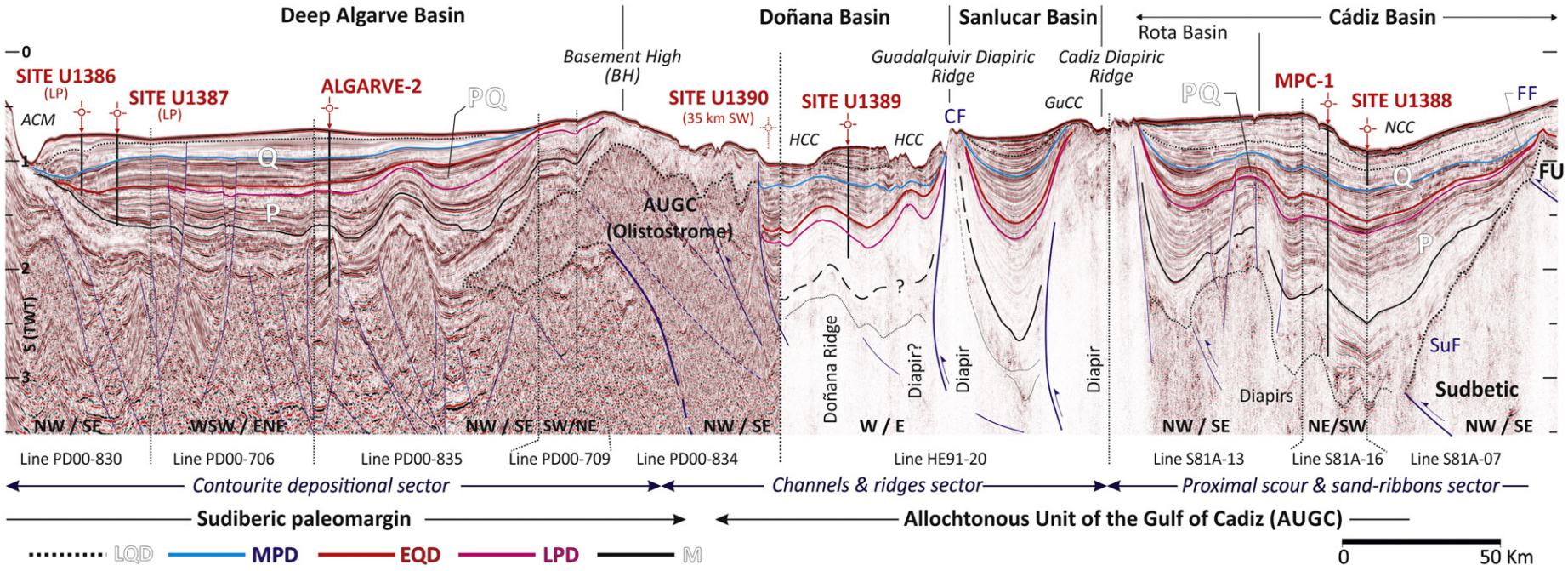

Fig. 4. Composite seismic profile (~500 km long) along the middle slope of the Gulf of Cadiz, from the proximal area near the Strait of Gibraltar (right) to the distal area along the Southern Algarve basin (left). Neogene sedimentary basins and the main morphosedimentary sectors of the contourite depositional system are shown within the regional tectonic framework. The Cadiz, Rota, Sanlucar and Doñana basins overly the Allochthonous Unit of the Gulf of Cadiz (AUGC). The Deep Algarve basin is located on the Sudiberic paleomargin. The major discontinuities occur at the Miocene–Pliocene boundary (M), late Pliocene (LPD), early Quaternary (EQD), mid Pleistocene (MPD) and late Quaternary (LQD).

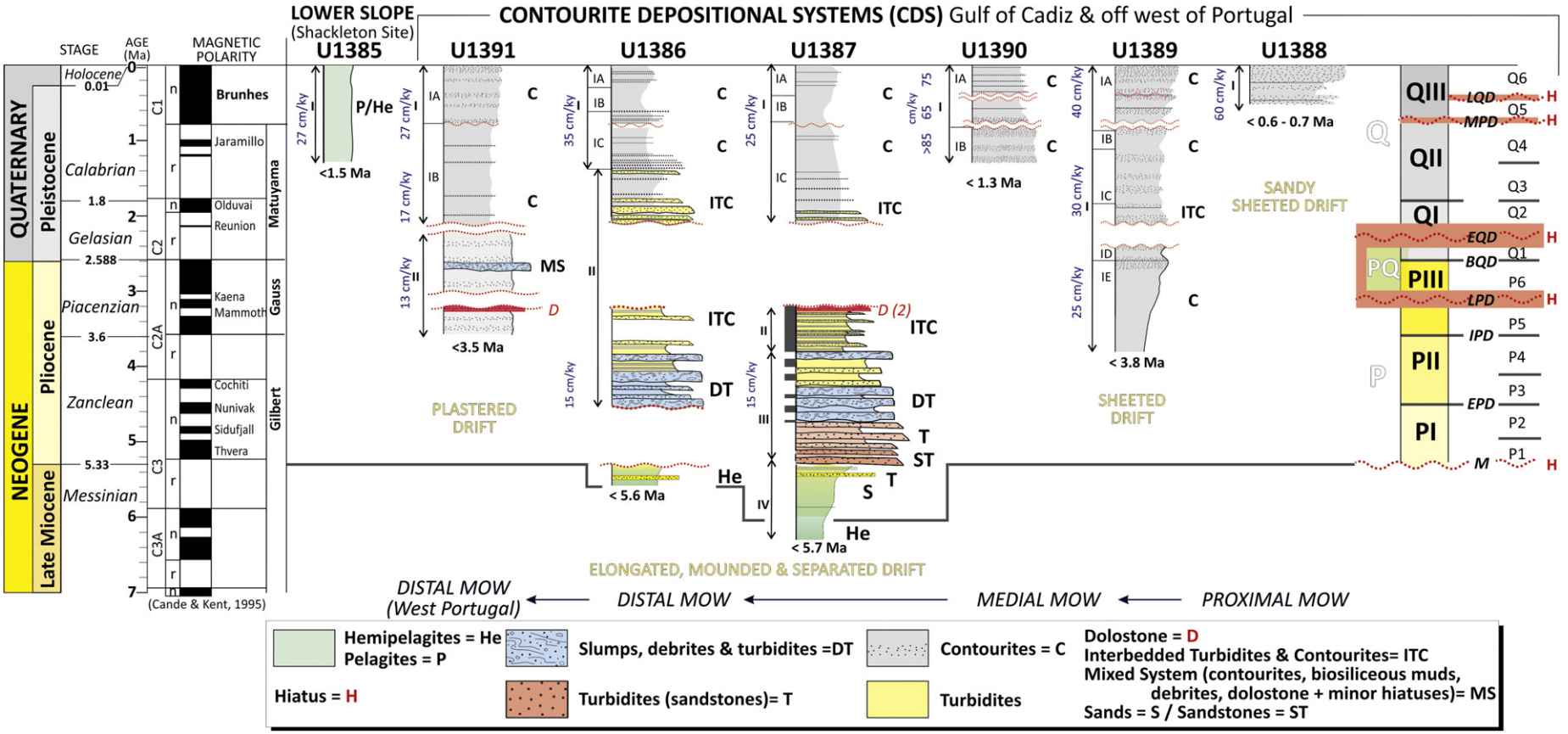

Fig. 5. Lithologic summary for sites drilled during IODP Exp. 339. A general interpretation for the proximal area close to the Strait of Gibraltar to the distal area off west Portugal indicates major hiatuses (H in red). Age models are based on biostratigraphic data and magnetostratigraphy (further details in Stow et al., 2913b; Hernández-Molina et al., 2014a, 2014b). Sedimentation rates for the Pliocene = 15–25 cm/ky and ~30 cm/ky to >100 cm/ky for the Quaternary. C = contourites; D = dolostone; DT = debrites and turbidites (terrigenous and bioclastic sands + chaotica); H = hemipelagites; ITC = interbeded turbidites and contourites; P/H = pelagites/hemipelagites; T = turbidites (sandstones); MS = mixed system (contourites, biosiliceous muds, debrites, dolostone + minor hiatuses). Major sequences (P, PQ and Q), units (PI–PIII and QI–QIII) and subunits (P1–P6 and Q1–Q6), as well as the main discontinuities and hiatuses are shown on the left. Site locations given in Figs. 2 and 3. Data from Cande and Kent, 1995.

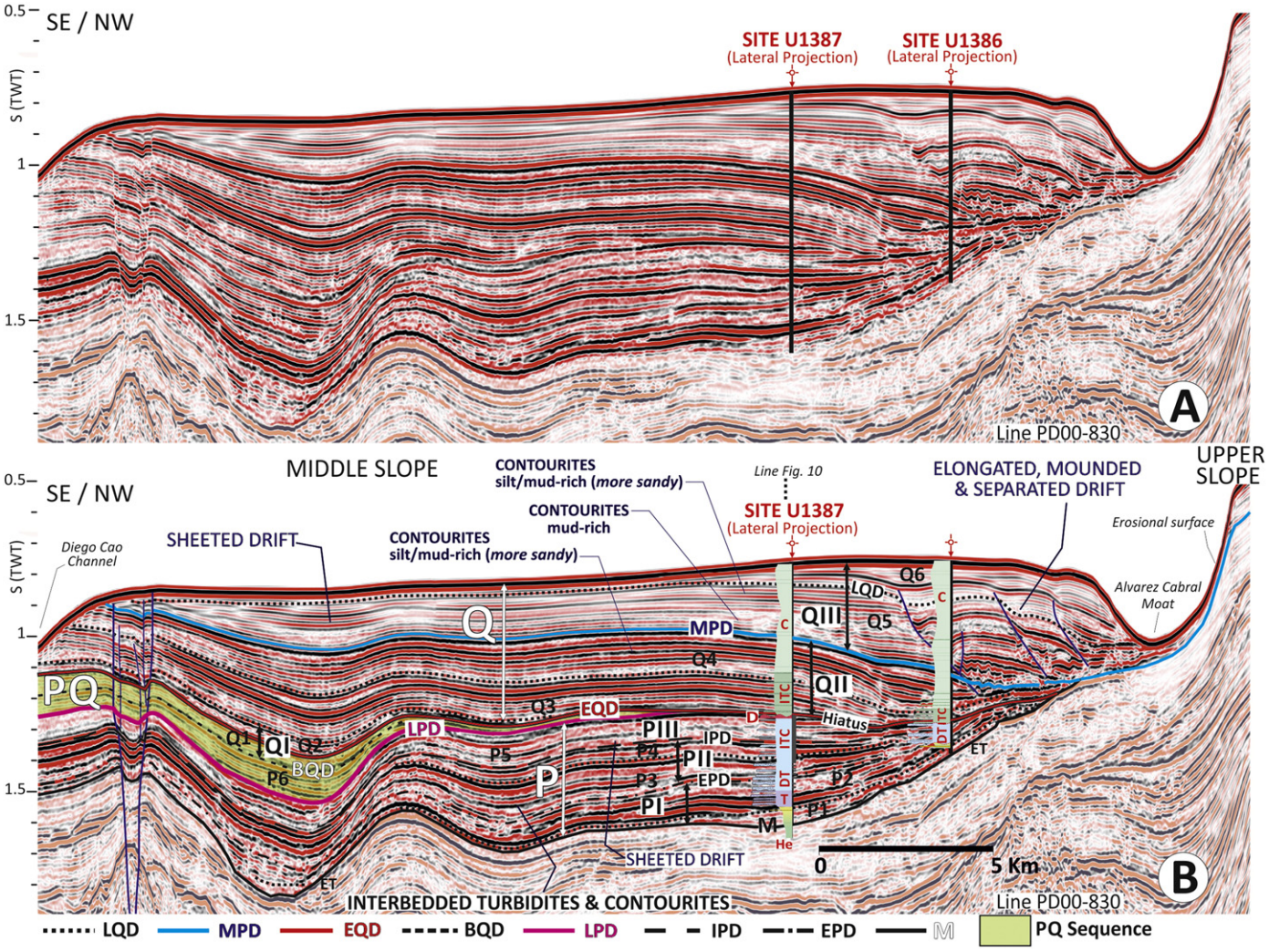

Fig. 6. Seismic profile (line PD00-830) of the Algarve basin showing the sedimentary stacking pattern for Pliocene sheeted drift to Quaternary separated drifts, based on correlations between sites U1386 and U1387. Both sites have been projected into this seismic profile. Site U1386 is place 1 km WSW from the line and Site U1387 is located 1.2 km ENW from the profile. Profile location given in Fig. 3. Major sequences (P, PQ and Q), units (PI–PIII and QI–QIII) and subunits (P1–P6 and Q1–Q6), as well as the main discontinuities and hiatuses are shown. See the text for further detail explanations (data courtesy of TGS–NOPEC Geophysical Company ASA). ET = Erosional truncation. Abbreviations for discontinuities (from bottom to top): M = Miocene–Pliocene boundary; EPD = early Pliocene discontinuity; IPD = intra Pliocene discontinuity; LPD = late Pliocene discontinuity; BQD = base of the Quaternary discontinuity; EQD = early Quaternary discontinuity, MPD = mid Pleistocene discontinuity; and LQD = late Quaternary discontinuity. Simplify sedimentary logs for U1386 and U1387 are included (see abbreviations in Fig. 5).

as recent re-analysis of the late Miocene, Pliocene and Quaternary onshore sections. Selected outcrops (Fig. 3) were specifically measured and re-sampled in order to date and characterize key stratigraphic horizons.

This paper updates and revises units, discontinuities and age assignments in the stratigraphic framework established by previous reports on the area. Inconsistencies in age assignments from previous works are a natural consequence of data processing methods as well as the different scales and resolution at which data was analyzed. Revisions also reflect recent modification of Quaternary chronostratigraphy by the International Commission on Stratigraphy (Mascarelli, 2009). The hierarchy of sedimentary units is described according to sedimentary sequences, units and subunits. The seismic-stratigraphic analyses were correlated with previous stratigraphic results from (Table 1): Sierro et al. (1996); Riaza and Martinez del Olmo (1996); Maldonado et al. (1999); Llave et al. (2001, 2007a, 2011); Hernández-Molina et al. (2002, 2006, 2014a, 2014b); Marchès et al. (2010); Roque et al. (2012); and Brackenridge et al. (2013). The term 'contourite' refers to sediments deposited or substantially reworked by the persistent action of bottom currents (e.g., Stow et al., 2002a; Rebesco, 2005; Rebesco and Camerlenghi, 2008). Contourites include a wide array of sediments that are affected to varying degrees by different types of currents (Rebesco et al., 2014). Thick, extensive sedimentary accumulations are referred to as contourite drifts or drifts. For the present work, we have adopted the classification of Faugères et al. (1999) (later updated by Faugères and Stow, 2008) and use the local and regional names for drifts described by previous authors (e.g., Faugères et al., 1985a, 1985b; Llave et al., 2007a; Hernández-Molina et al., 2003, 2014a; García et al., 2009; Marchès et al., 2007, 2010; Roque et al., 2012).

5. Results

A full assessment of the Neogene basins, the Late Miocene/Pliocene boundary, and the characteristics of the Pliocene to the Quaternary sedimentary record are outlined below. These are reported alongside the tectonic considerations of the results.

5.1. Neogene basins

Neogene basins in the study area include basins overlying the AUGC (Cadiz, Rota, Sanlucar and Doñana basins), a basin located on the Sudiberic paleomargin (Algarve basin) and the Alentejo basin off west

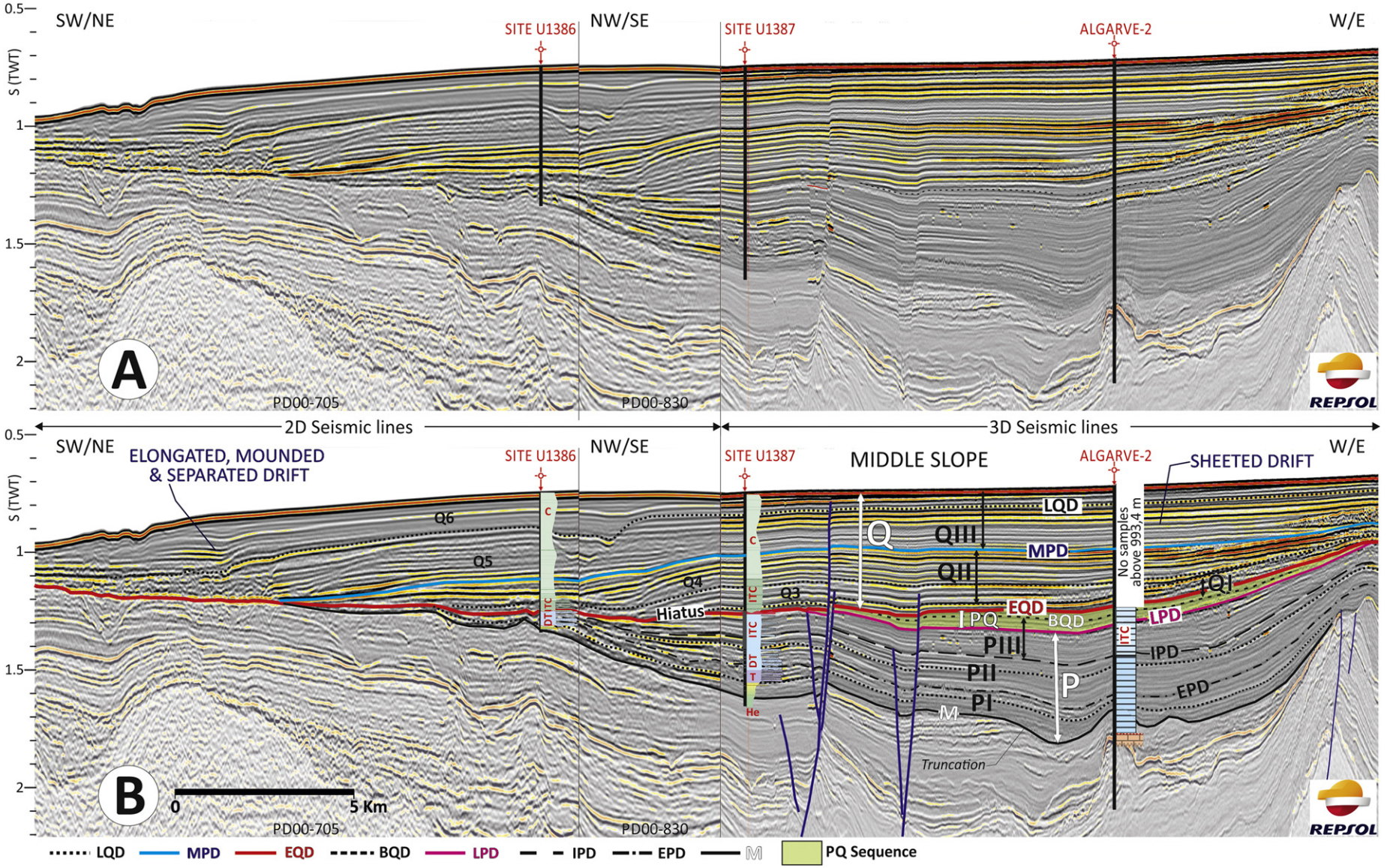

Fig. 7. Composite 2D (Line PD00-705) and 3D seismic data on the Algarve basin, integrating sites U1386, U1387 and Algarve-2. The Pliocene and Quaternary sedimentary stacking pattern including major sequences (P, PQ and Q), units (PI–PIII and QI–QIII) and subunits (P1–P6 and Q1–Q6) as well as the main discontinuities and hiatuses are shown (data courtesy of REPSOL). Profile locations given in Fig. 3. Abbreviations for discontinuities are in Fig. 6. Simplify sedimentary logs for U1386; U1387 and Algarve-2 are included (see abbreviations in Fig. 5).

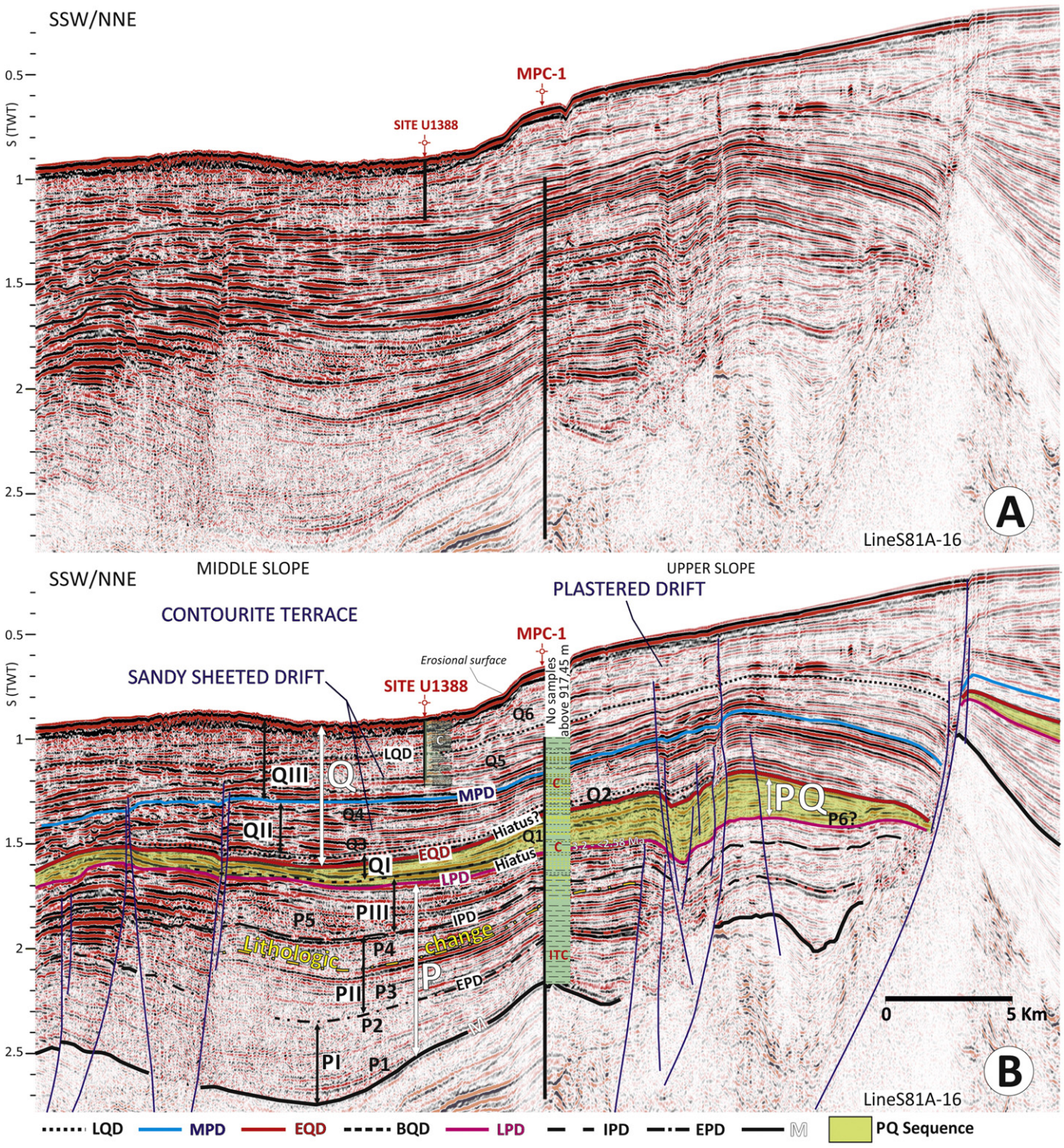

Fig. 8. Seismic profile (Line S81A-16) of the Cadiz basin across sites U1388 and MPC-1. Major sequences (P, PQ and Q), units (PI–PIII and QI–QIII) and subunits (P1–P6 and Q1–Q6), as well as the main discontinuities and hiatus are shown (Modified and updated from Hernández-Molina et al., 2014b). Profile location given in Fig. 3. Abbreviations for discontinuities are in Fig. 6. Simplify sedimentary logs for U1388 and MPC-1 are included (see abbreviations in Fig. 5).

Portugal (Fig. 1). Offshore slope areas of Algarve basin are considered as the Deep-Algarve basin. Tectonic features control the basins, their depocenter distribution and their main contourite sectors (1–5) described in Hernández-Molina et al. (2003, 2006) and Llave et al. (2007a, 2007b) (Fig. 4). The proximal scour and sand-ribbon sector (1) and the overflow sedimentary lobe sector (2) have developed within the Cadiz basin. The central channel and ridges sector (3) is found in the Sanlucar and Doñana basins and the main depositional sector (4) has formed within the Deep Algarve basin. The submarine canyon sector (5) covers the rest of the SIM westward including the Alentejo basin. Deformed sheeted drifts in the central sector coincide with the Doñana basin, which shows intensive recent and ongoing deformation.

Neogene Basins located in the Gulf of Cadiz are generally bound by westward thrusted Flysch and Subbetic material. The AUGC was thrust northwestwards into the Guadalquivir and Algarve basins. A set of

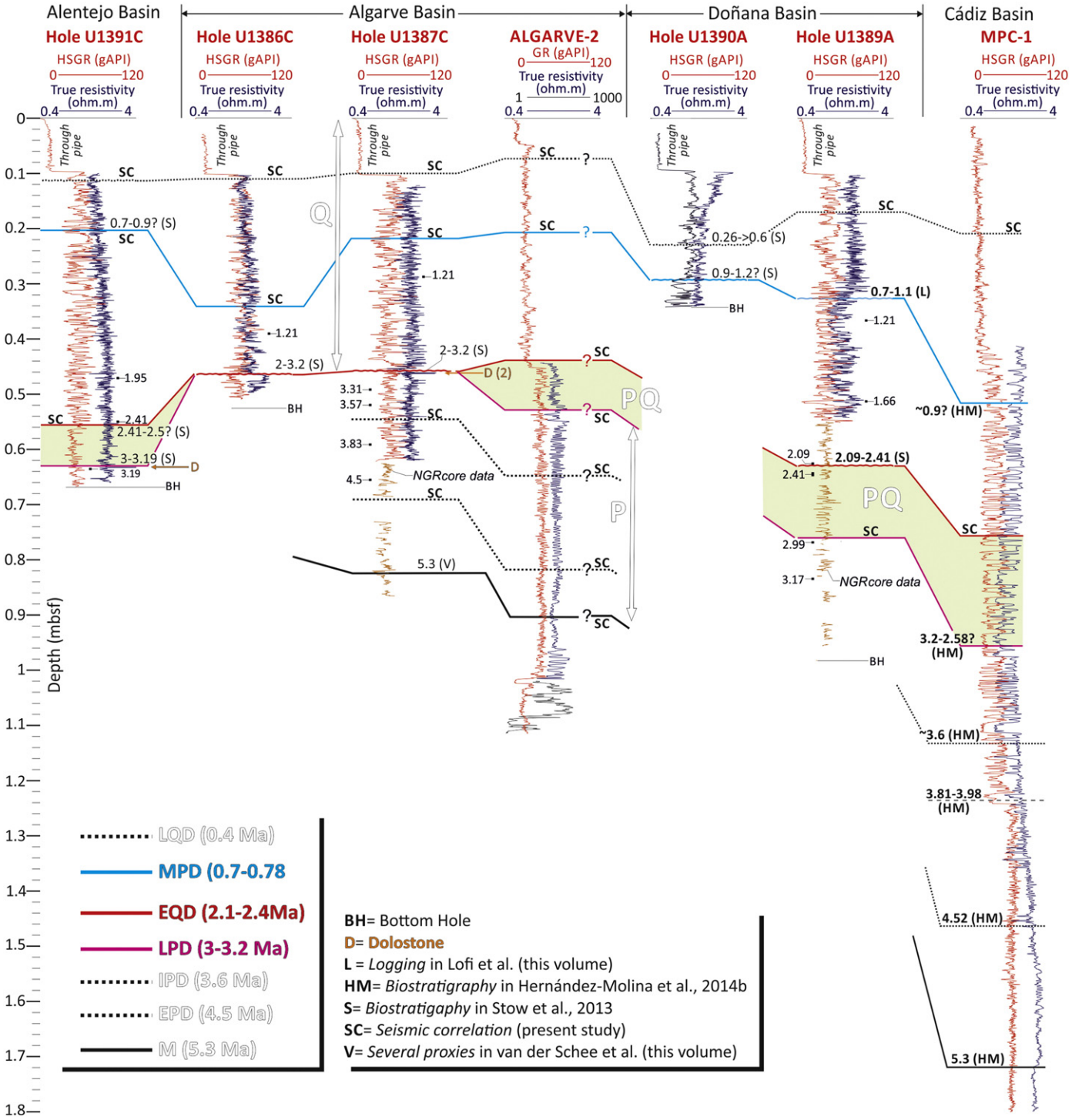

Fig. 9. Log data, gamma ray (HSGR) and resistivity, for IODP Exp. 339, Algarve-2 and MPC-1 boreholes shown with the main Pliocene and Quaternary discontinuities.

linear and segmented parallel ridges and highs trending in a NE–SW direction formed either exposed or buried structures, constructing the undulating sea-floor morphology that has been described by a number of works (e.g., Maldonado et al., 1999; Gutscher et al., 2002; Medialdea et al., 2004, 2009; Fernández-Puga et al., 2007; García et al., 2009). Diapirs appear as chaotic, highly diffractive bodies in seismic profiles (Fig. 4). Diapirs, as well as other highs and ridges are affected by SWIM strike-slip faults, which trend in a WNW–ESE direction, (Fig. 1) (Zitellini et al., 2009; Duarte et al., 2011). The influence of some of these structures on the Pliocene and Quaternary strata is shown in Figs. 4, 6–8 and 12–14.

The Cadiz basin occurs between frontal thrusted Flysch and Subbetic units (Fig. 4) and the Cadiz diapiric ridge (CDR). This basin trends in a NE–SW direction, and occupies an area 45 km wide and about 60 km in length, extending roughly to the present-day shelf break. The Pliocene and Quaternary sedimentary record is asymmetric and eastward thickening, with TWTTs of up to 1.7 s. This section of the record was sampled at site U1388, where drilling reached Pleistocene units (<0.6–0.7 Ma), and by the MPC-1 borehole which extends to the late Miocene. The CDR trends in a NNE direction and resides at a water depth of 400–800 m. It extends approximately 43 km in length, varies in width up to a maximum of 14 km and takes an asymmetric form. It

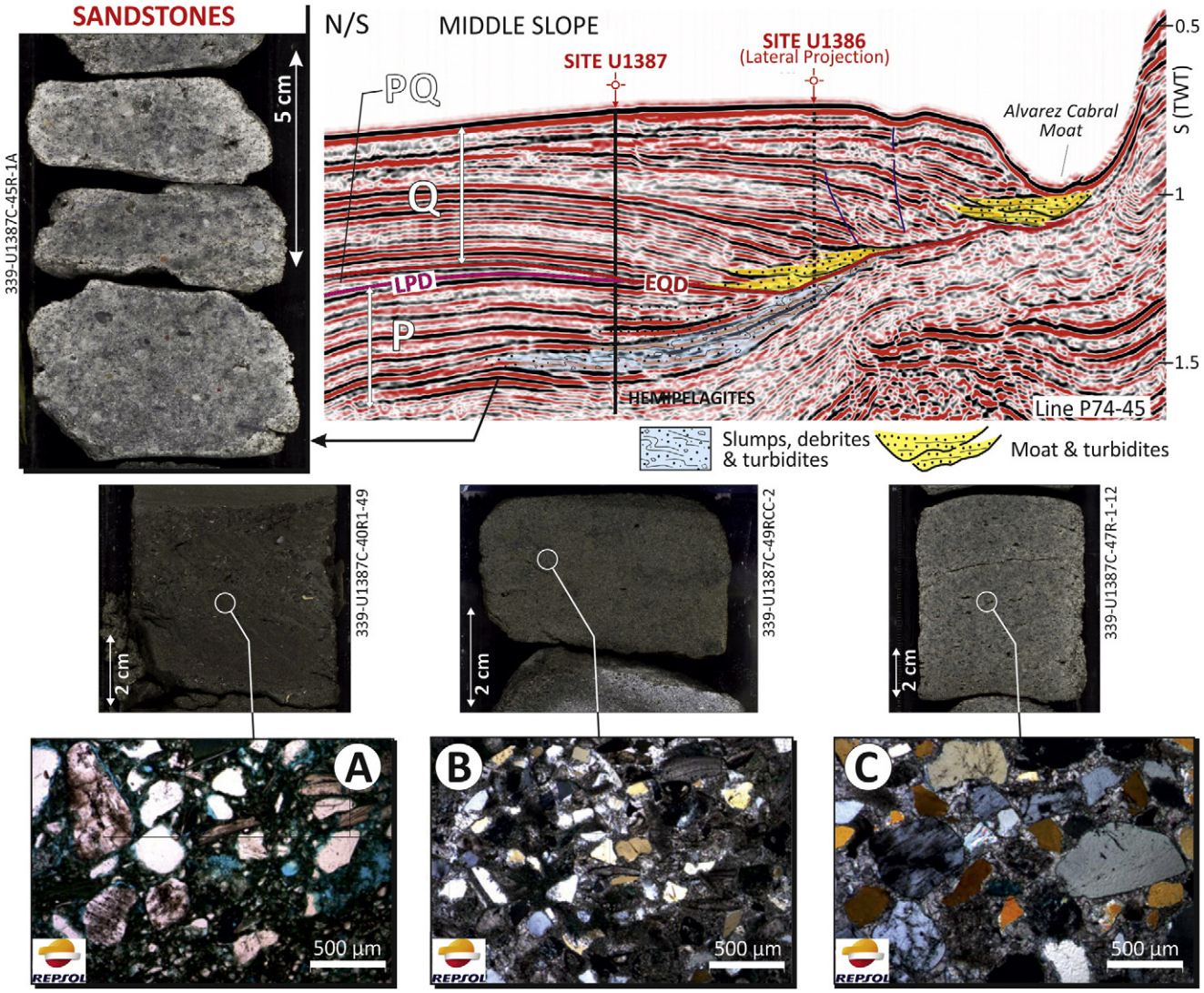

Fig. 10. Examples of early Pliocene sandstone petrofacies at site U1387C: A) petrofacies-1 with fine to very fine, very poorly sorted monocrystalline quartz sandstone (PP, plane polarized light.); B) petrofacies-2 with fine to very fine sandstone, moderate sorted and subrounded framework sandstone (XN, crossed nicols); and C) petrofacies-3 with well-rounded, poorly sorted sandstones (XN).

has gaps and is most strongly deformed along its eastern flank. The Rota basin is a smaller subordinate basin bounded by a diapiric structure and residing within the westernmost part of the Cadiz basin. It reaches widths of 20–25 km and thicknesses of approximately 1.5 s (TWTT).

The Sanlucar basin is of 25–30 km in width between the Cadiz and Guadalquivir diapiric ridges (GDR) (Fig. 4), and extends 70 km in length up to the shelf break. It has an asymmetric sedimentary thickness for the Pliocene and Quaternary section that reaches nearly 2 s (TWTT) along its eastern boundary. Although this basin was not sampled, upper slope and outer shelf deposits have been stratigraphically correlated with the adjacent Rota and Cadiz basins. The GDR trends in a NE–SW direction and reaches approximately 86 km in length. Its upper surface rests at water depths of 300–1100 m. This basin hosts the most extensive of the ridge systems found in the study area, and thus has a bathymetry characterized by numerous irregular highs, lows and gaps.

The Doñana basin is located to the west, between the Guadalquivir diapiric ridge and a set of elongated basement highs that trend in a NE–SW direction (Figs. 1 and 4). These occupy middle slope regions at 1200–1300 m depth and include the Guadalquivir bank (GB) and the Portimao and Albufeira basement highs (PH and AH, respectively). The Doñana basin is 25 km wide and extends 108 km in length up to the shelf break. It shows a Pliocene and Quaternary section of up to ~1.5 s (TWTT). Two sites have been drilled in the Doñana basin, the site U1389 borehole in the east of the basin, which penetrates down to the early Pliocene (<3.8 Ma) and the site U1390 borehole in a southwesterly area, which extends to the early Pleistocene (<1.3 Ma). The Doñana basin is bisected by the Doñana dipiric ridge (DDR) which is a 53 km long feature located to the north, at water depths ranging from 500 to 1100 m. This ridge outcrops in limited areas, and locally deforms the overlying sedimentary succession. The Guadalquivir bank (GB) is located in the southern part of the Algarve basin and represents a structural high located at water depths of around 300–500 m. The GB represents south Portugal's Variscan rifted basement (Medialdea et al., 2004; Roque et al., 2012). Due to its tectonic inversion and recent uplift, the adjacent western sector of the basin suffered subsidence allowing the formation of a sedimentary depocenter.

The Deep Algarve basin resides between the Algarve upper slope and the aforementioned basement highs (Fig. 4). It extends 40–50 km in width and 114 km in length. Pliocene and Quaternary sedimentary thickness in the basin reach about 1.2 s (TWTT). Sedimentary thickness is irregular in the Deep Algarve basin but much more tabular than that previously described basins. The Deep Algarve basin was sampled at sites U1386, U1387 down to the late Miocene (<5.75 Ma). The Algarve-2 borehole was also drilled down to the late Paleocene and

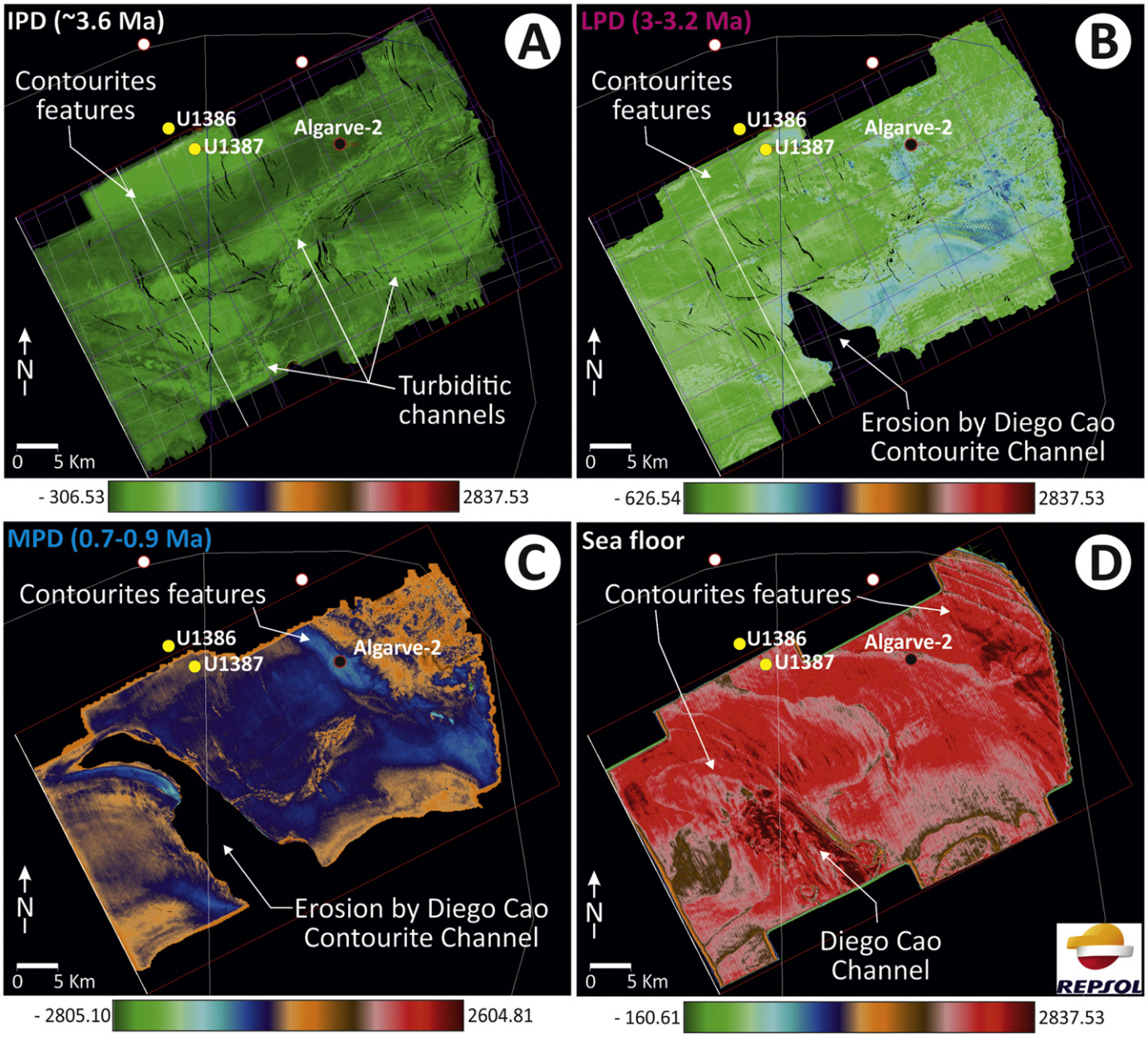

Fig. 11. Amplitude maps based on 3D seismic data from the Algarve basin (Fig. 3) for: A) Intra Pliocene Discontinuity (~3.6 Ma); B) late Pliocene Discontinuity (3–3.2 Ma); C) mid Pleistocene Discontinuity (0.7–0.9 Ma); D) present day bathymetry of study area (data courtesy of REPSOL). Area location is provided by a red square in Fig. 3. These maps show the change from a system of mixed contourite and turbidite deposition in the early Pliocene to the dominant contourite system from the Pleistocene to the present.

Eocene sections, the later of which is unconformably overlain by Late Miocene–Pliocene sediments. This basin contains diapiric structures, which follow NE–SW trends and include late Triassic and early Jurassic evaporites. The frontal part of the AUGC also appears in this basin and pinches out within late Miocene sediments (Roque et al., 2012; Hernández-Molina et al., 2014b). Finally, the Alentejo basin trends in a N–S direction between the San Vicente and Lisboa submarine canyons (Fig. 1) and hosts a Pliocene to Quaternary sediment thickness of <0.9 s (TWTT). The borehole at site U1391 sampled this basin down to the early Pliocene (<3.5 Ma).

Seismic and drilling results show significant spatial and vertical variation of sedimentary, seismic and logging facies along with numerous discontinuities in Neogene basins. The two most significant discontinuities (after the prominent Miocene–Pliocene boundary) occur at 3.2–3.0 Ma (late Pliocene Discontinuity, LPD) and 2.4–2 Ma (early Quaternary discontinuity, EQD) (Fig. 4) and divide the sedimentary record into three major sedimentary sequences of: Pliocene (P); Pliocene/Quaternary (PQ) and Quaternary (Q) age. These sequences consist of six seismic units (PI–PIII and QI–QIII) bounded by minor discontinuities (Table 1), which appear as high-amplitude seismic reflections. The distribution of these reflections indicates that they represent erosional surfaces along basin margins that develop into conformable surfaces basinwards. Sedimentary facies for the Pliocene and Quaternary sections consist primarily of pelagites, hemipelagites, contourites, turbidites, debrites and slump deposits (Figs. 5 and S2). Dolomitic mudstone, dolostones and sandstones are rare, but also appear in drill core material associated with the aforementioned hiatuses. Contourites include sand-rich, silt-rich and mud-rich contourites, and constitute about 50% of the recovered Pliocene core deposits, where debrites and turbidites are also common. Contourites predominate the sedimentary record Quaternary deposits (Fig. 5) above the 2.4–2 hiatus (up to 95% of recovered core deposits).

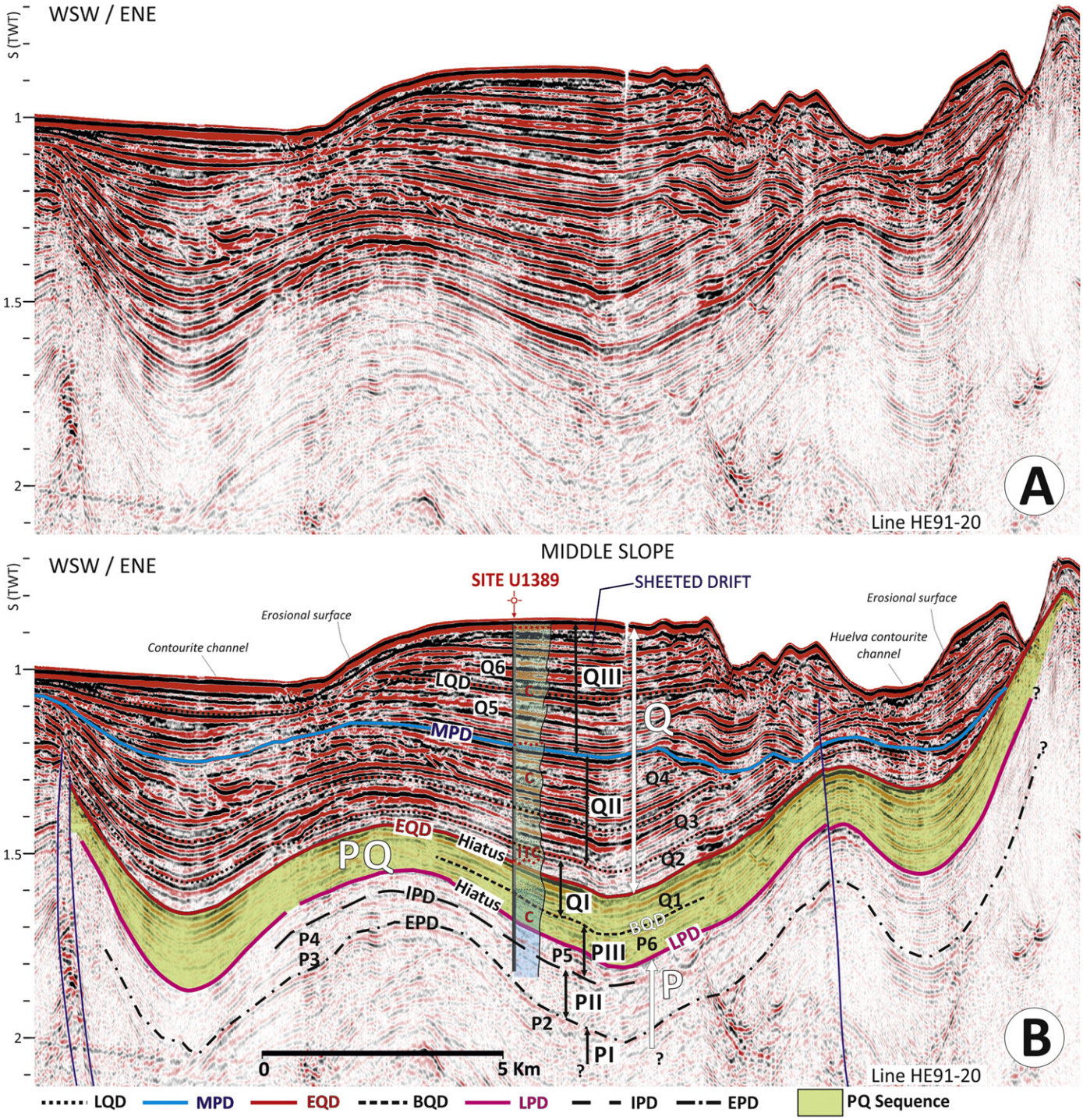

Fig. 12. Seismic profile (Line HE91-20) including site U1389 in the Doñana basin. Major sequences (P, PQ and Q), units (PI–PIII and QI–QIII) and subunits (P1–P6 and Q1–Q6), as well as the main discontinuities and hiatus are shown. Profile location given in Fig. 3. Abbreviations for discontinuities are in Fig. 6. Simplify sedimentary log for U1389 is included (see abbreviations in Fig. 5).

5.2. Late Miocene and Miocene/Pliocene boundary

Seismic facies for the entire late Miocene appear as very weak to semi-transparent seismic reflections. Some seismic reflections suggest slope progradation in a seaward direction. Locally high amplitude reflections occur in lateral association with incised erosional surfaces and channelized features (Figs. 6 and 7). Being Messinian in age, these deposits appear in the Deep Algarve basin at sites U1387 and Algarve-2 (Figs. 6 and 7) and in the Cadiz basin at the MPC-1 site (Fig. 8). The dominant regional sedimentary facies includes clays and marls with occasional layers of fine sand. This facies appears in the Deep Algarve basin at site U1387 as dark greenish to greenish, gray muds and muddy oozes with nannofossils. The facies forms in hemipelagic settings and shows subtle parallel lamination and pervasive bioturbation (Figs. S2-J). Siliciclastic abundances are up to 70% and carbonate abundances are 15%–30%.

The Miocene/Pliocene boundary (M) at 5.3 Ma was detected at borehole Algarve-2 at around 1455–1460 mbsf in the Deep Algarve Basin (Figs. 5 and 7). The seismic reflector marking the boundary was traced from Algarve-2 to sites U1387 and U1386. The boundary appears in

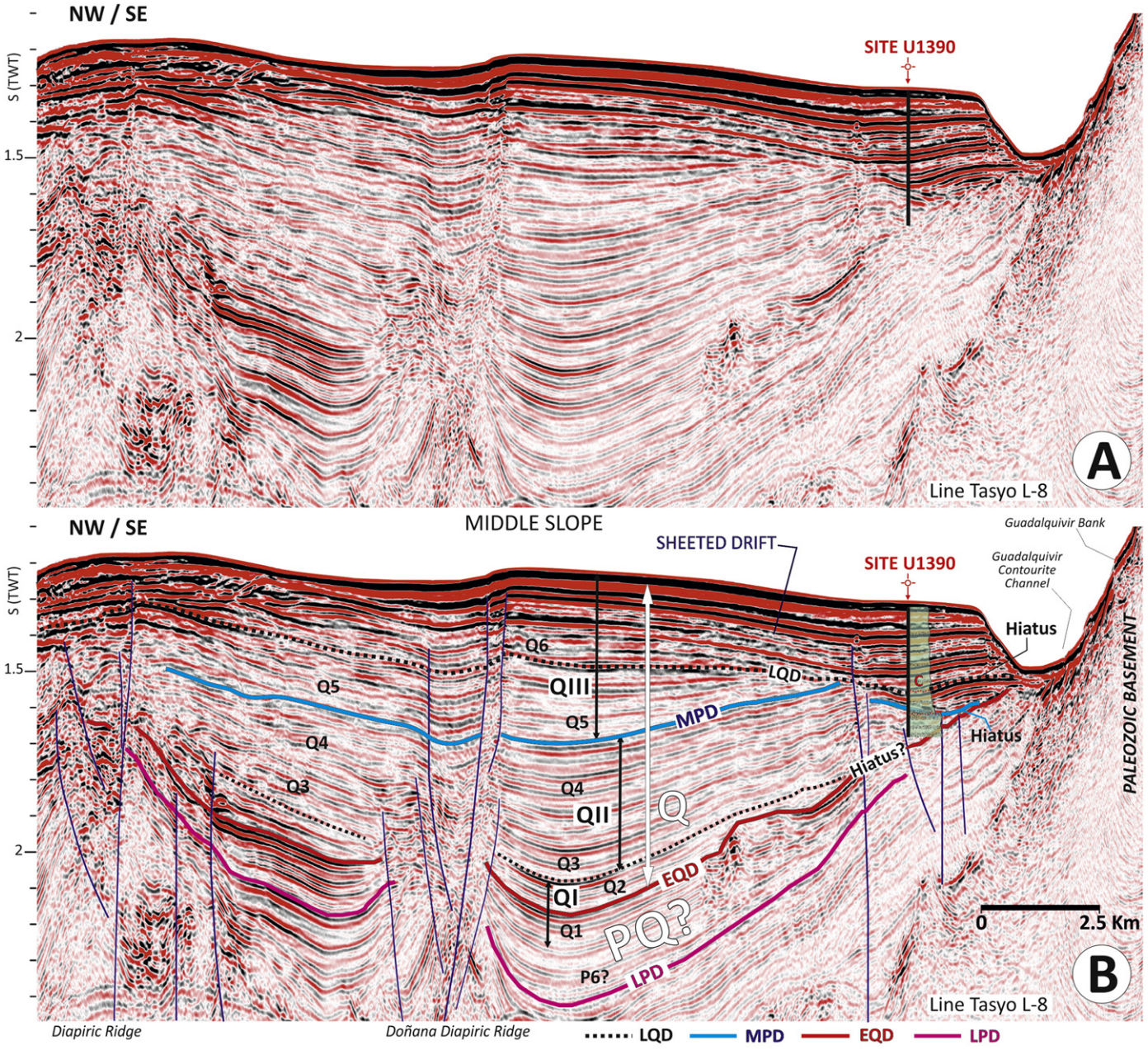

Fig. 13. Seismic profile (Line Tasyo L-8) of the Doñana basin across site U1390. Major sequences (P, PQ and Q), units (PI–PIII and QI–QIII) and subunits (P1–P6 and Q1–Q6), as well as the main discontinuities and hiatus are shown. Profile location given in Fig. 3. Abbreviations for discontinuities are in Fig. 6. Simplify sedimentary log for U1390 is included (see abbreviations in Fig. 5).

seismic profiles as an increase in reflection amplitudes (Fig. 7), which laterally correspond with an erosional surface along the axis of the Deep Algarve Basin (Figs. 6 and 7). These seismic characteristics also appear in profiles from the Cadiz, Rota and Sanlucar basins, but are less clear within the Doñana basin, due to its pervasive deformation. The transition does not appear in borehole log data (Fig. 9). The boundary at site U1387 is not consistently obvious in bio-, magneto- or cyclostratigraphic data. However Van der Schee et al. (2015) has recognized a significant change from hemipelagic muds to a sedimentary setting affected by bottom currents at around 826 mbsf in site U1387, which approximately coincides with the estimated depth for the aforementioned reflection. Above this boundary the sedimentation rate increases (from ~9.9 to 27.2 cm/ky in the Pliocene) and the sediment displays a greater relative siliciclastic component, an increase in the >63 μm grain size fraction, larger XRF Zr/Al ratios and lighter benthic oxygen isotope values.

5.3. Pliocene

The Pliocene succession was sampled at four sites from IODP Exp. 339 (U1386, U1387, U1389 and U1391, Fig. 5), as well as by the Algarve-2 and MPC-1 boreholes.

5.3.1. Early Pliocene to late Pliocene

Early Pliocene deposits appear as sheeted deposits with a general aggradational sedimentary stacking pattern and clear evidence of along- and across-processes interaction. These units correspond with the seismic units PI, PII and the lower part of PIII, which include a number of subunits (Table 1, Figs. 6–8). Seismic units vary between the Neogene basins in terms of seismofacies and sedimentation rates. In the Deep Algarve and Alentejo basins, these units exhibit well-stratified high amplitude reflections with good lateral continuity (PI and PII), which evolve

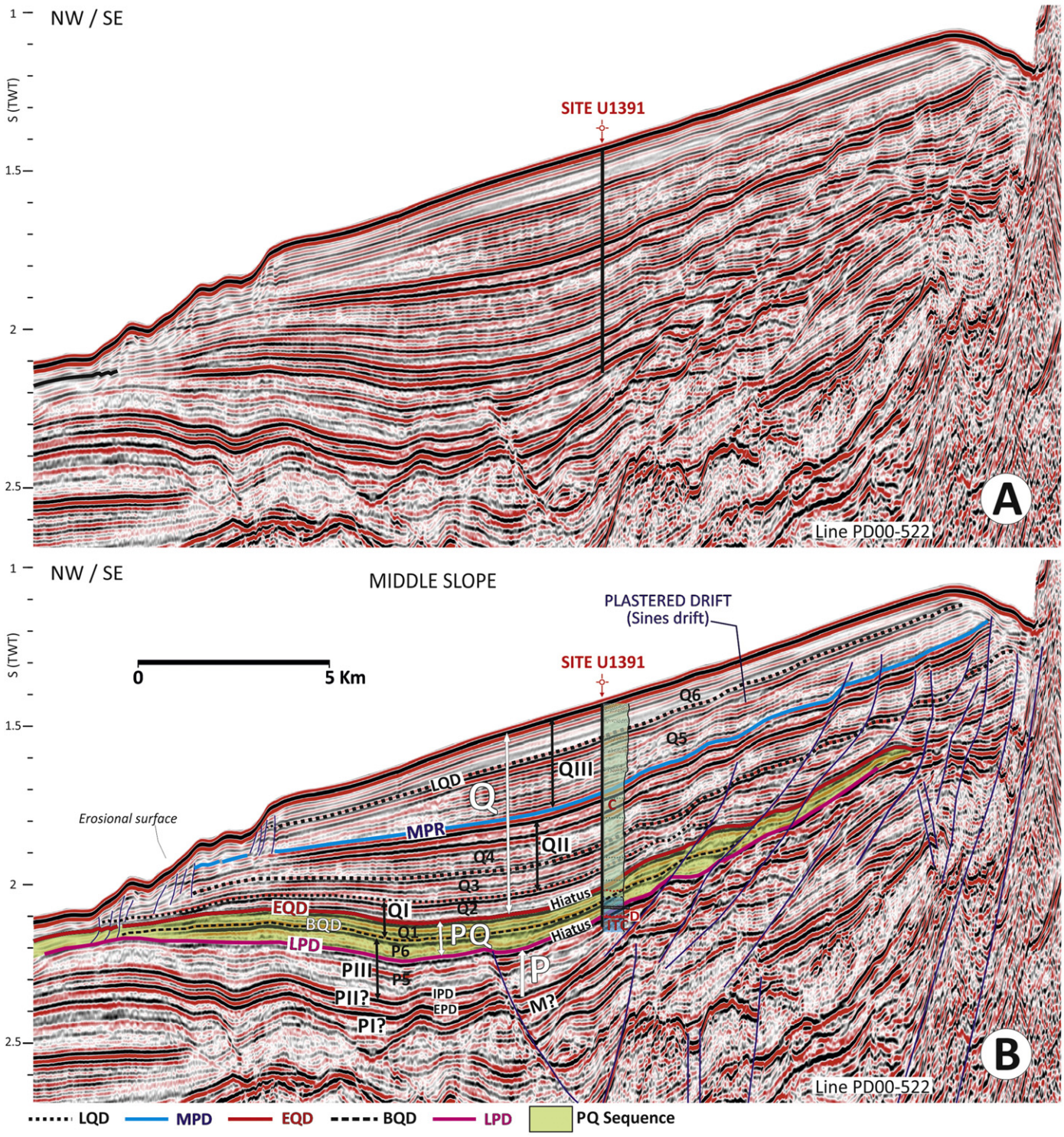

Fig. 14. Seismic profile (line PD00-522) of the Alentejo basin showing the Pliocene to Quaternary sedimentary record at site U1391. Major sequences (P, PQ and Q), units (PI–PIII and QI–QIII) and subunits (P1–P6 and Q1–Q6), as well as the main discontinuities and hiatus are shown (data courtesy of TGS–NOPEC Geophysical Company ASA). Profile location given Fig. 3. Abbreviations for discontinuities are in Fig. 6. Simplify sedimentary log for U1390 is included (see abbreviations in Fig. 5).

upward into deposits with weaker acoustic response (PIII). In basins hosting the AUGC, the early Pliocene deposits generaly show the opposite seismofacies trend (Figs. 4 and 6–8), with a weak acoustic response at the base (PI and PII) strengthening progressively upward to PIII. Sedimentation rates are moderate in the Deep Algarve and Alentejo basins (~15 cm/ky), but higher in the Doñana basin (~25 cm/ky; site U1389). A prominent precessional periodicity appears in log data from lower Pliocene records of the Gulf of Cadiz (Fig. 9). Sierro et al. (2000) first identified these cycles, being interpreted as rhythmic changes in clay content, reflecting precession-induced oscillations in annual rainfall. At sites U1386 and U1387, Pliocene logs record a strong lateral supply of terrigenous material.

The boundary between PI and PII represents an onlap surface (Fig. 6), referred to as the early Pliocene Discontinuity (EPD). Drilling data has constrained this surface to an age of ca. 4.5 Ma. This boundary correlates with the LPR horizon described in Llave et al. (2001,

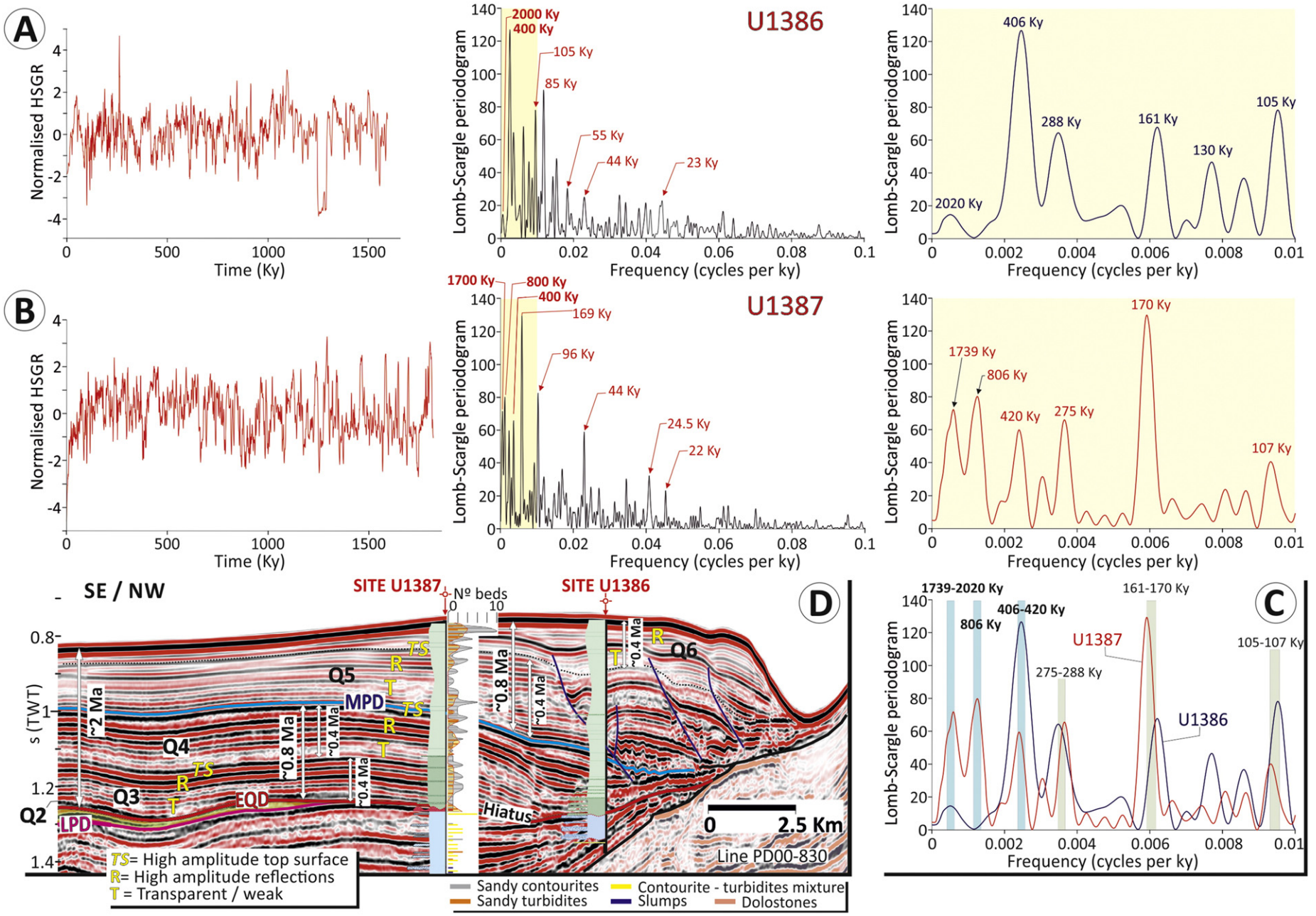

Fig. 15. Spectral analysis performed on HSGR logs at sites U1386C and U1387C (A and B) to determine orbital-scale variations in sediment from most active part of the CDS (C). D) Seismic line PD00-830 across sites U1386C and U1387C including the sedimentary cycles and the number of beds for the Quaternary sedimentary record above the early Quaternary discontinuity (EQD). Number of beds is taken from Stow et al. (2013b).

2007a, 2011); Hernández-Molina et al. (2002) and Marchès et al. (2010) and with the H1 discontinuity described in Roque et al. (2012) (Table 1).

Sub-unit PI has a basal tabular sub-unit (P1) that appears as moderate reflection amplitudes above the M discontinuity (Fig. 7). These deposits were drilled at site U1387. Although core recovery from this site was poor, core material exhibited thin sandy beds (silty sand and sand, Fig. S2-A), with common glauconite and dolomite, and was interbedded with nannofossil muds and occasional debrites. Above these sandy deposits, P2 occurs as a lobate to tabular shaped sub-unit with high to very high amplitude reflections at its base (Figs. 6 and 7). These seismofacies match the well-cemented, gray to dark greenish gray sandstones observed in core material from site U1387 (Fig. S2-B), which is interbedded locally with dark greenish gray, silty/muddy fine sands. Above the sandstones, chaotic seismic facies occur as tabular to wedge-shaped bodies (Fig. 6). These appear in drilling data from both U1386 and U1387, and correspond to thickly-bedded, chaotic, bioclastic debrites and slump deposits that reach thicknesses of up to 5 m (Figs. 5 and S2-C and D). These intervals appear as high resistivity values in borehole logs (Fig. 9, Ducassou et al., 2016).

The consolidated sandstone layers represent a shift in lithofacies at about 5 Ma, which corresponds to the marked change in seismofacies apparent in seismic profiles (Figs. 6 and 7). Sandstones show moderate to poor sorting and well-rounded grains of green glauconite but no bioturbation (Fig. 10). Sandstone clasts are supported by a matrix of clay and silt-sized carbonate, which is partly replaced by calcite cement. Silty material constitutes 30% of the matrix, siliciclastics make up 40% of the matrix (mostly quartz with trace feldspars, heavy minerals, and mica) and biogenic carbonate clasts makes up 30% (foraminifers and shell fragments). Most of the quartz grains are angular, although some grains of rounded quartz, polycrystalline quartz, or quartzite are also present. Petrographic analysis of sandstone thin sections revealed grain-supported, medium-grained sand with calcite cement filling in pore spaces (Fig. 10). This sample had a high relative abundance of feldspathic material, reaching 25% in arkose samples, as reported by Stow et al. (2013b). Recent analysis by REPSOL using IODP samples (Caja et al., 2013) identified three petrofacies in these sandstones. Petrofacies 1 has variable rounded, medium-fine to very fine, very poorly sorted monocrystaline quartz sandstones containing bioclasts of foraminifera and coral material (Fig. 10A). Petrofacies 3 consists of medium grained, rounded to well-rounded, poorly sorted sandstones with very little matrix and dominantly containing monocrystalline and polycrystalline quartz (Fig. 10C). Petrofacies 2 represents an intermediate between petrofacies 1 and 3 (Fig. 10B). All petrofacies share basic compositions that include K-feldspars, plagioclase, foraminifera and minor components of intrusive igneous rock fragments, carbonate, muscovite, hornblende, tourmaline and glauconite clasts (Fig. 10).

PII consists of two subunits (P3 and P4, Table 1) bounded by an extensive, high-amplitude reflection surface dated at ~3.8 to 3.9 Ma (Figs. 6 and 7). Within the AUGC, this horizon represents a lithologic shift in which sedimentary input to the Cadiz basin assumed a sandier composition (Hernández-Molina et al., 2014a) (Fig. 8). PIII and PII are separated by a high amplitude horizon dated at ~3.6–3.5 Ma and interpreted as the intra Pliocene discontinuity (IPD) (Figs. 6, 7 and 8, Table 1). Above this surface, PIII assumes a sandier composition in the Cadiz basin (Fig. 8).

Nannofossil mud, silty mud and silty sand with biogenic carbonate comprise the dominant sedimentary facies found in PII and PIII core material from site U1387 (Figs. 5 and S2). The relative abundance of nannofossil mud decreases significantly through the early Pliocene up to unit PII. This compositional shift is manifested as a seismic amplitude increases for the overlying unit PIII in the Algarve basin. Interbedded turbidite and contourite deposits commonly appear as parallel- to slightly inclined-laminations with normally graded bedding (Fig. S2). For the intra Pliocene discontinuity (IPD), amplitude anomaly maps based on 3D seismic profiles of the Deep Algarve Basin, clearly show the common occurrence of turbiditic channels throughout the basin and their lateral association with contourite features (Fig. 11). Core material from PII and PIII subunits consists of cyclical alternation of sediments with light and dark layers of 1 to 5 m thickness (Figs. 5 and S2-H). The base of each cycle generally consists of light-colored silty sands with biogenic carbonate and normal graded bedding that passes upward into light- or dark-colored muds (Stow et al., 2013b). In general, the mud facies constitute >80% of each cycle. The muds contain trace amounts of siliceous microfossils (e.g., radiolarians, diatoms, and sponge spicules). Lithologic contacts within a cycle are gradational or bioturbated, whereas the basal contact of the silty sands is sharp, erosional and sometimes bioturbated.

5.3.2. The late Pliocene hiatus

A regional discontinuity, termed the late Pliocene Discontinuity (LPD) appears as a laterally continuous, high amplitude reflection in the Deep Algarve basin (Figs. 6 and 7), basins covering the AUGC (Figs. 8, 12 and 13) and the Alentejo basin (Fig. 14). This discontinuity represents a local erosional surface with the hiatus increasing towards local highs. The hiatus appears at around 3.0–3.2 Ma in core material from site U1391, or as reduced rates of sedimentation at other sites. The amplitude anomalies map for the LPD in the Deep Algarve basin (Fig. 11) shows no turbiditic channels and an increase in reflectivity (associated to coarser grain sizes) in the southern part of the basin, near the basement highs. Dolostone deposits are closely linked to this hiatus (Figs. 5 and S2-I), indicating shallow diagenetic processes and appearing as high resistivity peaks in borehole logs (Fig. 9).

5.4. The late Pliocene–Quaternary

The Pliocene–Quaternary (PQ) sequence is bounded by the LPD at its base and by the early Quaternary discontinuity (EQD) along its upper surface. The sequence includes the upper part of the PIII seismic unit (P6) and the lower part of the QI seismic unit (Q1) (Table 1). PQ was sampled at sites U1389 and U1391 (Fig. 5), as well as by the Algarve-2 and MPC-1 boreholes, but did not appear in records from other sites. Sedimentation rates corresponding to this sequence reach ~25 cm/ky in the Doñana basin (site U1389) and 13 cm/ky in the Alentejo basin (site U1391). On seismic profiles, the EQD completely erodes the PQ sequence in areas near the upper slope, diapirs and basement highs. The sequence is continuous in the deepest part of the basins (Figs. 6–8 and 12–14). Erosional processes have resulted in a wedge or lenticular shaped PQ sequence. Seismic profiles show PQ as high amplitude reflections indicating sheeted drift deposits and enhanced acoustic response in upper parts of the sequence, especially in areas adjacent to highs and banks. Borehole logs for this sequence show cyclic swings in amplitude that are generally lower than those observed for the Q sequence, except when sampling the most proximal site, MPC-1 (Fig. 9). Logs from site U1390 shows low amplitude variation for the lower part of the sequence, increasing to higher amplitude variation for the upper parts of the sequence.

Sedimentary facies for the latest Pliocene (P6) in the Doñana basin (site U1389) consist of calcareous mud (Fig. S2-K). Bi-gradational sequences are scarce and normally graded bedding is absent. In the Alentejo basin (site U1391), above subunit P6, dominant calcareous muds alternate with biogenic muds (Fig. S2-L) and debrites. The earliest Pleistocene sedimentary record (Q1) is bounded at its base by a laterally extensive and high amplitude reflection, which corresponds to the basal Quaternary discontinuity (BQD). This surface correlates with the H3 discontinuity in Roque et al. (2012) and with horizons BQD and D1 in Llave et al. (2011) and Marchès et al. (2010), respectively (Table 1). Q1 is typically eroded by the EQD, but where observed, it appears as high- to very high-amplitude, laterally extensive seismic reflections that outline aggradational features and internal erosional truncations

(Figs. 6–8 and 12–14). Core material revealed lithologies that include nannofossil muds, calcareous silty muds, and silty sands with biogenic carbonate (Figs. 5 and S2). There are frequent bioturbation structures throughout.

5.4.1. The early Quaternary hiatus

The early Quaternary discontinuity (EQD) is the most prominent discontinuity in the study area. This horizon marks a shift in the sedimentation pattern, a considerable increase in sedimentation rates and the onset of the present-day contourite depositional and erosional features. The surface appears as a high-amplitude reflection outlining a penetrative erosional truncation surface that is especially evident in areas near the upper slope and adjacent to relief (diapirs and basement highs) (Figs. 6–8 and 12–14). Core material shows the hiatus occurs at 2 and 2.4 Ma at different sites. The volume of sediment eroded varies, but increases considerably towards highs. The surface evolves to a more conformable horizon basinwards. Several well-cemented dolomite horizons occur below the EQD at site U1387, where beds appear as high resistivity peaks in borehole logs (Fig. 9). Dolostones consist of almost pure dolomite (3–10 μm dolomite grains) but contain a few quartz grains, opaque minerals, and ghosts of siliceous microfossils, including radiolarians and diatoms (Fig. S2-I). The dolomite beds are overlain by turbidite sands (Figs. 5–7).

5.5. The Quaternary (<2 Ma)

The Quaternary sequence (Q) younger than 2 Ma consists of the upper part of the QI, as well as seismic units QII and QIII (Table 1). It unconformably overlies the Pliocene deposits and was sampled at all IODP Exp. 339 sites, partially by MPC-1, but did not appear at the Algarve-2 site. The primary contourite sedimentary facies include nannofossil mud, calcareous silty mud and silty bioclastic sand lithologies (Figs. 5 and S2). These three facies generally occur as bi-gradational sequences, the most complete of which coarsen upward from nannofossil muds to calcareous silty muds to silty bioclastic sands, and then fine upwards through calcareous silty mud to nannofossil mud (Fig. S2-N and O). Partial sequences are also common (Fig. S2-P and Q) and episodic turbidite intercalations with normally graded sequences occur at several sites (Fig. 5). As a result, some of the contourite muds retain a distinctive lamination, albeit discontinuous in character, whereas the thicker sands are especially clean and well sorted. The Q sequence appears in well logs from all sites. HSGR logs show the sequence as medium-amplitude cyclic swings, varying on decimeter to sub-meter scale, with no major steps in base levels (Fig. 9). High NGR values indicate layers with high clay content and low carbonate content, whereas lower NGR values indicate either the opposite and/or coarser grained clastic material characteristic of contourite beds. Prominent precessional and eccentricity periodicities appear in log data (Lofi et al., 2015. Fig. 9). HSGR log patterns correlate very well across sites sampled by IODP Exp. 339, enabling regional mapping of certain well expressed contourite beds (Lofi et al., 2015). Q1 sequences exhibit cycles consistent with orbital forcing at precessional and eccentricity-related timescales. The PQ and Pliocene intervals below also exhibit cyclic swings in both HSGR and resistivity logs, but with lower amplitude and at lower frequencies than those observed for the Q sequence (Fig. 9).

5.5.1. From 2 Ma to the middle Pleistocene

The early and middle Pleistocene deposits (upper part of QI and Q2) are bound by the EQD at their base and by the Mid Pleistocene Discontinuity (MPD) along the upper surface. Internal discontinuities distinguish minor subunits (Q2, Q3 and Q4, Table 1). These deposits have middle to high amplitude acoustic response but occur as different seismic facies among the Neogene basins. In the basin covering the AUGC, these deposits appear as high to very high amplitude acoustic responses with a well-layered internal structure, indicating sheeted drifts in aggradational configuration. The facies show a few thin intervals of lateral progradation within the Cadiz and Doñana basins (Figs. 8, 12 and 13). In the Deep Algarve basin these deposits exhibit clear upslope progradation of certain well-stratified high amplitude and laterally continuous reflections (Figs. 6 and 7), which represent a mounded elongated and separated drift (Faro Drift). This mounded geometry evolves in a seaward direction to an aggradational geometry characteristic of a sheeted drift. A similar sequence of seismic facies appears within Q3 and Q4 in all the basins, wherein weak to transparent acoustic facies evolve upwards into a high-reflectivity facies truncated by a subtle erosional surface (Figs. 6–8 and 12–14).

Although these early and middle Pleistocene deposits are mud-dominated, they represent a period of increased sand and silt deposition and a marked increase in sediment supply to the slope (sedimentation rates of 25 and 40 cm/ky), relative to previous deposits (Fig. 5). Sedimentary facies of Q2 and Q3 record the interbedding of contourites with sandy and silty turbidites. The higher relative proportion of sand in contourites/turbidites explains the higher acoustic response of these subunits, especially in the Deep Algarve basin (Fig. 6). In the Doñana basin (sites U1389 and U1390) Q2 and Q3 are slightly enriched in the clay sized fraction (51%) and the sandy mud with biogenic carbonate as a subordinate lithology. These horizons at site U1389 exhibit fewer and finer-grained contourite sequences, all without sand, and higher proportions of biosiliceous sediment (diatoms and sponge spicules). These sediment types indicate a low-energy depositional environment. Silty and sandy units are generally poorly sorted, with subrounded to rounded detrital siliciclastic material. Detrital carbonate grains are generally subrounded to subangular, many with abraded margins indicative of reworking.

5.5.2. The mid Pleistocene discontinuity (MPD)

Another important change in the sedimentary stacking pattern occurs at the mid Pleistocene discontinuity (MPD). This discontinuity correlates with the MPR discontinuity (Mid-Pleistocene Revolution) identified by Hernández-Molina et al. (2002, 2006); Llave et al. (2007a, 2007b, 2011); Marchès et al. (2010) and Roque et al. (2012). Although it is clearly evident in seismic profiles (Figs. 6, 7, 8, 12, 13 and 14) as an erosional surface in areas adjacent to diapirs and basement highs, core material from the Doñana basin (sites U1389 and U1390) indicates it represents only a short hiatus of variable duration (around 0.7–0.9 Ma). In the Cadiz basin, the sheeted drifts become even sandier above the MPD. Thick sands also appear around this horizon in the Doñana basin (site U1390). The amplitude anomaly map for Deep Algarve basin (Fig. 11), show contourites features along slope in the vicinity of the MPD horizon.

5.5.3. Middle Pleistocene to Holocene

Middle Pleistocene to Holocene deposits (QIII, Table 1) overlie the MPD at their base and extend up to the present-day seafloor. In the seismic profiles, they exhibit different seismofacies across different Neogene basins (Figs. 6–8 and 12–14). In basins covering the AUGC, they appear as a sandy sheeted drift (Cadiz basin) that transitions to muddy sheeted and mounded drifts in a northwesterly direction. These are then incised by contourite channels in the Doñana and Deep Algarve basins. The deposits have a well-layered internal acoustic structure, very high to massive acoustic response (with a few very high reflections), aggradational seismic configuration and abundant internal erosional surfaces (Figs. 8 and 12–13). In the Deep Algarve basin, these deposits exhibit a weaker acoustic response, with a sigmoidal to oblique reflection configuration suggestive of upslope progradation in proximal areas of the slope, and parallel to sub-parallel reflectors, outlining enhanced mounded morphology (Figs. 6 and 7). Laterally, the mounds features transition into an aggradational pattern characteristic of a large sheeted drift. Sedimentation rates for these deposits are moderate (~30 cm/ky) in the Deep Algarve and Alentejo basins (sites U1386, U1387 and U1391), to extremely high in the Cadiz (60 cm/ky at site U1388) and Doñana basins, where the highest sedimentation

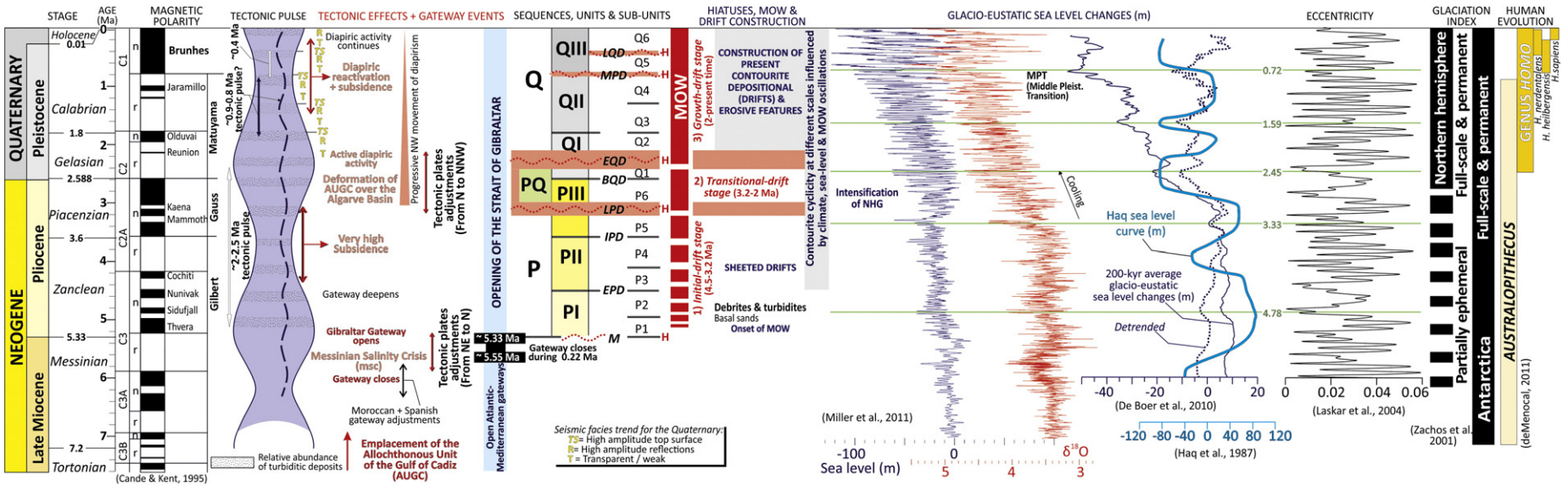

Fig. 16. Neogene and Quaternary CDS evolution in the Gulf of Cadiz and off west Portugal. Hiatuses, sequences, units and sub-units and the main stages of the contourite depositional systems are integrated with main tectonic and sedimentary pulses. Tectonic pulsing arises from changes in the interaction between the African and European tectonic plates. Glacio-eustatic sea-level changes, eccentricity cycles and major climatic and human evolution steeps are also included. See text for further details. Data from Cande and Kent, 1995 and De Boer et al., 2010.

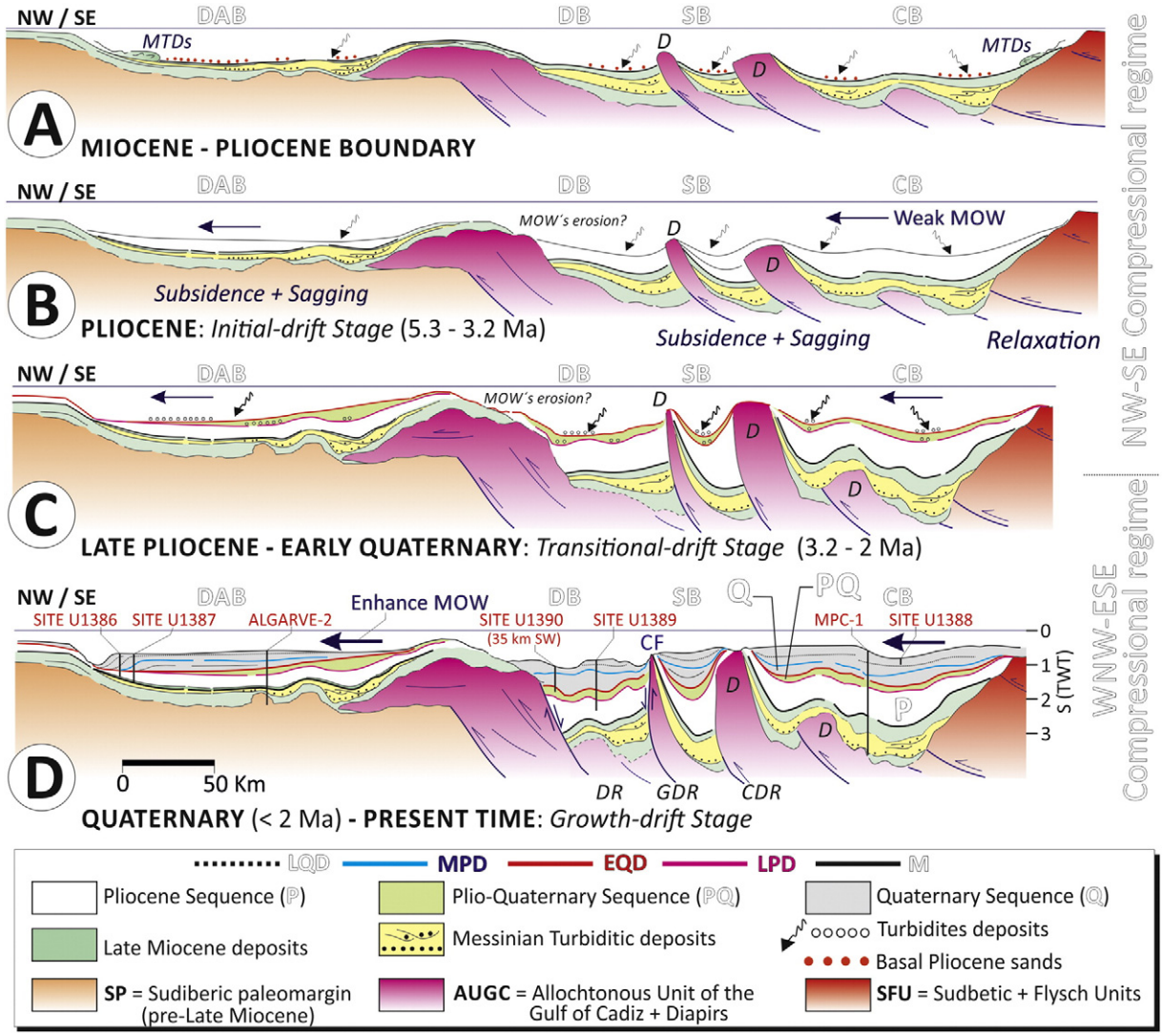

Fig. 17. Simplified evolutionary cartoons (not at scale) for the sedimentary evolution since the late Miocene to the present time of Neogene basins in the Gulf of Cadiz. After a compressional period associated with the late Miocene and early Pliocene (<4.5 Ma), two major compressional events affecting to the Neogene basins at 3.2–3 Ma and 2–2.3 Ma help constrain the three main stages of CDS evolution. The stages include: 1) the initial-drift stage (5.33–3.2 Ma) with a weak MOW, 2) a transitional-drift stage (3.2–2 Ma) and 3) a growth-drift stage (2 Ma-present time) with enhanced MOW circulation into the Atlantic and associated contourite development due to greater bottom-current velocity. See text for further details and discussion. Abbreviations for discontinuities are in Fig. 6. CF, Cadiz Fault; D, Diapirs. Legend for the sedimentary basins: DAB = Deep Algarve basin; CB = Cadiz basin; DB = Doñana basin; SB = Sanlucar basin.

rates were observed (>100 cm/ky at site U1390). Sheeted drifts in the Doñana basin are highly deformed due to tectonic activity.

Internal discontinuities within QIII allow identification of two internal subunits (Q5 and Q6). These are bounded by the late Quaternary Discontinuity (LQD) discontinuity, locally identified as a short hiatus around 0.3–0.6 Ma in the Doñana basin (site U1390). A coarse layer is observed in association with the LQD in the Doñana basin, as is a shift from very poorly sorted below, to poorly sorted sediment above the discontinuity. The LQD correlates with the H5 discontinuity reported by Roque et al. (2012) and with the ID12 and D3 horizons identified by Llave et al. (2001, 2007a, 2011) and Marchès et al. (2010) (Table 1), respectively.

Sedimentary facies for QIII vary depending of the basin, with contourites as the dominant deposits, occurring as bi-gradational sequences, but also as top- and/or base-cut-out sequences (Fig. S2). Cadiz basin sediment from site U1388 shows sand, silty sand and silty muds as the principle lithologies from this horizon. Core material also includes numerous beds of calcareous sand and sand with biogenic carbonate (Fig. S2-R) reaching thicknesses of up to several meters. This subunit also includes many intervals of mud with biogenic carbonate that exceed thicknesses of 15 m. In the Doñana basin, sedimentary facies consist primarily of calcareous mud, but also include silty mud, sandy mud, and silty sand with biogenic carbonate. In the Alentejo basin, sandy contourites and alternating reddish/brownish and greenish gray/greenish calcareous mud make up QIII. Subunits Q5 and Q6 exhibit sequences of seismic facies similar to those of Q3 and Q4, wherein weak to transparent acoustic facies transition upwards into high-reflectivity facies truncated by an erosional surface (Figs. 6–8 and 12–14). Drilling data from the Deep Algarve basin indicate that the weak to transparent seismic facies represent a mud dominated contourite succession that includes a higher proportion of nannofossil muds and calcareous silty muds. The greater reflectivity of overlying facies corresponds to increasing grain size and detrital content and to decreasing proportions of biogenic carbonate.

5.5.4. Quaternary Cyclostratigraphic analysis

A well-developed cyclostratigraphic pattern on normalized HSGR logs time-series is recognized in sites U1386 and U1387

(Figs. 9 and 15), showing high-significant cycles (higher than 99% CL) at different frequencies and periods. In general both sites show similar, common peaks, located in the following four frequency bands (Fig. 15):

a) At the higher frequency band, two main peaks at 24.5 ky and 22 ky are registered in site U1387C that could be correlated with that at 23 ky in site U1386C (Fig. 15B).
b) At the middle frequency band, a common cycle at 44 ky is observed, as well as one at 55 ky in site U1386C (15A).
c) At the middle-lower frequency band, two main peaks at 85 ky and 105 ky were registered at site U1386C that could be correlated with that at 96 ky in site U1387C (Fig. 15A).
d) At the lower frequency band several peaks from 0.4 Ma to 2 Ma are observed at both sites. The significant peak at 0.8 Ma is only registered in site U1387 (Fig. 15C).

Detailed analysis of this cyclostragraphic results for site U1386 reveal slight differences in compared to site U1387 in all but the higher frequency bands. The Site U1386 records a reduced Quaternary sedimentary record since sub-unit Q3 pinches out close to the site and its younger record above the discontinuity MPD is affected by sinsedimentary faults (Fig. 15D).

5.6. Tectonic considerations

The late Miocene, Pliocene and Quaternary sediments are deformed by folding and faulting. Chronostratigraphic constraints presented in this work suggest asynchronous timing for such deformation events. At a local scale they are related mainly to 1) emplacement of the AUGC in the Gulf of Cadiz and Deep Algarve, 2) fault-activity, some of them bounding structural highs, 3) salt flowage. In fact, local deformation is evident from folding and faulting of late Miocene to Quaternary sedimentary cover overlying diapirs and structural highs. The structural grain of some of these features indicates continuous deformation up to present.

Late Miocene and Pliocene sediments overlying the AUGC are folded, in some cases slightly due to blind-thrust. These sediments are locally offset by the reactivation of the some AUGC imbricated thrust-faults (Fig. 4). Uplift of structural highs, such as the case of the Guadalquivir Bank, has also deformed the overlying sedimentary cover (Fig. 4). Basins covering the AUGC and Deep Algarve basin are faulted, primarily by NE and NW trending normal faults (Figs. 4, 6–8 and 12–13). Normal faults affecting the Alentejo basin trend primarily in a N–S direction (Fig. 14), cutting through the Pliocene and Quaternary. In this basin the sediments overlying LQD are underformed.

Salt flowage seems to be one of the main mechanisms leading to folding and faulting of the late Miocene through Quaternary in Deep Algarve, Doñana, Cadiz and Sanlucar basins. Inverted reactivated salt diapirs are found in the Algarve basin nearby the Diego Cão Channel (Fig. 6), probably induced either by regional shortening or local reactivation of a pre-existent normal fault of Mesozoic rifting phases. In the same basin, the presence of deeper salt domes is inferred from folded sediments, defining an asymmetrical anticline topped by EQD and a symmetrical one topped by MPD. Synkinematic sediments (seismic units P1–P5 and Q1) are thicker on the flanks than on the top of the salt dome indicating the upward movement of the salt. The associated rim syncline constituted a major local depocenter, and is generally thicker in the SE sector. Sediment folding has been attenuated since the deposition of unit Q2. In the Doñana Basin, sediments from Pliocene through Late Quaternary have been folded into symmetrical anticlines and synclines (Fig. 12). These structures are probably residual highs related to interdomal evolution occurring well below the Pliocene–Quaternary sequence, as there is no significant thickness variation of the seismic units. Contourite channels, such as the Huelva channel, have developed along the axis of the rim synclines. Diapiric ridge crests have been truncated by LQD, which marks the end of the folding phase, since younger sediments seem to be undeformed (Fig. 12). However, other NE–SW diapiric ridges are outcropping in the Doñana Basin, Sanlucar Basin and Cadiz Basin, such as the Guadalquivir and Cadiz Diapiric Ridges, suggesting a recent activity formed these structures. The upward salt flowage in the Doñana diapiric ridge occurred mainly between LPD and MPD. This induced compensatory subsidence and created rim synclines bounding the diapir, which acted as major depocenters during this phase (Fig. 4). Rising-up of salt in the Doñana diapiric ridge seems to have stopped, or at least decreased, during late Quaternary as marked by LQD (Fig. 12).

Two kinds of normal faults have been identified in close relation to diapiric domes and ridges: stretch faults and growth faults. In the Algarve basin the apex of salt diapirsm has been extended by stretching faults, which affected the entire Pliocene and Quaternary sedimentary column, and almost reached the seafloor. Several stretch faults developed in the apex of the Doñana diapiric ridge (Fig. 13) cutting through Pliocene and Quaternary sediments, although showing insignificant offsets. These extensional structures can be created by local stresses in the apex of diapirs due to salt flowage, independently of the regional tectonic regime. Some of these faults reached the seafloor and formed stair-step scarps (Fig. 13). The majority of stretch faults seem to be contemporaneous to diapir growth and sedimentation (e.g. Figs. 4 and 6) but some show evidences of posterior activity, cutting through undeformed sediments (e.g. Fig. 13). In the Cadiz basin, Quaternary sediments are locally affected by growth-faults, probably related to lateral salt flowage in a reactivated diapir (Fig. 8). Some of these faults are still active offsetting the present-day seafloor (Fig. 8). Growth-fault reactivation is recorded by EQD, with movement occurring largely until LQD and decreasing through present. Several episodes of fault movement created accommodation space in the SSW block, allowing the development of thicker Quaternary units.

Deformation of the early to late Pliocene (P) sequence varies in different basins. Basins covering the AUGC primarily exhibit folding, due to the diapiric structures and uplift of highs (Figs. 12, 13 and 14).

Two deformation events related to the LPD and EQD also affected the late Pliocene to early Quaternary sequence (PQ), mainly resulting in diapir growth and fault reactivation. Deformation appears as frequent faults and as reactivation of previous faults (evident from offset trends) and folds. Folded structures however are broader than those affecting early Pliocene sediments (Figs. 4, 6–8 and 12–14).

The Quaternary sequence (Q) is also locally deformed, particularly in areas adjacent to structural highs and diapirs. These areas show folds, faults and features indicating reactivation of blind-thrusts (Figs. 4, 6–8 and 12–14). The major, active regional scale faults operating in the Gulf of Càdiz are the WNW–ESE SWIM faults, which apply dextral strike-slip or normal deformation to the seafloor, as well as their conjugates NE–SW structures. The Doñana basin records more intensive deformation of sediments deposited after the middle Pleistocene.

6. Discussion

6.1. The Miocene–Pliocene boundary

The Miocene–Pliocene boundary (M discontinuity) represents a major stratigraphic surface within the Neogene basins along the SIM, but one whose expression varies laterally. Nelson et al. (1993) and Maldonado et al. (1999) described its basin-scale characteristics in basins covering the AUGC from single and multi-channel seismic profiles. In basins covering the AUGC, and in particular the Cadiz basin, this boundary forms a noticeable truncation surface clearly evident in seismic profile (Fig. 4). Along the flanks of the basement highs and diapirs it is very clear, but it become less obvious in central areas. Onshore (outcrop) expressions of this part of the basin show unconformable deposition of Pliocene sediments over late Miocene and AUGC sediments (IGME, 1990, 1994; Aguirre et al., 2010). The Fuente del Gallo north section (Cadiz, Spain; Figs. 3 and S3), provides a good example of this,

wherein early Pliocene sands unconformably overly upper Miocene (Messinian) marls (Aguirre et al., 2010). Our analysis of marls below the unconformity identified abundant *Globorotalia menardii* form 4. The last common occurrence of this foram species was recorded in North Atlantic (Sierro et al., 1993) and Mediterranean sediments during the late Tortonian age (7.51 Ma; Hilgen et al., 1995). Other Tortonian species such as *Globorotalia suterae* are also present in marls beneath the unconformity. Horizons above the unconformity (Fig. S3) contain *Globorotalia margaritae* but not *Globorotalia puncticulata*. Because the first occurrence of *G. puncticulata* has been astrochronologically dated at 4.52 Myr (Lourens et al., 2004), we interpret these horizons to be early Pliocene in age, specifically dating between 5.33 (base of the Pliocene) and 4.52 Ma. However, a latest Messinian age cannot be entirely ruled out since *G. margaritae* was common at that time. The Miocene–Pliocene boundary is thus marked by a hiatus and lithological shift. Furthermore, Messinian deposits are all but absent from the section. A coeval lithological shift appears at the Miocene–Pliocene boundary in sediments from the Gulf of Cadiz continental shelf, where channel-filled turbidites are replaced by hemipelagites (Sierro et al., 2000, 2008). More inland, in the Guadalquivir basin the Miocene Pliocene boundary is identified by a pronounced reflector that separates Messinian seismic units with dominant northward progradation from Pliocene ones in a southward direction (Ledesma, 2000). The Miocene–Pliocene boundary is a conformable surface in the central part of the Deep Algarve basin at site U1387, only marked by local erosional along the axis of the basin and along its margins. The contact between the Cacela (marine) and Ludo (mainly fluvial) formations marks the approximate area of the Miocene–Pliocene boundary in Algarve basin outcrop (onshore). Moura and Boski (1999) and CachÃo and da Silva (2000) interpreted a hiatus of 2.5 Ma and found the Messinian section absent from this part of the study area. The Miocene–Pliocene boundary has not yet been identified in the Alentejo basin, where the middle Miocene–Quaternary section consists of one big unit (C3) (Alves et al., 2009; Pereira et al., 2011; Pereira and Alves, 2013). In many areas of the Mediterranean continental margins, the Miocene–Pliocene boundary appears as a prominent erosive surface referred to as the 'M reflector' (Hsü et al., 1973; Ryan et al., 1973; Lofi et al., 2011). It is typically interpreted to represent penetrative desiccation and erosion during the Messinian salinity crisis (5.6–5.5 Ma) and the subsequent Zanclean flooding event (5.33 Ma) (e.g., Bache et al., 2009; Garcia-Castellanos et al., 2009; Estrada et al., 2011; Roveri et al., 2014; Flecker et al., 2015).

Above the Miocene–Pliocene boundary, fine sand deposits are found in units PI and PII. Onshore outcrops, adjacent to the Cadiz Basin, host extensive deposits of similar sands (e.g., see Fig. S3), which also appear regionally in the Neogene Guadalquivir foreland basin where they are described as glauconite and Huelva sands (Sierro et al., 1991, 1996; Gonzalez-Delgado et al., 2013), as well as in the basins covering the AUGC (IGME, 1990, 1994).

Several authors have interpreted the local erosional character of the Miocene–Pliocene boundary along the SIM as resulting from Messinian sea-level fall at about 5.5 Ma (Riaza and Martinez del Olmo, 1996; Nelson et al., 1993; Maldonado et al., 1999; Hernández-Molina et al., 2002). Hoddel et al. (2001) however demonstrated that sea-level began to rise below this boundary, and argued that the section lacked evidence of any other glacio-eustatic fall associated with the Miocene–Pliocene boundary. Sierro et al. (2008) and Flecker et al. (2015) found little evidence of major sea-level variations. These authors therefore proposed tectonic activity as a driving factor in boundary-related depositional changes. Results presented here support this hypothesis, as they describe compressional deformation of the AUGC and areas near the Strait of Gibraltar up until 4.5 Ma.

6.2. Sedimentary stacking pattern

The Pliocene to Quaternary sedimentary record in the Neogene basins shows a clear hierarchy of sedimentary units. Major sequences PI–PII and QI–QIII units consist of P1–P6 and Q1–Q6 subunits, respectively. These subunits represent sedimentary cycles at different scales that are bounded by major and minor discontinuities. Seismic profiles show that the sedimentary thicknesses of Pliocene units and subunits are less than those of Quaternary units and subunits (Figs. 6–8 and 12–14). Shifts in sedimentary thickness coincide with major increases in sedimentation rates occurring above the early Quaternary discontinuity (EQD) at 2–2.4 Ma. A more pronounced change in sedimentary thickness occurred both above and below the Mid Pleistocene Discontinuity (MPD, Figs. 6–8 and 12–14). The estimated stratigraphic ages of around 0.8–0.9 Ma and 0.4–0.5 Ma for the subunits agrees well with cycles identified in the spectral analysis of HSGR logs (Fig. 15).

Cyclostratigraphic analysis of sites U1386 and U1387 evidences the incidence of an orbital control in the range of the Milankovitch temporal cycles (Berger, 1977, 1978; Berger et al., 1989). Thus, registered cycles at 22 ky, 23 ky and 24.5 ky can be assigned to precession, those at 44 ky and 55 ky to the obliquity signal, while cycles of 85 ky, 96 ky, and 105 ky fit well with the short-term eccentricity. These data confirm the forcing of precession and eccentricity on deposition after the discontinuity MPD (as previously reported by Llave et al., 2001, 2007a and Hernández-Molina et al., 2002, 2006), and probably a comparatively minor incidence of the obliquity-induced cyclicity (Lofi et al., 2015).

In respect to the lower frequency band, that constitutes those cycles with a periodicity higher than that of the short-term eccentricity cycle (>100 ky), and orbital influence can be also envisaged. The common cycle at similar periods of 406 ky and 420 ky, can be clearly correlated with the well-known long-term eccentricity cycle of approximately 0.4 Ma (Berger, 1977, 1978). These cycles show a high stability and have been used as a basic calibration period for cyclostratigraphy (Laskar et al., 2004, 2011; Hinnov and Hilgen, 2012). The peaks recognized around 2 Ma (Fig. 15C), could be tentatively correlated with the approximately 2.4 Ma eccentricity term. Modulation of the 0.4 Ma components of the eccentricity shows actually a dominant component at a period of around 2.4 Ma related with Earth–Mars secular resonance (Laskar et al., 2004, 2011; Hinnov, 2000; Hinnov and Hilgen, 2012). This cycle has been also frequently identified in the geological record as a long-term cycle, from the Triassic, with periods of around 1.6 to 2 Ma (see Boulila et al., 2012 and Ikeda and Tada, 2013 for recent reviews). However, differences in the periodicities corresponding to the modulated eccentricity at around 2.4 My, and those here registered at around 1.7 Ma and 2.0 Ma could reveal the incidence of different driving processes that induce new signals or distort the 2.4 Ma orbital one. The cycle at around 0.8 Ma registered in site U1387C has been related to a possible non linear combination of other periods or a double mode of the eccentricity period (Ripepe and Fischer, 1991; Kashiwaya et al., 1998). The absence of these cycles at site U1386 could be associated to local conditions disturbing its record (for example faulting, Fig. 6), although other global signals at higher (0.4 Ma) and lower (2 Ma) frequencies have been recognized.

These lower frequency cycles correspond with 3rd- and 4th-order asymmetric sequences identified in middle and high-resolution seismic profiles by Llave et al. (2001, 2007a) and Hernández-Molina et al. (2002, 2006). Sedimentary cycles can be identified regionally at seismic scale in all the Neogene basins. The Quaternary sequence shows the cycles more clearly than the Pliocene sequence, however. The cyclicity is evident as a consistent facies trend within each subunit that includes (a) a transparent zone at the base, (b) smooth, parallel reflectors of moderate-to-high amplitude in the upper section and (c) a continuous, high amplitude, erosive surface at the top (Fig. 6, 7 and 15D). This facies trend has previously been documented within the Faro-Albufeira Drift (Llave et al., 2001, 2006; Stow et al., 2002b), the Porcupine Drift (Van Rooij et al., 2003) and the Eirik Drift (Hunter et al., 2007). According to IODP Exp. 399 sampling, weak seismic facies at the unit scale (~0.8–0.9 Ma) correspond to mud dominated sediments. The higher reflectivity facies above correspond to an increase in grain size and detrital content, and a decrease in biogenic carbonate. Most of the sandy

turbidites deposits during the Quaternary are coincident with the upper reflective part in each sequence, but also with a higher number of coarser (sandy) contourites (Fig. 15D). Preliminary results from IODP Exp. 399 identify turbiditic deposits having similar periodicities (Stow et al., 2013b) in the upper and higher reflectivity part of the unit (Figs. 6 and 7). Whyte and Lovell (1997) described similar turbidite deposition cycles in North Sea deposits. Future works with higher resolution should clarify this interesting interrelation between along- and across sedimentary processes and products at these scales.

6.3. The significance of hiatuses

Regionally extensive erosional discontinuities are often used to identify contourites (Faugères et al., 1999; Rebesco et al., 2014). This is the case along the SIM, where discontinuities evident in seismic profiles as high amplitude reflections represent key, basin-scale stratigraphic horizons and important transitions in sedimentary staking patterns (Table 1 and Figs. 4, 6–8 and 12–14). The M, LPD and EQD in particular mark angular erosional unconformities along basin margins and areas surrounding highs and diapirs. Discontinuities grade laterally into conformable contacts towards the basin central areas. This demonstrates that the thickness eroded increases towards highs implicating uplift as a mechanism for erosion. In cases of more pronounced hiatuses, uplift appears to occur coeval to enhanced bottom current velocity. The association of hiatuses, discontinuities, correlative conformities and changes in sedimentation rate represents a major finding of IODP Exp. 339 (Stow et al., 2013b; Hernández-Molina et al., 2014b; Lofi et al., 2015). The two most significant discontinuities in the sedimentary record after the Miocene–Pliocene boundary (M), are associated with LPD (3–3.2 Ma) and EQD (2–2.4 Ma) (Figs. 4, 6–8 and 12–14).

The late Pliocene hiatus, around 3–3.2 Ma (LPD), suggest a compressional tectonic event along the SIM. This coincides with an intra-Pliocene unconformity previously recognized in onshore outcrop of the Betic–Rif Cordillera (Montenat et al., 1990; Aguirre et al., 1995; Azdimousa et al., 2006), including sections between El Puntalejo and Cabo Roche adjacent to the Cadiz Basin (Cadiz, Spain; Fig. S4). The unconformity appears in this area between marine sands (Unit I) and the littoral Unit III, as defined by Aguirre (1991, 1992, 1995) and Aguirre et al. (1993, 1995, 2010). Our analysis showed that just beneath the unconformity, yellow sand deposits are found containing *G. puncticulata* and with *G. margaritae*, which constrains the sediment to a 3.81–4.52 Ma age range, based on the latest occurrence of *G. margaritae*, as astronomically dated by Lourens et al. (2004). The unconformity could thus correlate with a late Pliocene discontinuity, as has been proposed by Aguirre et al. (1995, 2010). The hiatus is coeval with tectonic activity in the Betic Cordillera (Montenat et al., 1990), but also with thrusting of the allochtonous unit on top of the Moroccan Meseta (Flinch and Vail, 1998), and the most intensive phase of AUGC emplacement in the Algarve basin (Hernández-Molina et al., 2014b). These events could also occur synchronously with uplift of the Serra do Caldeirão in the Algarve basin (Dias and Cabral, 1997, 2000).

For the early Quaternary, the EQD prominently marks a hiatus representing a major shift in sedimentation between 2 and 2.4 Ma (Figs. 6–8 and 12–14), and the probable onset of a new compressional event. This hiatus appears in the Cadiz basin (Hernández-Molina et al., 2014a), and may correlate with the extensive erosional surface observed in adjacent onshore outcrops (Fig. S4). The onshore unconformity is overlain by extensive continental facies deposits (Zazo et al., 1985; IGME, 1990, 1994; Aguirre, 1991, 1992, 1995; Aguirre et al., 1993, 1995, 2010), and shows the end of sediment supply from any Guadalquivir river branch (Zazo et al., 1985; Aguirre, 1995) towards the Cadiz basin. The EQD also coincides with hiatuses observed in the northeast Atlantic between Gibraltar and equatorial areas. These form coevally with slump facies indicative of tectonic instabilities (Stein et al., 1986). In areas that experienced higher erosion, the EQD incised the entire late Pliocene section and base of the Quaternary. The only hiatus longer than the EQD in these regions is the interval spanning about 1.4 Ma, incising sediment from 3.4 to 2 Ma in the Deep Algarve basin sections sampled at sites U1386 and U1387. A similar hiatus appears in the Alboran Sea section (Comas et al., 1996; Martínez-García et al., 2013).

Two other younger and minor discontinuities within the Quaternary record (Figs. 6–8 and 12–14) represent key stratigraphic horizons recording erosion and possible renewed tectonic activity at around 0.7–0.9 Ma for MPD (MIS 19-17) (Lofi et al., 2015) and between 0.3–0.6 Ma (MIS 11 and 13) for the LQD. Borehole log data record the MPD as a short hiatus within the Doñana basin that also affected the sedimentation rate at site U1391 (Lofi et al., 2015). A similar hiatus, coeval with tectonic activity occurs in sediments of the northeast Atlantic (Stein et al., 1986). The LQD corresponds to a hiatus in sediment from sites U1390 and U1391 (Lofi et al., 2015), and with a condensed interval in sediment from site U1385 (Hodell et al., 2015).

The aforementioned hiatuses coincide with sedimentary and paleoceanographic changes and regional tectonic activity. Conceptual depositional models for foreland basins (e.g., DeCelles and Giles, 1996; Einsele, 2000; Nichols, 2009) suggest that turbidites develop during initial stages after the thrusting. Messinian turbidites forming after the Tortonian emplacement of the AUGU likely reflect this phase of development (Riaza and Martinez del Olmo, 1996; Sierro et al., 1996; Ledesma, 2000). Hiatuses associated with turbidites demonstrate that similar sequences of events apparently occurred in the early Pliocene, late Pliocene and early Quaternary. These sedimentary features also indicate minor pulses of westward compression recorded in deformed wedges of the AUGC.

6.4. Evolutionary model and paleoceanographic implications

Neogene basins along the SIM record the complex interplay of tectonics, climate, sea-level and bottom current circulation from the latest Miocene to present-day. Around 50 km of convergence occurred in a NW direction between the Eurasian and African plates in the vicinity of the Alboran Sea and Gulf of Cadiz during this period (Dewey et al., 1989).

Neogene basin initiation began at the end of the early Miocene, as a consequence of downward flexure of pre-existing basement in response to loading of thrusted and imbricated overburden of Betic and Rif orogen (Sierro et al., 1996, 2008; Berástegui et al., 1998; Fernàndez et al., 1998; Maldonado et al., 1999; Ledesma, 2000; Roque, 2007; Terrinha et al., 2009; Vergés and Fernàndez, 2012). Tectonic inversion of Mesozoic extensional structures occurred simultaneously in the Deep Algarve and Alentejo basins (Terrinha et al., 2002; Roque, 2007). During the Tortonian, the regional compressional regime shifted towards a NW–SE direction, which remobilized the primarily westward emplacement of the AUGC (Maldonado et al., 1999; Medialdea et al., 2004; Sierro et al., 2008). Around the Tortonian–Messinian boundary (~7.2 Ma), regional tectonic activity caused narrowing of the Betic gateways (Fig. 16) between the Atlantic and Mediterranean (Sierro et al., 2008) and extensive turbidite deposition within Neogene basins (Riaza and Martinez del Olmo, 1996; Ledesma, 2000). Subsequent tectonic uplift in the Guadalquivir basin and Gibraltar area triggered the final closure of the Rifian and Iberian gateways (~6 Ma), isolation of the Mediterranean Sea and onset of the Messinian Salinity Crisis at 5.55 Ma (Hsü et al., 1973). This was a short-lived event that ended with opening of the Strait of Gibraltar at about 5.33 Ma (Duggen et al., 2003; Roveri et al., 2014; Flecker et al., 2015).

These events preceding Pliocene and Quaternary deposition conditioned the asymmetric shape of basins overlying the AUGC to an eastward deepening geometry. The results described here suggest this phase of tectonic activity was associated with the Miocene–Pliocene boundary and ended by 4.5 Ma. Younger Pliocene and Quaternary compressional events between 3.2–3 Ma and 2–2.3 Ma further pinpoint

three stages of subsequent development and evolution of the contorite depositional systems (Figs. 16 and 17).

I. *Initial-drift stage* (Pliocene, from 5.3–3.2 Ma);

This stage began at the end of the compressional period associated with the late Miocene and early Pliocene. In the Deep Algarve basin, sandier deposits at the base of the Pliocene formed first, and were immediately followed by extensive mass transport deposits (MTDs). These included sands, sandstones, debrites and slumps. Based on sedimentologic and petrofacies analysis, the sandstones are categorized as turbidites and debrites. Like other MTDs, these derive primarily from the adjacent shelf and upper slope (Ducassou et al., 2016), which contributed quartz, lithics and carbonates. MTDs suggest resedimented facies and margin instability until 4.5 Ma (Fig. 16). These deposits are coeval with early Pliocene debrites (>4.5 Ma) that outcrop in areas adjacent to the Cadiz basin (Fig. S3), and with gravitational collapse breccias described from the Strait of Gibraltar by Esteras et al. (2000) and Blanc (2002). Thrusting and westward compression of the frontal areas of deformed AUGC wedges compressed the basin during late Miocene and created several isolated basins (Cadiz, Sanlucar and Doñana). Regional depocenters migrated westward, and underwent subsidence, sagging and diapiric processes, as evidenced by morphological highs and diapiric ridges parallel to thrust structures. Fragmentation of Miocene basins into minor complex basins was by this point likely sufficient for development of piggyback basins (Figs. 16 and 17).

These events coincided with a major sea-level highstand (Haq et al., 1987; Raymo et al., 2011; Miller et al., 2011), evident from early Pliocene marine deposition in onshore localities (IGME, 1990, 1994; Sierro et al., 1996; Salvany et al., 2011). These events generated pronounced angular unconformities and a major hiatus between late Miocene and early Pliocene deposition near the Strait of Gibraltar (Figs. 4 and S3). This truncation may document folding and uplift due to the westward thrusting of Subbetic and Flysch units. Uplift occurred onshore, adjacent to the Algarve basin CachÃo and da Silva (2000), probably due to the regional forebulge position during this time. These events, along with widespread tectonic activity, compression and slope instability relate to late Miocene tectonic uplift in the Guadalquivir basin and Strait of Gibraltar area, the final closure of the Rifian and Betic gateways at 5.96 Ma, the Messinian Salinity crisis (MSC) (Duggen et al., 2003; CIESM, 2008; Flecker et al., 2015), and ultimately, the opening of the Strait of Gibraltar (Maldonado et al., 1999; Estrada et al., 2011), which caused the Zanclean flooding (Garcia-Castellanos et al., 2009; Estrada et al., 2011). Similar compressional stages have been determined in the Alboran Sea (Martínez-García et al., 2013) and other areas of the Mediterranean (Cloetingh et al., 1990). These events are attributed to a major reorganizational phase of the Africa-Eurasia plate boundary. During this time, compression shifted from NE to N (Duggen et al., 2003; Sierro et al., 2008), the Betic–Rif Cordillera basins experienced differential subsidence and the Gibraltar area was uplifted (Sierro et al., 2008).

These compressional events (>4.5 Ma) were followed by a period of relaxation, initiated by the elastic response to thrust loading. This period of sagging and high subsidence rates coincided with local extensional collapse affecting the AUGC (Maldonado et al., 1999; Medialdea et al., 2004, 2009), which likely deepened the Strait of Gibraltar.

The opening of the Strait of Gibraltar had major paleoceanographic implications. Bottom current indicators however show little evidence of this event. Indicators also suggest that MOW intensity was relatively weak during this time (Stow et al., 2013b; Hernández-Molina et al., 2014b, Van der Schee et al., 2015). The MOW strengthened progressively after 4.5 Ma as indicated by the development of the large, muddy sheeted drifts in the Neogene basins recorded during PI, PII and the lower part of PIII units. Periodic turbidites are observed in these early Pliocene horizons (Roque et al., 2012; Brackenridge et al., 2013; Stow et al., 2013b). As the MOW developed into a source of intermediate water for the North Atlantic, its warm, saline outflow enhanced both the production of NADW and northward ocean heat transport in the Atlantic (Hay, 1996). Evidence for enhanced bottom current circulation in the early Pliocene (about 4.5 Ma) appears along the Porcupine margin (Van Rooij et al., 2003), north Atlantic (Hunter et al., 2007), continental margins of NW Europe (Laberg et al., 2005, Praeg et al., 2005; Stoker et al., 2005), Faeroe-Shetland Channel (Knutz and Cartwright, 2003) and south of the Greenland-Scotland Ridge (Wold, 1994). Evidence for enhanced MOW also occurs above the intra-Pliocene discontinuity (IPD) according to paleoceanographic proxies in the North Atlantic (Khélifi et al., 2011, 2014).

II. *Transitional-drift stage* (late Pliocene to early Quaternary, 3.2–2 Ma).

This stage documents the most important changes in the sedimentary stacking pattern and development of Neogene basins development, about 2.5 Ma after late Miocene to early Pliocene events. The upper part of unit PIII (P6) and lower part of unit QI (Q1) consist of interbedded contourites and turbidites, with occasional debrites. Synsedimentary deformation, active halokinesis, lower subsidence rates, thrusting and folding occurred during a widespread phase of shortening affecting all basins. This phase began around the LPD (3–3.2 Ma) but ended with the EQD (2–2.4 Ma Ma) (Figs. 16 and 17). Hiatuses are accompanied by dolostones, debrite and more downslope sedimentation. Previous research has also detected the decrease in subsidence rates in the Gulf of Cadiz (Nelson et al., 1993; Maldonado et al., 1999; Maestro et al., 2003; Medialdea et al., 2004; Roque et al., 2012) and other areas of the North Atlantic (Cloetingh et al., 1990; Praeg et al., 2005; Stoker et al., 2005). Signs of continental deposition appear at the end of this stage, with the Guadalquivir basin (Salvany et al., 2011) and basins covering onshore AUGC units (Zazo et al., 1985; IGME, 1990, 1994; Aguirre et al., 1995, 2010), finalizing the separation of early Pliocene onshore units from Quaternary offshore marine basins. These events coincided with regional compression and deformation related to a directional change in the Iberia and Nubia convergent boundary from NW–SE to WNW–ESE (Zitellini et al., 2009; Duarte et al., 2013). The shift in convergence direction for the southwest Iberian margin coincided with a decline in westward migration and thrusting activity for the AUGC. Reactivated blind-thrusts accommodated shortening and thus exhibit only minor sedimentary subsidence (Gutscher et al., 2002). The oblique convergence between the sub-plates generated a new transpressional regime and reactivated WNW–ESE dextral strike-slip faults as well as shallower W–NW directed thrusts (Duarte et al., 2011). Evidence for compressional events around this age has been detected in the Betic (Viguier, 1974; Benkhelil, 1976), Rif (Guillemin and Houzay, 1982; Morel, 1988; Aït, 1991; Azdimousa, 1991), Alboran Sea (Bourgois et al., 1992; Martínez-García et al., 2013), easternmost Mediterranean (Cyprus) (Robertson et al., 1998; Kinnaird, 2008), Himalaya (Derbyshire, 1996), other areas of the Northern Hemisphere (Cloetingh et al., 1990) and offshore Central America (Vannucchi et al., 2013). These events are associated with global plate tectonic reorganization and final closure of the Central American Seaway, which led to the establishment of Northern Hemisphere glaciations and a shift to a globally cooler climate conditions (Zachos et al., 2001; Miller et al., 2011) coeval with the emergence of the genus *Homo* between 2.8–2.4 Ma (deMenocal, 2011; Villmoare et al., 2015) (Fig. 16).

The MOW progressively strengthened from 3.2 to 2 Ma (Fig. 16), in tandem with enhanced deep-water convection in the Mediterranean Sea and with more active circulation in the North Atlantic (Khélifi et al., 2011, 2014). The MOW intensification contributed with saltwater to intermediate depths of northerly latitude Atlantic Waters, thus enhancing Thermohaline Circulation (THC), Atlantic Meridional Overturning Circulation (AMOC) and overall Northern Hemisphere deep-water formation (Hernández-Molina et al., 2014a). These changes coincided with long-term global cooling trends (Zachos et al., 2001) marked by the final NHG intensification (Bartoli et al., 2005). The shift

included a decline in atmospheric CO_2 levels, global cooling (Zachos et al., 2001) and sea-level fall (Miller et al., 2011). The 41 ky obliquity cycles replace the 23 ky precessional cycles as the primary orbital mechanism influencing climate. This shift is also associated with a progressive increase in the amplitude of Earth's orbital obliquity (Bartoli et al., 2005).

III. *Growth-drift stage* (Quaternary, from 2 Ma to present).

Over the last 2 Ma, the Quaternary section (upper part of unit QI and units II and III) exhibited major depositional changes with maximal sedimentation rates and a pronounced phase of contourite deposition and drift development throughout the Neogene basins. Interestingly, most of the North Atlantic contourite drifts show decreasing accumulation rates at this time (Knutz, 2008). Quaternary depocenters are located west of underlying sequences due to the displacement of preceding compressional stages. High sedimentation rates could arise from the combination of more vigorous bottom-current influence and substantially higher volumes of MOW input into the Atlantic, as well as from greater transport to offshore depocenters, due to the progradation of Guadalquivir and Rharb basin sediments into the Gulf of Cadiz (Sierro et al., 1991; Flinch and Vail, 1998; Riaza and Martinez del Olmo, 1996; Ledesma, 2000; Salvany et al., 2011).

Two phases of MOW and bottom current intensification (Fig. 16) led to the fully established MOW. We attribute its formation to tectonic constriction and deformation in the basins related to the mid Pleistocene discontinuity (MPD, 0.7–0.9 Ma, MIS 19-17) and LQD (~0.4 Ma, between MIS 11 and 13). These events are especially evident in the Doñana basin, which experienced more deformation and the highest sedimentation rate observed from the MPD up to the present. The MPD represents the beginning of a new phase in the sedimentary stacking pattern of drifts, with enhanced upslope progradation and mounded drift morphologies (Llave et al., 2001, 2007a; Roque et al., 2012). Lateral migration of sandier deposits and of morphological features from proximal to central areas of the CDS co-occurred with MOW enhancement. Together these events coincide with a significant eustatic drop in sea-level (Miller et al., 2005; Rogerson et al., 2012), and intensification of the AMOC (Knutz, 2008). MOW density increased during subsequent glacial stages, as it did during the last glaciation when slope morphologies indicate that MOW flow rates were higher (Rogerson et al., 2012; Hernández-Molina et al., 2014a). The period between 0.9–0.7 Ma, coeval with the MPD, marked another important step in human evolution as pre-human primates disappeared (Fig. 16) and *Homo heielbergensis*, the ancestor of modern humans, emerged (deMenocal, 2011).

6.5. Conceptual implications

6.5.1. Drift construction

Contourite drift types are classified according to their external morphology (McCave and Tucholke, 1986; Faugères et al., 1999; Rebesco and Stow, 2001; Stow et al., 2002b; Nielsen et al., 2008; Rebesco et al., 2014). The three aforementioned evolutionary stages for the CDS imply the following phases of drifts. First, mixed drifts formed during the initial-drift stage (Pliocene) due to the interplay between across- and along- slope processes, resulting in large sheeted drifts, which appear primarily as sub-parallel reflections onlapping previous relief. Second, a transitional-drift stage (Late Pliocene to the base of the Quaternary) began up-slope migration and moat development (non-deposition) marked by gently downlapping reflections in seismic profiles. Finally, a growth-drift stage (Quaternary, <2 Ma) is dominated by contourite deposition. Drifts evolve into elongated mounds with a deep moat in the Deep Algarve and Alentejo basins and sandier sheeted drifts in the rest of the basins overlying the AUGC. Drifts therefore became more prominent high-relief features that regionally migrated up- and along-slope (downcurrent). When considered with the configuration of internal seismic units and dominant deposits, this shift in the drift's external geometry conceptually agrees with the vertical first-order variation in drift evolution proposed by other authors (Faugères et al., 1985a; Stow et al., 2002b; Nielsen et al., 2008), demonstrating the case for intensified bottom-currents along the SIM during the last 2 Ma.

The same cyclicity in seismic facies trends is frequently found at different scales with (1) a transparent zone at the base, (2) smooth, parallel reflectors of moderate-to-high amplitude in the upper part, and (3) a continuous, high-amplitude erosional surface at the top. The integration of IODP Exp. 399 drilling data with multichannel seismic data presented here suggests that this cyclic pattern of seismic facies most likely represents repeated coarsening-upward sequences bounded by erosional surfaces at unit and sub-unit scales. The duration of these cycles identified in multichannel seismic is much greater (0.8–0.9 Ma and 0.4–0.5 Ma, Fig. 15) than cycles identified by Llave et al. (2001, 2006, 2007a) in sparker source seismic profiles. These authors demonstrated links between grain size variation, climate and MOW variability for the last eustatic/climate cycle, which experienced enhanced MOW during cold intervals. Additional research has corroborated these findings (Voelker et al., 2006; Toucanne et al., 2007; García et al., 2009; Rogerson et al., 2012; Bahr et al., 2014; Hernández-Molina et al., 2014a). Longer frequency cyclicities in seismic facies trends observable at seismic scales however raise questions as to whether differently scaled cycles arise from the same processes. The relative abundance of turbiditic deposits occupying upper sections of these cycles and their protracted periodicity, which resembles that of longer repetitions identified from IODP sites (Stow et al., 2013b), and their genetic relation to some of the short identified hiatus suggest that CDS reflect tectonic activity, relative sea-level change and margin instability rather than orbital-scale variation at these longer scales.

6.5.2. Tectonics versus climate

Eustatic sea-level variation occurs at different time scales (Vail et al., 1977) and exerts primary influence on sequence architecture and basin evolution (e.g., Coe, 2003; Catuneanu, 2006). However, the causes for eustatic variations are not fully understood (Lovell, 2010). Previous regional stratigraphic analysis of the SIM considered eustatic changes a primary depositional factor at unit and subunit scales (Flinch and Vail, 1998; Riaza and Martinez del Olmo, 1996; Llave et al., 2001, 2007a, 2011; Hernández-Molina et al., 2002, 2006; Marchès et al., 2010; Roque et al., 2012; Brackenridge et al., 2013). These studies linked prominent discontinuities to major sea-level drops, global cooling events and cyclic shifts in the climate system. In their interpretation, the continental margin (including contourite deposits) formed primarily by stacking of regressive and lowstand sedimentary deposits in every depositional sequence, and building its observed progradational morphology. Transgressive and highstand deposits are also present in each depositional sequence but occur as condensed sections. This interpretation is consistent with high-resolution seismic studies for the last eustatic hemicycle and last 4th-order and 5th-order sequences (Llave et al., 2001, 2006) and with lithological changes observed in calypso piston and gravity cores (Llave et al., 2006, 2007a; Voelker et al., 2006; Toucanne et al., 2007; Bahr et al., 2014), and IODP Sites (Bahr et al., 2015).

The present work describes a clear and more protracted cyclicity in units and subunits of around 0.8–0.9 and 0.4–0.5 Ma (Fig. 15). These sedimentary cycles correspond with 3rd- and 4th-order asymmetric sequences identified in the region with mid- to high-resolution seismic profiles by Llave et al. (2001, 2007a) and Hernández-Molina et al. (2002, 2006). Results described here however indicate significant tectonic influence at long- and short-term scales, on margin development, downslope sediment transport and contourite drift evolution in Neogene basins. This activity also exerts primary influence on seafloor morphology, which in turn has determined MOW pathways and CDS

architecture. According to the timing of these different events, we propose tectonic pulses of approximate 0.8–0.9 Ma duration overprinted by more significant 2/2.5 Ma compressive-flexural stress cycles, which caused uplift/compression or active subsidence (Fig. 16). Westward roll back of subducted oceanic lithosphere with simultaneous tectonic shortening and gravitational spreading in the Gulf of Cadiz (Gutscher et al., 2002, 2009; Duggen et al., 2003) provides a consistent explanation for these cycles. Compressional tectonic regimes along the northeast Atlantic margin apparently correlate with the development of major deep-sea unconformities (Andersen et al., 2000; Stoker et al., 2005) and sedimentary pulses (Whyte and Lovell, 1997; Lovell, 2010). Interestingly, compressional events similar to those described here also occurred in the Himalaya (Cochran, 1990; Derbyshire, 1996) and North Atlantic regions (Cloetingh et al., 1990; Knutz, 2008). Atlantic plate reorganization entailed similar tectonic cycles of compression and sagging related to episodic, small-scale convective flow in the upper mantle plume (Cloetingh et al., 1990; Whyte and Lovell, 1997; Praeg et al., 2005; Stoker et al., 2005). Convection in the Earth's mantle thus occurs in punctuated pulses on geologic times scales (Rudge et al., 2008; Lovell, 2010) and has been interpreted as "blobby" flow (Jones et al., 2012). Surface uplift due to plate interactions (subsidence, rift activity, etc.), magmatic underplating and plume activity also affects sea-level (White and McKenzie, 1989; Whyte and Lovell, 1997; Maclennan and Lovell, 2002; Lovell, 2010; Jones et al., 2012) on time scales of 2nd- and 3rd order cycles from 2 to 4 Ma down to 1 Ma or less (Rudge et al., 2008; Lovell, 2010).

Consideration of these global cycles demonstrates that both tectonic and climatic factors determined sedimentary evolution of the Gulf of Cadiz and the margin off west Portugal. Changes in rates and geometries of plate boundaries as well as long-term plate reorganization lead to fluctuations in the magnitude of intraplate stresses. Modifications imparted by these factors on climate, relative sea-level and the seafloor morphology also affected bottom-current circulation. Tectonics thus influence deep-water sedimentation on geological scales of 2.5–>0.4 Ma. Tectonic pulses occurring around 2–2.5 Ma and 0.8–0.9 Ma align with long-period variation in orbital (eccentricity) cycles as is reported above, and with 3rd-order (1–3 Ma) eustatic cycles (Lourens and Hilgen, 1997), but not with cycles operating on shorter time-scales (Fig. 16). Tectonic events could thus control 3rd-order cycles on time scales of about 0.8–2.5 Ma. We interpret variation occurring on significantly shorter time-scales in Quaternary contourites as related to climate variability, sediment supply and sea-level fluctuation. Sediments analyzed here also show evidence of orbital-scale effects (Fig. 15) as identified by other studies (Sierro et al., 1999, 2000; Hernández-Molina et al., 2014b; Lofi et al., 2015). Orbital cycles (variation in insolation) influences climate on shorter times scales ≤0.4 Ma generating high to very high frequency (4th-order) depositional sequences of 0.1–0.2 Ma duration (Flinch and Vail, 1998) to submillennial scale variation in the sedimentary record (Schönfeld and Zahn, 2000; Llave et al., 2007a; Voelker et al., 2006; Toucanne et al., 2007; Rogerson et al., 2012; Bahr et al., 2014).

7. Conclusion

Semi-permanent bottom currents shape continental margin architecture and generate extensive contourite depositional systems (CDS). The large CDS along the Southwest Iberian margin (SIM) records unmistakable signs of Mediterranean Outflow Water (MOW) as it exits the Strait of Gibraltar, which reopened at the end of the Miocene. The SIM also records the pronounced effects of tectonic activity on margin sedimentation and evolution. The complexity of the SIM record results from the interaction of tectonic, climate and eustatic changes with additional bottom current circulation variations.

Integration of new core, borehole and outcrop data with previously collected seismic and drilling data revealed that significant changes in sedimentary style and processes often co-occurred with widespread depositional hiatuses. Tectonic influence on margin development, downslope sediment transport and sediment evolution began around the time of the narrowing of the Atlantic–Mediterranean gateways at 7 Ma and opening of the Strait of Gibraltar (5.33 Ma). The periodicity of these different events suggests an ~0.8–0.9 Ma duration for tectonic pulsing. A pronounced overprint of ~2–2.5 Ma cycles related to the westward roll back of subducted lithosphere as the Africa-Eurasia collision transitioned from a predominantly NW–SE to WNW–ESE direction. Following the temporal decrease of tectonic activity near the Miocene–Pliocene boundary, major compressional events affecting Neogene basins between 3.2–3 Ma and 2–2.3 Ma differentiate three stages of CDS evolution. These include 1) an initial-drift stage (Pliocene, from 5.3–3.2 Ma) with a weak MOW and the formation of a mixed across- and along slope deposits, 2) a transitional-drift stage (late Pliocene and early Quaternary, 3.2–2 Ma) and 3) a growth-drift stage (Quaternary, from 2 Ma to present) where the prevalence of contourites demonstrates increased bottom-current velocity due to a fully established MOW. Two younger and more minor Pleistocene discontinuities at 0.7–0.9 Ma and about 0.3–0.6 Ma in the Doñana basin record the effects of renewed tectonic activity.

A pronounced sedimentary cyclicity with a periodicity of about 0.8–0.9 Ma in sedimentary units, and 0.4–0.5 Ma sub-units appears throughout the sedimentary record, but is most clearly observed in the Quaternary section. Tectonics, sea-level and climate all exert primary external influence on sedimentation. The specific cause-and-effect relationships between them and their relative importance on temporal scales remain contentious. We propose that tectonic effects represent a long-term factor in controlling deep-marine sedimentation, especially at scales of 2.5–>0.4 Ma, whereas climatic (orbital) variation constitutes a short-term factor clearly dominant at scales of ≤0.4 Ma.

This work generally outlines the case for revisiting the role of bottom water circulation and associated processes in shaping the seafloor, controlling sedimentary stacking patterns on continental margins and influencing global climate. CDS preserve specific information on bottom-current circulation not available from other types of proxies. This information can be related to tectonic changes, climate and other sedimentary processes. High resolution, basin-level analysis of CDS requires integration of borehole, core and outcrop records with seismic data. Further research can help establish more refined interpretation of CDS, including their interaction with gravitational processes and their role in deep water systems. Refined interpretation workflows are necessary due to the common occurrence of sandy contourites in deep water settings with the potential of hydrocarbon resources and, most importantly, their role in recording Earth's paleoceanographic history.

Supplementary data to this article can be found online at http://dx.doi.org/10.1016/j.margeo.2015.09.013.

Acknowledgments

This research used samples and data collected through the Integrated Ocean Drilling Program (IODP). The research was partially supported through the CTM 2008-06399-C04/MAR, CTM 2012-39599-C03, CGL2011-26493, CTM2012-38248, SA263U14, IGCP-619, INQUA 1204 and FWF P25831-N29 Projects. Some data were collected with 94-1090-C03-03 (FADO) and MAR-98-0209 (TASYO) Projects. Research was conducted in the framework of the Continental Margins Research Group of the Royal Holloway University of London, People and the Program (Marie Curie Actions) of the European Union's Seventh Framework Program FP7/2007-2013/ under REA Grant Agreement No. 290201 MEDGATE'. We are very grateful to REPSeOL, TGS–NOPEC, and the CSIC-Institut Jaume Almera (http://geodb.ictja.csic.es) for allowing us to use an unpublished seismic data from the Gulf of Cadiz. We thank *J. Aguire* (UGR, Spain) for comments and suggestions concerning the Pliocene and Quaternary outcrops, *B. van den Berg* (USAL) for organizing a thought-provoking field-trip to Cadiz, Spain in November, 2014, *M. Ángel Caja*, *L. García Diego*, and *J. Tritlla* (REPSOL) for

provenance and diagenetic analysis of early Pliocene sandstones and debrites, and *L.J. Lourens* (Utrecht University) for providing us the eccentricity and 200-Kys glacio-eustatic sea-level curves included in the Figure 16. Both *Prof. D.A.V. Stow* (Heriot-Watt Univ., UK) and *F.J. Hernández-Molina* (RHUL, UK), as the main co-proponents of the IODP Proposal 644 and the co-chiefs of the IODP Exp. 339, thanks to IODP, Exp. IODP 339 Scientists; JR crew and technicians, as well as all people, institutions and companies involved in making IODP a success since 2003. Finally, we also thank the editor, Gert J. De Lange and the reviewers T. Mulder (Bourdeaux Univ.); D. Van Rooij (Ghent Univ) and J. Duarte (Monash Univ.) for their very positive and helpful feedback and discussions in publishing this research.

References

Aguirre, J., 1991. Estratigrafía del plioceno de la Costa de Cadiz entre chiclana y conil. Geogaceta 9, 84–87.

Aguirre, J., 1992. Evolución de las asociaciones fósiles del plioceno Marino de cabo Roche (Cadiz). Rev. Esp. Paleontol. volumen Extra 3–10.

Aguirre, J., 1995. Implicaciones paleoambientales y paleogeográficas de dos discontinuidades estratigráficas en los depósitos pliocénicos de Cadiz (SW de españa). Rev. Soc. Geol. Esp. 8, 153–166.

Aguirre, J., Braga, J.C., Martín, J.M., 1993. Algal nodules in the late Pliocene deposits at the coast of Cadiz (S Spain). In: Barattolo, F., De Castro, P., Parente, M. (Eds.), Studies on fossil benthic algae: Bolletino della Societa Paleontologica Italiana Special Volume, pp. 1–7.

Aguirre, J., Castillo, C., Agustí, J., Férriz, F.J., Oms, O., 1995. Marine-continental magnetobiostratigraphic correlation of the dolomys subzone (middle of late Pliocene): implications for the late ruscinian age. Palaeogeogr. Palaeoclimatol. Palaeoecol. 117, 139–152.

Aguirre, J., Gibert, J.M., Puga-Bernabeu, A., 2010. Proximal–distal ichnofabric changes in a siliciclastic shelf, early Pliocene, Guadalquivir basin, southwest Spain. Palaeogeogr. Palaeoclimatol. Palaeoecol. 291 (2010), 328–337.

Aït, B.L., 1991. Tectoniques et états de contrainte récents du Maroc Nord. Résultats de la cinématique des plaques Afrique-Europe et du bloc d'Alboran. Univ. Mohammed V, Fac. Sci. Rabat (Thèse d'Etat). (252 pp.).

Alves, T.M., Gawthorpe, R.L., Hunt, D.W., Monteiro, J.H., 2003. Cenozoic tectono-sedimentary evolution of the western Iberian margin. Mar. Geol. 195, 75–108.

Alves, T.M., Moita, C., Cunha, T., Ullnaess, M., Myklebust, R., Monteiro, J., Manuppella, G., 2009. Diachronous evolution of late Jurassic–cretaceous continental rifting in the northeast Atlantic (west Iberian margin). Tectonics 28, TC4003. http://dx.doi.org/10.1029/2008TC002337 (32 pp.).

Ambar, I., Howe, M.R., 1979. Observations of the Mediterranean outflow-II. The deep circulation in the vicinity of the Gulf of Cadiz. Deep-Sea Res. 26 (A), 555–568.

Ambar, I., Serra, N., Neves, F., Ferraira, T., 2008. Observations of the Mediterranean undercurrent and eddies in the gulf of cádiz during 2001. J. Mar. Syst. 71 (1–2), 195–220.

Andersen, M.S., Nielsen, T., Sørensen, A.B., Boldreel, O.L., Kuijpers, A., 2000. Cenozoic sediment distribution and tectonic movements in the Faroe region. Glob. Planet. Chang. 24, 239–259.

Argus, D.F., Gordon, R.G., DeMets, C., Stein, S., 1989. Closure of the Africa–Eurasia–North America plate motion circuit and tectonics of the Gloria fault. J. Geophys. Res. 94, 5585–5602.

Azdimousa, A., 1991. La Géologie des Bordures Méridionales de la mer d'Alboran des Temsamane Jusqu'Au Cap des Trois Fourches (Rif Oriental, Maroc) (Thèse de 3ème Cycle), Université Mohammed 1, Fac. Sci. Oujda 219 pp.

Azdimousa, A., Poupeau, G., Rezqi, H., Asebriy, L., Bourgois, J., Aït Brahim, L., 2006. Géodynamique des bordures méridionales de la mer d'Alboran; application de la stratigraphie séquentielle dans le bassin néogène de Boudinar (Rif oriental, Maroc). Bulletin de l'Institut Scientifique, Rabat, section Sciences de la Terre n°28, pp. 9–18 (2006).

Bache, F., Olivet, J.L., Gorini, C., Rabineau, M., Baztan, J., Aslanian, D., Suc, J.-P., 2009. Messinian erosional and salinity crises: view from the Provence basin (gulf of lions, western Mediterranean). Earth Planet. Sci. Lett. 286, 139–157.

Bahr, A., Jiménez-Espejo, F., Kolasinac, N., Grunert, P., Hernández-Molina, F.J., Röhl, U., Voelker, A., Escutia, C., Stow, D.A.V., Hodell, D., Alvarez-Zarikian, C.A., IODP Expedition 339 Scientists, 2014. Deciphering bottom current strength and paleoclimate signals from contourite deposits in the gulf of Cadiz during the last 140 kyr: an inorganic geochemical approach. G-Cubed 15 (8), 3145–3160.

Bahr, A., Kaboth, S., Jiménez-Espejo, F.J., Sierro, F.J., Voelker, A.H.L., Lourens, L., Röhl, U., Reichart, G.J., Escutia, C., Hernández-Molina, F.J., Pross, J., Friedrich, O., 2015. Persistent monsoonal forcing of Mediterranean Outflow dynamics during the late Pleistocene. Geology. http://dx.doi.org/10.1130/G37013.1 (in press).

Baringer, M.O., Price, J.F., 1997. Mixing and spreading of the Mediterranean outflow. J. Phys. Oceanogr. 27, 1654–1677.

Baringer, M.O., Price, J.F., 1999. A review of the physical oceanography of the Mediterranean outflow. Mar. Geol. 155, 63–82.

Bartoli, G., Sarnthein, M., Weinelt, M., Erlenkeuser, H., Garbe-Schönberg, D., Lea, D.W., 2005. Final closure of panama and the onset of northern hemisphere glaciation. Earth Planet. Sci. Lett. 237, 33–44.

Benkhelil, J., 1976. Etude néotectonique de la terminaison occidental dans les Cordilléres Bétiques (Espagne) (Thése de 3em cycle), Univ. Nice (180 pp.).

Berástegui, X., Banks, C., Puig, C., Taberner, C., Waltham, D., Fernández, M., 1998. Lateral diapiric emplacement of Triassic evaporites at the southern margin of the Guadalquivir basin, Spain. In: Mascle, A., Puigdefa'bregas, C., Luterbacher, H.P., Fernández, M. (Eds.), Cenozoic foreland basins of western Europe. Geol. Soc. London Spec. Publ. 134, pp. 49–68.

Berger, A., Loutre, M.F., Dehant, V., 1989. Milankovitch frequencies for pre-quaternary. Nature 342, 133.

Berger, A.L., 1977. Support for the astronomical theory of climatic change. Nature 269, 44–45.

Berger, A.L., 1978. Long-term variations of daily insolation and Quaternary climatic changes. J. Atmos. Sci. 35, 2362–2367.

Blanc, P.-L., 2002. The opening of the plio-Quaternary Gibraltar strait: assessing the size of a cataclysm. Geodin. Acta 15 (5–6), 303–317.

Borenäs, K.M., Wahlin, A.K., Ambar, I., Serra, N., 2002. The Mediterranean outflow splitting- a comparison between theoretical models and CANIGO data. Deep-Sea Res. II 49, 4195–4205.

Boulila, S., Galbrun, B., Laskar, J., Pälike, H., 2012. A ~9 myr cycle in Cenozoic $\delta^{13}C$ record and long-term orbital eccentricity modulation: is there a link? Earth Planet. Sci. Lett. 317–318, 273–281.

Bourgois, J., Mauffret, A., Ammar, A., Demnati, A., 1992. Multichannel seismic data imaging of inversion tectonics of the alboran ridge (western Mediterranean sea). Geo-Mar. Lett. 12, 117–122.

Brackenridge, R.A., Hernández-Molina, F.J., Stow, D.A.V., Llave, R., 2013. A Pliocene mixed contourite-turbidite system offshore the Algarve Margin, Gulf of Cadiz: Seismic response, margin evolution and reservoir implications. Mar. Pet. Geol. 46: 36–50. doi.org/http://dx.doi.org/10.1016/j.marpetgeo.2013.05.015.

Bryden, H.L., Stommel, H.M., 1984. Limiting processes that determine basic features of the circulation in the Mediterranean sea. Oceanol. Acta 7, 289–296.

Bryden, H.L., Candela, J., Kinder, T.H., 1994. Exchange through the strait of Gibraltar. Prog. Oceanogr. 33, 201–248.

Buitrago, J., García, C., Cajebread-Brow, J., Jiménez, A.y., Martínez del Olmo, W., 2001. Contouritas: Un excelente almacén casi desconocido (Golfo de Cadiz, SO de España). 1er Congreso Técnico Exploración y Producción REPSOL-YPF, pp. 24–27 (Madrid).

CachÃo, M., da Silva, C.M., 2000. The three main marine depositional cycles of the neogene of Portugal. Ciênc. Terra (UNL). 14, 303–312.

Caja, M.A., Diego, L.G., Tritlla, J., 2013. Advance Provenance and Diagenetic Study for Algarve Turbiditic Systems Technical Report. REPSOL Technology – E&P and Gas (42 pp.).

Cande, S.C., Kent, D.V., 1995. Revised calibration of the geomagnetic polarity timescale for the late cretaceous and Cenozoic. J. Geophys. Res. 100, 6093–6095.

Catuneanu, O., 2006. Principles of Sequence Stratigraphy. Elsevier, Amsterdam.

Cherubin, L., Carton, X., Paillet, J., Morel, Y., Serpatte, A., 2000. Instability of the Mediterranean water undercurrents southwest of Portugal: effects of baroclinicity and topography. Oceanol. Acta 23 (5), 551–573.

CIESM, 2008. The Messinian Salinity Crisis from mega-deposits to microbiology — a consensus report. In: Biand, F. (Ed.), Nº 33 in CIESM workshop Monographs Monaco: (168 pp.).

Cloetingh, S., Gradstein, F.M., Kooi, H., Grant, A.C., Kaminski, M., 1990. Plate reorganization: a cause of rapid late neogene subsidence and sedimentation around the north Atlantic? J. Geol. Soc. Lond. 147, 495–506.

Cochran, J.R., 1990. Himalayan uplift, sea level, and the record of Bengal Fan sedimentation at the ODP Leg 116 sites. In: Cochran, J.R., Stow, D.A.V., et al. (Eds.), Proc. ODP, Sci. Results 116. Ocean Drilling Program, College Station, TX, pp. 397–414.

Coe, A.L. (Ed.), 2003. The Sedimentary Record of sea-Level Change. Cambridge University Press, Cambridge.

Comas, M.C., Zahn, R., Klaus, A., et al., 1996. Proceedings of the Ocean Drilling Program, Initial Reports. vol. 161.

Copard, K., Colin, C., Frank, N., Jeandel, C., Montero-Serrano, J.-C., Reverdin, G., Ferron, B., 2011. Nd isotopic composition of water masses and dilution of the Mediterranean outflow along the southwest European margin. Geochem. Geophys. Geosyst. 12, 864, Q06020.

De Boer, B., Van de Wal, R.S.W., Bintanja, R., Lourens, L.J., Tuenter, E., 2010. Cenozoic global ice-volume and temperature simulations with 1-D ice-sheet models forced by benthic δ18O records. Ann. Glaciol. 51 (55), 23–33.

DeCelles, P.G., Giles, K.A., 1996. Foreland basin systems. Basin Res 8, 05–123.

Derbyshire, E., 1996. Quaternary glacial sediments, glaciation style, climate and uplift in the Karakoram and nortwest Himalaya: review and speculations. Palaeogeogr. Palaeoclimatol. Palaeoecol. 120, 147–157.

Dewey, J.F., Helman, M.L., Turco, E., Hutton, D.H.W., Knott, S.D., 1989. Kinematics of the western Mediterranean. In: Coward, M. (Ed.), Alpine Tectonics. Spec. Publ. Geol. Soc., London 45, pp. 265–283.

Dias, R.P., Cabral, J., 1997. Plio-Quaternary crustal movements in southern Portugal-Algarve. IV Reunião do Quaternário Ibérico, pp. 61–68 Huelva.

Dias, R.P., Cabral, J., 2000. Deformações neotectónicas na região do Algarve. 3° Simpósio da Margem Ibérica Atlântica, pp. 189–190 Faro.

Duarte, J.C., Rosas, F.M., Terrinha, P., Schellart, W.P., Boutelier, D., Gutscher, M.A., Ribeiro, A., 2013. Are subduction zones invading the Atlantic? Evidence from the southwest Iberia margin. Geology http://dx.doi.org/10.1130/G34100.1.

Duarte, J.C., Rosas, F.M., Terrinha, P., Gutscher, M.-A., Malavieille, J., Silva, S., Matias, L., 2011. Thrust–wrench interference tectonics in the gulf of Cadiz (Africa–Iberia plate boundary in the north-east Atlantic): insights from analog models. Mar. Geol. 289, 135–149.

Ducassou, E., Fournier, L., Sierro, F.J., Alvarez Zarikian, C.A., Lofi, J., Flores, J.A., Roque, C., 2016. Origin of the large Pliocene and Pleistocene debris flows on the Algarve margin. Mar. Geol. 377, 58–76.

Duggen, S., Hoernle, K., van den Bogaard, P., Rüpke, L., Morgan, J.P., 2003. Deep roots of the Messinian salinity crisis. Nature (London, U. K.) 422 (6932), 602–606.

Einsele, G., 2000. Sedimentary Basins. Evolution, Facies, and Sediment Budget, 2nd ed. Springer-Verlag, Berlin 792 pp.
Esteras, M., Izquierdo, J., Sandoval, N.G., Bahmad, A., 2000. Evolución morfológica y estratigráfica plio-cuaternaria del umbral de camarinal (estrecho de Gibraltar) basada en sondeos marinos. Rev. Soc. Geol. Esp. 13 (3–4), 539–550.
Estrada, F., Ercilla, G., Gorini, C., Alonso, B., Vázquez, J., García-Castellanos, D., Juan, C., Maldonado, A., Ammar, A., Elabbassi, M., 2011. Impact of pulsed Atlantic water inflow into the alboran basin at the time of the zanclean flooding. Geo-Mar. Lett. 31, 361–376.
Expedition 339 Scientists, 2012. Mediterranean outflow: environmental significance of the Mediterranean outflow water and its global implications. IODP Preliminary Report, p. 339 http://dx.doi.org/10.2204/ iodp.pr.339.2012.
Faugères, J.-C., Stow, D.A.V., 2008. Contourite Drifts: Nature, Evolution and Controls. In: Rebesco, M., Camerlenghi, A. (Eds.), ContouritesDevelopments in Sedimentology 60. Elsevier, Amsterdam, pp. 257–288.
Faugères, J.-C., Cremer, M., Monteiro, H., Gaspar, L., 1985a. Essai de reconstitution des processus d'edification de la ride sedimentaire de faro (Marge Sud-portugaise). Bull Inst. Géol. Bassin Aquitaine 37, 229–258.
Faugères, J.-C., Frappa, M., Gonthier, E., Grousset, F., 1985b. Impact de la veine d'eau méditerranéenne sur la sedimentation de la Marge Sud et Ouest iberique au quaternaire recent. Bull Inst. Géol. Bassin Aquitaine 37, 259–287.
Faugères, J.-C., Stow, D.A.V., Imbert, P., Viana, A.R., 1999. Seismic features diagnostic of contourite drifts. Mar. Geol. 162, 1–38.
Fernàndez, M., Berástegui, X., Puig, C., García-Castellanos, D., Jurado, M.J., Torné, M., Banks, C., 1998. Geophysical and geological constraints on the evolution of the Guadalquivir foreland basin, Spain. In: Mascle, A., Puigdefàbregas, C., Luterbacher, H.P., Fernàndez, M. (Eds.), Cenozoic Foreland Basins of Western Europe: Geological Society Special Publications. 134, pp. 29–48.
Fernández-Ibánez, F., Soto, J.I., Zoback, M.D., Morales, J., 2007. Present-day stress field in the Gibraltar arc (western Mediterranean). J. Geophys. Res. 112, 1–25.
Fernández-Puga, M.C., Vázquez, J.T., Somoza, L., Díaz del Río, V., Medialdea, T., Mata, M.P., León, R., 2007. Gas-related morphologies and diapirism in the gulf of Cadiz. Geo-Mar. Lett. 27 (2–4), 213–221.
Flecker, R., Krijgsman, W., Capella, W., Martins, C., De, C., Demitrieva, E., Mayser, J.P., Marzocchi, A., Modestu, S., Ochoa Lozano, D., Simon, D., Tulbure, M., van den Berg, B., van der Schee, M., de Lange, G., Ellam, R., Govers, R., Gutjahr, M., Hilgen, F., Kouwenhoven, T., Lofi, J., Meijer, P., Sierro, F.J., Bachiri, N., Barboun, N., Chakor Alami, A., Chacon, B., Flores, J.A., Gregory, J., Howard, J., Lunt, D., Ochoa, M., Pancost, R., Vincent, S., Yousfi, M.Z., 2015. Evolution of the late Miocene Mediterranean-Atlantic gateways and their impact on regional and global environmental Change. Earth-Sci. Rev. 150, 365–392.
Flinch, J.F., Vail, P.R., 1998. Plio-Pleistocene sequence stratigraphy and tectonic of the Gibraltar Arc. In: de Graciansky, P.C., Hardenbol, J., Jacquin, T., Vail, P.R. (Eds.), Mesozoic and Cenozoic Sequence Stratigraphy of European Basins SEM, Spec. Pub. vol. 60, pp. 199–208
García, M., Hernández-Molina, F.J., Llave, E., Stow, D.A.V., León, R., Fernández-Puga, M.C., Díaz del Río, V., Somoza, L., 2009. Contourite erosive features caused by the Mediterranean outflow water in the gulf of Cadiz: Quaternary tectonic and oceanographic implications. Mar. Geol. 257, 24–40.
Garcia-Castellanos, D., Estrada, F., Jiménez-Munt, I., Gorini, C., Fernàndez, M., Vergés, J., De Vicente, R., 2009. Catastrophic flood of the Mediterranean after the Messinian salinity crisis. Nature (London, U. K.) 462 (7274), 778–781.
Gardner, J.V., Kidd, R.B., 1983. Sedimentary processes on the Iberian continental margin viewed by long-range side-scan sonar. 1: gulf of Cadiz. Oceanol. Acta 6 (3), 245–254.
George, D., 2011. TGS–Nopec's Portugal Survey Suspended. Oil and Gas Online.
Gonthier, E.G., Faugères, J.C., Stow, D.A.V. 1984. Contourite facies of the faro drift, gulf of Cadiz. En: Stow, D.A.V., Piper, D.J.W. (Eds.), Fine-Grained Sediments, Deep-Water Processes and Facies. Geological Society Special Publication, 15: 275-292.
Gonzalez-Delgado, J.A., Dabrio, C.J., Sierro, F.J., Civis, J., 2013. The Neogene of Huelva (western Guadalquivir basin, SW Spain). Fieldtrip guide. STRATI 2013. 1st International Congress on Stratigraphy, Lisbon.
Gràcia, E., Danobeitia, J., Verges, J., Bartolome, R., 2003. Crustal architecture and tectonic evolution of the gulf of Cadiz, SW Iberia, at the convergence of the Eurasian and African plates. Tectonics 22 (4), 1033.
Guillemin, M., Houzay, J.-P., 1982. Le néogène post-nappes et le quaternaire du Rif Nord oriental. Stratigraphie et tectonique des bassins de Melilla, de kert, de boudinar et du piedmont des kebdana. Notes Mém. Serv. Géol. Maroc 314, 7–239.
Gutscher, M.-A., Dominguez, S., Westbrook, G.K., Gente, P., Babonneau, N., Mulder, T., Gontier, E., Bartolome, R., Luis, J., Rosas, F., Terrinha, P., Delila, T., Teams, D.S.I.S., 2009. Tectonic shortening and gravitational spreading in the gulf of Cadiz accretionary wedge: observations from multi-beam bathymetry and seismic profiles. Mar. Pet. Geol. 26, 647–659.
Gutscher, M.-A., Malod, J., Rehault, J.-P., Contrucci, I., Klingelhoefer, F., Mendes-Victor, L., Spakman, W., 2002. Evidence for active subduction beneath Gibraltar. Geology 30, 1071–1074.
Habgood, E.L., Kenyon, N.H., Masson, D.G., Akhmetzhanov, A., Weaver, P.P.E., Gardner, J., Mulder, T., 2003. Deep-water sediment wave fields, bottom current sand channels and gravity flow channel-lobe systems: gulf of Cadiz, NE Atlantic. Sedimentology 50, 483–510.
Hanquiez, V., Mulder, T., Lecroart, P., Gonthier, E., Marchès, E., Voisset, M., 2007. High resolution seafloor images in the gulf of Cadiz, Iberian margin. Mar. Geol. 28, 42–59.
Haq, B.U., Hardenbol, J., Vail, P.R., 1987. Chronology of fluctuating sea levels since the Triassic. Science 235, 1156–1167.
Hay, W.W., 1996, Tectonic and climate. Geol. Rundsch, v. 85, p. 409–437.
Hernández-Molina, F.J., Llave, E., Preu, B., Ercilla, G., Fontan, A., Bruno, M., Serra, N., Gomiz, J.J., Brackenridge, R.E., Sierro, F.J., Stow, D.A.V., García, M., Juan, C., Sandoval, N., Arnaiz, A., 2014a. Contourite processes associated to the Mediterranean outflow water after its exit from the Gibraltar strait: global and conceptual implications. Geology 42, 227–230.
Hernández-Molina, F.J., Llave, E., Somoza, L., Fernández-Puga, M.C., Maestro, A., León, R., Barnolas, A., Medialdea, T., García, M., Vázquez, J.T., Díaz del Río, V., Fernández-Salas, L.M., Lobo, F., Alveirinho Dias, J.M., Rodero, J., Gardner, J., 2003. Looking for clues to paleoceanographic imprints: a diagnosis of the gulf of Cadiz contourite depositional systems. Geology 31, 19–22.
Hernández-Molina, F.J., Llave, E., Stow, D.A.V., García, M., Somoza, L., Vázquez, J.T., Lobo, F.J., Maestro, A., Díaz del Río, V., León, R., Medialdea, T., Gardner, J., 2006. The contourite depositional system of the gulf of Cadiz: a sedimentary model related to the bottom current activity of the Mediterranean outflow water and its interaction with the continental margin. Deep-Sea Res. II 53, 1420–1463.
Hernández-Molina, F.J., Serra, N., Stow, D.A.V., Llave, L., Ercilla, E., Van Rooij, D., 2011. Along-slope oceanographic processes and sedimentary products around the Iberian margin. Geo-Mar. Lett. 31 (5–6), 315–341.
Hernández-Molina, F.J., Somoza, L., Vazquez, J.T., Lobo, F., Fernandez-Puga, M.C., Llave, E., Diaz-del Rio, V., 2002. Quaternary stratigraphic stacking patterns on the continental shelves of the southern Iberian peninsula: their relationship with global climate and palaeoceanographic changes. Quat. Int. 92, 5–23.
Hernández-Molina, F.J., Stow, D.A.V., Alvarez-Zarikian, C., Expedition IODP 339 Scientists, 2013. IODP expedition 339 in the gulf of Cadiz and off west Iberia: decoding the environmental significance of the Mediterranean outflow water and its global influence. Sci. Drill. 16, 1–11.
Hernández-Molina, F.J., Stow, D.A.V., Alvarez-Zarikian, C.A., Acton, G., Bahr, A., Balestra, B., Ducassou, E., Flood, R., Flores, J.A., Furota, S., Grunert, P., Hodell, D., Jimenez-Espejo, F., Kim, J.K., Krissek, L., Kuroda, J., Li, B., Llave, E., Lofi, J., Lourens, L., Miller, M., Nanayama, F., Nishida, N., Richter, C., Roque, C., Pereira, H., Sanchez Goñi, M.F., Sierro, F.J., Singh, A.D., Sloss, C., Takashimizu, Y., Tzanova, A., Voelker, A., Williams, T., Xuan, C., 2014b. Onset of Mediterranean outflow into the north Atlantic. Science 344, 1244–1250.
Hilgen, F.J., Krijgsman, W., Langereis, C.G., Lourens, L.J., Santarelli, A., and Zachariasse, W.J., 1995. Extending the astronomical (Polarity) time scale into the Miocene. Earth Planet. Sci. Lett., v. 136, p. 495–510.
Hinnov, L.A., 2000. New perspectives on orbitally forced stratigraphy. Annu. Rev. Earth Planet. Sci. 28, 419–475.
Hinnov, L.A., Hilgen, F.J., 2012. Cyclostrtaigraphy and Astrochronology. In: Gradstein, F.M., Ogg, J.G., Schmitz, M., Ogg, G. (Eds.), The Geologic Time Scale 2012. Elsevier, pp. 63–88.
Hoddel, D., Curtis, J.H., Sierro, F.J., Raymo, M.E., 2001. Correlation of late Miocene to early Pliocene sequences between the Mediterranean and north Atlantic. Paleoceanography 16 (2), 164–178.
Hodell, D., Lourens, L., Crowhurst, S., Konijnendijk, T., Tjallingii, R., the Shackleton Site Project Members, 2015. A reference time scale for Site U1385 (Shackleton Site) on the Iberian Margin.
Hodell, D., Lourens, L., Stow, D.A.V., Hernández-Molina, F.J., Alavarez-Zarikian, C.A., the Shackleton Site Project Members, 2013. The "shackleton site" (IODP site U1385) on the Iberian margin. Scientific Drilling. Sci. Drill. 16 (13–19), 2013. http://dx.doi.org/10.5194/sd-16-13-2013.
Hsü, K.J., Cita, M.B., Ryan, W.B.F., 1973. The Origin of the Mediterranean Evaporites. Initial Reports of the Deep Sea Drilling Project. U.S. Government Printing Office, Washington, DC, pp. 1203–1231.
Hunter, S.E., Wilkinson, D., Stanford, J., Stow, D.A.V., Bacon, S., Akhmetzhanov, A.M., Kenyon, N.H., 2007. The Eirik Drift: A Longterm Barometer of North Atlantic Deepwater Flux South of Cape Farewell, Greenland. In: Viana, A., Rebesco, M. (Eds.), Economic and Paleoceanographic Importance of Contourites. Geological Society of London Special Publication 276, pp. 245–263.
IGME, 1990. Mapa Geológico de España escala 1:50.000. Vejer de la Frontera. Instituto Tecnológico GeoMinero de España. Madrid.
IGME, 1994. Mapa Geológico de España. Escala 1:200.000. Hoja 86, 3–12. Instituto Geológico y Minero de España. Ministerio de Industria y Energía.
IGMP, 1998, Carta Geológica de Portugal (1:1 000 000) Instituto Geológico e Mineiro, Portugal.
Ikeda, M., Tada, R., 2013. Long period astronomical cycles from the Triassic to Jurassic bedded chert sequences (inuyama, Japan); geologice evidences for the chaotic behavior of solar planest. Earth Planets Space 65, 351–360.
Iorga, M., Lozier, M.S., 1999. Signatures of the Mediterranean outflow from a north Atlantic climatology. 1. Salinity and density fields. J. Geophys. Res. 194, 25985–26029.
Iribarren, L., Vergés, J., Camurri, F., Fullea, J., Fernàndez, M., 2007. The structure of the Atlantic– Mediterranean transition zone from the alboran sea to the horseshoe abyssal plain (Iberia– Africa plate boundary). Mar. Geol. 243, 97–119.
Jones, S.M., Lovell, B., Crosby, A.G., 2012. Comparison of modern and geological observations of dynamic support from mantle convection. J. Geol. Soc. 169, 745–758.
Kashiwaya, K., Ryugo, M., Sakai, H., Kawai, T., 1998. Long-term climate-limnological oscillation during the past .2–.5 million years printed in lake Baikal sediments. Geophys. Res. Lett. 25, 659–662.
Khélifi, N., Sarnthein, M., Andersen, N., Blanz, T., Frank, M., Garbe-Schönberg, H., B.A., Stumf, R., Einelt, M., 2011. A major and long-term Pliocene intensification of the Mediterranean outflow, 3–5–3.3 Ma ago. Geology 37, 811–814.
Khélifi, N., Sarnthein, M., Frank, M., Andersen, N., Garbe-Schönberg, D., 2014. Late Pliocene Variations of the Mediterranean Outflow. Mar. Geol. 357, 182–194.
Kinnaird, T.C., 2008. Tectonic and Sedimentary Response to Oblique and Incipient Continental - Continental Collision the Easternmost Mediterranean (Cyprus) (Thesis submitted for the degree of Doctor of), Philosophy University of Edinburgh (380 pp.).
Knutz, P.C., 2008. Palaeoceanographic significance of contourite drifts. In: Rebesco, M., Camerlenghi, A. (Eds.), ContouritesDevelopments in Sedimentology 60. Elsevier, Amsterdam, pp. 511–535.

Knutz, P.K., Cartwright, J., 2003. Seismic stratigraphy of the west Shetland drift: implications for Late Neogene paleocirculation in the Faeroe–Shetland gateway. Paleoceanography 18, 1093. http://dx.doi.org/10.1029/2002PA000786.
Laberg, J.S., Stoker, M.S., Torbjørn Dahlgren, K.I., De Haas, H., Haflidason, H., Hjelstuen, B.O., Nielsen, T., Shannon, P.M., Vorren, T.O., Van Weering, T.C.E., Ceramicola, S., 2005. Cenozoic alongslope processes and sedimentation on the NW European Atlantic margin. Mar. Pet. Geol. 22, 1069–1088.
Laskar, J., Fienga, A., Gastineau, M., Manche, H., 2011. La2010: a new orbital solution for the long term motion of the earth. Astron. Astrophys. 532. http://dx.doi.org/10.1051/0004-6361/201116836.
Laskar, J., Robutel, P., Joutel, F., Gastineau, M., Correia, A.C.M., Levrard, B., 2004. A long term numerical solution for the insolation quantities of the earth. Astron. Astrophys. Paris 428 (n° 1), 261–285.
Ledesma SM (2000) Astrobiocronología y estratigrafía de alta resolución del Neógeno de la Cuenca del Guadalquivir-Golfo de Cadiz. (PhD Thesis), University of Salamanca, Salamanca. Unpublished, (464 pp.)
Llave, E., Hernández-Molina, F.J., Somoza, L., Stow, D.A.V., Díaz del Río, V., 2007a. Quaternary evolution of the contourite depositional system in the gulf of Cadiz. In: Viana, A., Rebesco, M. (Eds.), Economic and Paleoceanographic Importance of Contourites. Geol Soc London Sp Publ 276, pp. 49–79.
Llave, E., Hernández-Molina, F.J., Stow, D., Fernández-Puga, M.C., García, M., Vázquez, J.T., Maestro, A., Somoza, L., Díaz del Río, V., 2007b. Reconstructions of the Mediterranean outflow water during the Quaternary since the study of changes in buried mounded drift stacking pattern in the gulf of Cadiz. Mar. Geophys. Res. 28, 379–394.
Llave, E., Hernández-Molina, F.J., Somoza, L., Díaz-del-Río, V., Stow, D.A.V., Maestro, A., Alveirinho Dias, J.M., 2001. Seismic stacking pattern of the faro-albufeira contourite system (gulf of Cadiz): a Quaternary record of paleoceanographic and tectonic influences. Mar. Geophys. Res. 22, 487–508.
Llave, E., Matias, H., Hernández-Molina, F.J., Ercilla, G., Stow, D.A.V., Medialdea, T., 2011. Pliocene–Quaternary contourites along the northern gulf of Cadiz margin : sedimentary stacking pattern and 46 lim adu distribution. Geo-Mar. Lett. 31 (5/6). http://dx.doi.org/10.1007/s00367-011-0241-3.
Llave, E., Schönfeld, J., Hernández-Molina, F.J., Mulder, T., Somoza, L., Díaz del Río, V., I. Sánchez-Almazo, I. 2006. High-resolution stratigraphy of the Mediterranean outflow contourite system in the gulf of Cadiz during the late Pleistocene: the impact of Heinrich events. Mar. Geol., 227: 241-262.
Lofi, J., Déverchère, J., Gaullier, V., Gillet, H., Gorini, C., Guennoc, P., Loncke, L., Maillard, A., Sage, F., Thinon, I., 2011. Atlas of the "Messinian Salinity Crisis" seismic markers in the Mediterranean and Black seas. CCGM & Mém. SGF n.s., t.179, (72 pp.).
Lofi, J., Voelker, A.H.L., Ducassou, E., Hernández-Molina, F.J., Sierro, F.J., Bahr, A., Galvani, A., Lourens, L.J., Pardo-Igúzquiza, E., Rodríguez-Tovar, F.J., William, T., 2015. Quaternary record in the gulf of Cádiz and Portuguese contourite depositional systems. Mar. Geol. (in this volume).
Lopes, F.C., Cunha, P.P., Le Gall, B., 2006. Cenozoic seismic stratigraphy and tectonic evolution of the Algarve margin (offshore Portugal, southwestern Iberian peninsula). Mar. Geol. 231, 1–36.
Louarn, E., and Morin, P., 2011, Antarctic intermediate water influence on Mediterranean sea water outflow, Deep-Sea Res. I Oceanogr. Res. Pap., v. 58, p. 932–942, doi:http://dx.doi.org/10.1016/j.dsr.2011.05.009.
Lourens, L.J., Hilgen, F.J., 1997. Long-periodic variation in the earth's obliquity and their relation to third-order eustatic cycles and late neogene glaciations. Quat. Int. 40, 43–52.
Lourens, L.J., Hilgen, F.J., Shackleton, N.J., Laskar, J., Wilson, D., 2004. The Neogene Period. In: Gradstein, F.M., Ogg, J.G., Smith, A.G. (Eds.), Geological Time Scale 2004. Cambridge University Press, Cambridge, UK, pp. 409–440.
Lovell, B., 2010. A pulse in the planet: regional control of high-frequency changes in relative sea level by mantle convection. J. Geol. Soc. 167, 637–648.
Maclennan, J., Lovell, B., 2002. Control of regional sea level by surface uplift and subsidence caused by magmatic underplating of earth's crust. Geology 30 (8), 675–678.
Madelain, F., 1970. Influence de la topographie du fond sur l'ecoulement méditerranéen entre le Detroit de Gibraltar et le cap saint-Vincent. Cah. Oceanogr. 22, 43–61.
Maestro, A., Somoza, L., Medialdea, T., Talbot, C.J., Lowrie, A., Vázquez, J.T., Díaz-del-Río, V., 2003. Large-scale slope failure involving triassic and middle Miocene salt and shale in the gulf of Cadiz (Atlantic Iberian margin). Terranova 15, 380–391.
Maldonado, A., Somoza, L., Pallares, L., 1999. The betic orogen and the Iberian-African boundary in the gulf of Cadiz, geological evolution central north Atlantic. Mar. Geol. 155, 9–43.
Marchès, E., Mulder, T., Cremer, M., Bonnel, C., Hanquiez, V., Gonthier, E., Lecroart, P., 2007. Contourite drift construction influenced by capture of Mediterranean outflow water deep-sea current by the portimao submarine canyon (gulf of Cadiz, south Portugal). Mar. Geol. 242, 247–260.
Marchès, E., Mulder, T., Gonthier, E., Cremer, M., Hanquiez, V., Garlan, T., Lecroart, R., 2010. Perched lobe formation in the gulf of Cadiz: interactions between gravity processes and contour currents (Algarve margin, southern Portugal). Sediment. Geol. 229, 81e94.
Martinez del Olmo, W., Garcia-Mallo, J., Leret, J., Serrano-Oñate, A., Suarez-Alba, J., 1984. Modelo tectosedimentario del bajo Guadalquivir. I Congreso Español de Geologia. Tomo I, 199–213.
Martínez-García, P., Comas, M., Soto, J.I., Lonergan, L., Watts, A.B., 2013. Strike-slip tectonics and basin inversion in the western Mediterranean: the post-messinian evolution of the alboran sea. Basin Res. 25, 361–387. http://dx.doi.org/10.1111/bre. 12005.
Mascarelli, A.L., 2009. Quaternary geologists win timescale vote. Nature 459, 264.
McCave, I.N., Tucholke, B.E. 1986. Deep current controlled sedimentation in the western North Atlantic. En: Vogt, P.R., Tucholke, B.E. (Eds.), The Geology of North America, vol. M, The Western North Atlantic Region. Geological Society Am Boulder (CO), pp 451–468
Medialdea, T., Somoza, L., Pinheiro, L.M., Fernández-Puga, M.C., Vázquez, J.T., León, R., Ivanov, M.K., Magalhaes, V., Díaz-del-Río, V., Vegas, R., 2009. Tectonics and mud volcano development in the gulf of cádiz. Mar. Geol. 261, 48–63.
Medialdea, T., Vegas, R., Somoza, L., Vazquez, J.T., Maldonado, A., Díaz-del-Río, V., Maestro, A., Córdoba, D., Fernández-Puga, M.C., 2004. Structure and evolution of the "olistostrome" complex of the Gibraltar arc in the gulf of Cadiz (eastern central Atlantic): evidence from two long seismic cross-sections. Mar. Geol. 209, 173–198.
deMenocal, P.B., 2011, Climate and human evolution. Science, V. 331(6017), p. 540-542.
Michard, A., Saddiqi, O., Chalouan, A., Frizon de Lamotte, D. (Eds.), 2008. Continental Evolution: The Geology of Morocco: Structure, Stratigraphy and Tectonics of the Africa–Atlantic–Mediterranean Triple Junction. Springer-Verlag, Berlin Heidelberg (424 pp.).
Miller, K.G., Kominz, M.A., Browning, J.V., Wright, J.D., Mountain, G.S., Katz, M.E., Sugarman, P.J., Cramer, B.S., Christie-Blick, N., Pekar, S.F., 2005. The phanerozoic record of global sea-level change. Science 310, 1293–1298.
Miller, K.G., Mountain, G.S., Wright, J.D., Browning, J.V., 2011. A 180-million-year record of sea level and ice volume variations from continental margin and deep-sea isotopic records. Oceanography 24 (2), 40–53. http://dx.doi.org/10.5670/oceanog.2011.26.
Millot, C., 2009. Another description of the Mediterranean outflow. Prog. Oceanogr. 82 (2), 101–124.
Montenat, C., Ott d'Estevou, P., De La Chapelle, G., 1990. Le bassin de nijar-carboneras et le couloir du bas-andarax. In: Montenat, C. (Ed.), Les bassins néogènes du domaine bétique oriental (espagne). tectonique et sédimentation darts un couloir de décrochement. Doc. Trav. IGAL. 12–13, pp. 129–164.
Morel, J.-L., 1988. Evolution récente de l'orogène rifain et de son avant-pays, depuis la fin de la mise en place des nappes (Rif, maroc). Mém. Géodiffusion 4 (226 pp.).
Mougenot, D., 1988. Geologie de la Marge Portugaise VI. Univ. Pierre et, Marie Curie, Paris Thése 3éme Cicle. 259 pp.
Moura, D., Boski, T., 1999. Unidades litostratigráficas do pliocénico e plistocénico no Algarve. Commun. Inst. Geol. Min. 86, 85–106.
Mulder, T., Voisset, M., Lecroart, P., Le Drezen, E., Gonthier, E., Hanquiez, V., Faugères, J.-C., Habgood, E., Hernández-Molina, F.J., Estrada, F., Llave, E., Poirier, D., Gorini, C., Fuchey, Y., Volker, A., Freitas, P., Lobo Sanchez, F., Fernandez, L.M., Morel, J., 2003. The gulf of Cadiz: an unstable giant contouritic levee. Geo-Mar. Lett. 23 (1), 7–18.
Nelson, C.H., Baraza, J., Maldonado, A., 1993. Mediterranean undercurrent sandy contourites, gulf of Cadiz. Spain. Sediment. Geol. 82, 103–131.
Nelson, C.H., Baraza, J., Rodero, J., Maldonado, A., Escutia, C., Barber Jr., J.H., 1999. Influence of the Atlantic inflow and Mediterranean outflow currents on late Pleistocene and Holocene sedimentary facies of gulf of Cadiz continental margin. Mar. Geol. 155, 99–129.
Nichols, G., 2009. Sedimentology and stratigraphy. 2nd ed. Wiley-Blackwell (419 pp.).
Nielsen, T., Knutz, P.C., Kuijpers, P.C.A., 2008. Seismic expression of contourite depositional systems. In: Rebesco, M., Camerlenghi, A. (Eds.), ContouritesDevelopments in Sedimentology 60. Elsevier, Amsterdam, pp. 301–322.
Ochoa, J., Bray, N.A., 1991. Water mass exchange in the Gulf of Cadiz. Deep-Sea Research 38 (1), S465–S503.
Pardo-Igúzquiza, E., Rodríguez-Tovar, F.J., 2000. The permutation test as a non-parametric method for testing the statistical significance of power spectrum estimation in cyclostratigraphic research. Earth Planet. Sci. Lett. 181, 175–189.
Pardo-Igúzquiza, E., Rodríguez-Tovar, F.J., 2005. MAXENPER: a program for máximum entropy spectral estimation with assessment of statistical significance by the permutation test. Comput. Geosci. 31, 555–567.
Pardo-Igúzquiza, E., Rodríguez-Tovar, F.J., 2006. Maximum entropy spectral analysis of climatic time series revisited: assessing the statistical significance of estimated spectral peaks. J. Geophys. Res. 111, D10102. http://dx.doi.org/10.1029/2005JD006293.
Pardo-Igúzquiza, E., Rodríguez-Tovar, F.J., 2011. Implemented lomb-scargle periodogram: a valuable tool for improving cyclostratigraphic research on unevenly sampled deep sea stratigraphic sequences. Geo-Mar. Lett. 31, 537–545.
Pardo-Igúzquiza, E., Rodríguez-Tovar, F.J., 2012. Spectral and cross-spectral analysis of uneven time series with the smoothed lomb–scargle periodogram and Monte Carlo evaluation of statistical significance. Comput. Geol. 49, 207–216.
Perconig, E., 1960–1962. Sur la constitution ge'ologique de l' andalousie occidentale, en particulier du bassin du Guadalquivir (espagne meridionale). livre me'moire du professeur Paul fallot. Mem. Hors-Ser. Soc. Geol. Fr. 1, 229–256.
Pereira, R., Alves, T.M., 2013. Margin segmentation prior to continental break-up: a seismic–stratigraphic record nof multiphased rifting in the north Atlantic (southwest Iberia). Tectonophysics 505, 17–34.
Pereira, R., Alves, T.M., Cartwright, J., 2011. Post-rift compression on the SWIberian margin (eastern north Atlantic): a case for prolonged inversion in the ocean–continent transition zone. J. Geol. Soc. 168, 1249–1263.
Potter, P.E. and Szatmari, P., 2009, Global Miocene tectonics and the modern world. Earth Sci. Rev., v.96, p. 279-295.
Praeg, D., Stoker, M.S., Shannon, P.M., Ceramicola, S., Hjelstuen, B., Laberg, J.S., Mathiesen, A., 2005. Episodic Cenozoic tectonism and the development of the NW European "passive" continental margin. Mar. Pet. Geol. 22, 1007–1030.
Raymo, M.E., Mitrovica, J.X., O'Leary, M.J., DeConto, R.M., Hearty, P.J., 2011. Departures from eustasy in Pliocene sea-level records. Nat. Geosci. 4, 328–332.
Rebesco, M., 2005. Contourites. En: Richard, C., Selley, R.C., Cocks, L.R.M., Plimer, I.R. (Eds.), Encyclopedia of Geology, vol. 4. Elsevier, London, pp. 513–527.
Rebesco, M., Camerlenghi, A. (Eds.), 2008. ContouritesDevelopments in Sedimentology vol. 60. Elsevier, Amsterdam.
Rebesco, M., Stow, D., 2001. Seismic expression of contourites and related deposits: a preface. Mar. Geophys. Res. 22, 303–308.
Rebesco, M., Hernández-Molina, F.J., Van Rooij, D., Wåhlin, A., 2014. Contourites and associated sediments controlled by deep-water circulation processes: state of the art and future considerations. Mar. Geol. 352, 111–154.
Riaza, C., Martinez del Olmo, W., 1996. Depositional model of the Guadalquivir-Gulf of Cadiz tertiary basin. In: Frien, P.F., Dabrio, C.J. (Eds.), Tertiary Basins of Spain: The Stratigraphic Record of Crustal Kinematics. Cambridge University Press, Cambridge, pp. 330–338.
Ripepe, M., Fischer, A.G., 1991. Stratigraphic rhythms synthesized from orbital variations. In: Franseen, K., Watney, W.L., Kendall, C.G., St., C., Ross, W. (Eds.), Sedimentary

Modelling: Computer Simulations and Methods for Improved Parameter Definition. Kansasa state geol. Surv. Bull. 233, pp. 335–344.
Roberts, D.G., 1970. The Rif–betic orogen in the gulf of Cadiz. Mar. Geol. 9, M31–M37.
Significance of lower pliocene mass-flow deposits for the timing and process of collision of the Eratosthenes seamount with the Cyprus active margin. In: Robertson, A.H.F., Emeis, K.-C., Richter, C., Camerlenghi, A. (Eds.), Proceedings of the Ocean Drilling Program, Scientific Results. vol. 160, pp. 465–481.
Rodrigo-Gámiz, M., Martínez-Ruiz, F., Rodríguez-Tovar, F.J., Jiménez-Espejo, F., Pardo-Igúzquiza, E., 2014. Millennial- to centennial-scale climate periodicities and forcing mechanisms in the westernmost Mediterranean for the past 20,000 years. Quat. Res. 81, 78–93.
Rogerson, M., Rohling, E.J., Bigg, G.R., and Ramirez, J., 2012, Paleoceanography of the Atlantic-Mediterranean exchange: Overview and first quantitative assessment of climatic forcing: Rev. Geophys., v. 50, RG2003, doi:http://dx.doi.org/10.1029/2011RG000376.
Roque, C., 2007. Tectonostratigrafia do Cenozóico das Margens Continentais Sul e Sudoeste Portuguesas: um Modelo de Correlação Sismostratigráfica. Departamento de Geologia, Universidade de Lisboa.
Roque, C., Duarte, H., Terrinha, P., Valadares, V., Noiva, J., Cachão, M., Ferreira, J., Legoinha, P., Zitellini, N., 2012. Pliocene and Quaternary depositional model of the Algarve margin contourite drifts (gulf of Cadiz, SW Iberia): seismic architecture, tectoni control and paleoceanographic insights. Mar. Geol. 303–306, 42–62.
Rosas, F.M., Duarte, J., Terrinha, P., Valadares, V., Matias, L., Gutscher, M.A., 2009. Major bathymetric lineaments and soft sediment deformation in NW gulf of Cadiz (Africa–Iberia plate boundary): new insights from high resolution multibeam bathymetry data and analogue modelling experiments. Mar. Geol. 261 (1–4), 33–47.
Roveri, M., Flecker, R., Krijgsman, W., Lofi, J., Lugli, S., Manzi, V., Sierro, F.J., Bertini, A., Camerlenghi, A., De Lange, G., Govers, R., Hilgen, F.J., HÅNubscher, C., Meijer, P.T., Stoica, M., 2014. The Messinian Salinity Crisis: Past and future of a great challenge for marine sciences. Mar. Geol. 352, 25–58.
Rudge, J.F., Shaw Champion, M.E., White, N., McKenzie, D., Lovell, B., 2008. A plume model of transient diachronous uplift at the earth's surface. Earth Planet. Sci. Lett. 267, 146–160.
Ryan, W.B.F., Hsü, K.J., Cita, M.B., Dumitrica, P., Lort, J., Maync, W., Nesteroff, W.D., Pautot, G., Stradner, H., Wezel, F.C., 1973. Western Alboran Basin-Site 121. In: Initial Reports of the Deep Sea Drilling Project. (Ed. by W.B.F. Ryan & K.J. Hsu¨ al.), 13, 43–89. Govt. Printing Office, Washington D.C.
Salvany, J.M., Larrasoaña, J.C., Mediavilla, C., Rebollo, A., 2011. Chronology and tectono-sedimentary evolution of the upper Pliocene to Quaternary deposits of the lower Guadalquivir foreland basin, SW Spain. Sediment. Geol. 241, 22–39.
Sarnthein, M., Bartoli, G., Prange, M., Schmittner, A., Schneider, B., Weinelt, M., Andersen, N., Garbe-Schönberg, D., 2009. Mid-Pliocene shifts in ocean overturning circulation and the onset of Quaternary-style climates. Clim. Past 5, 269–283.
Scargle, J.D., 1982. Studies in astronomical time series analysis. II. Statistical aspects of spectral analysis of unevenly spaced data. Astrophys. J. 263, 835–853.
Schönfeld, J., Zahn, R., 2000. Late glacial to Holocene history of the Mediterranean outflow. Evidence from benthic foraminiferal assemblages and stable isotopes at the Portuguese margin. Palaeogeogr. Palaeoclimatol. Palaeoecol. 159, 85–111.
Serra, N., Ambar, I., Boutov, D., 2010. Surface expression of Mediterranean water dipoles and their contribution to the shelf/slope–open ocean exchange. Ocean Sci. 6, 191–209.
Serra, N., Ambar, I., Käse, R.H., 2005. Observations and numerical modelling of the Mediterranean outflow splitting and eddy generation. Deep-Sea Res. II 52, 383–408.
Sierro, F.J., Flores, J.A., Civis, J., González-Delgado, J.A., Francés, G., 1993. Late Miocene globorotaliid event-stratigraphy and biogeography in the NE Atlantic and Mediterranean. Mar. Micropaleontol. 21, 143–168.
Sierro, F.J., Flores, J.A., Zamarreño, I., Vazquez, A., Utruilla, R., Frances, G., Hilgen, F.J., Krigsman, W., 1999. Messinian climatic oscilations, astronomic cyclicity and reef growth in the western Mediterranean. Mar. Geol. 153, 137–146.
Sierro, F.J., Glez Delgado, J.A., Dabrio, C., Flores, J.A., Civis, J., 1991. Paleontologia y Evolució Mem. Iberian Neogene basins especial 2, 209–250.
Sierro, F.J., González-Delgado, J.A., Dabrio, C.J., Flores, J.A., Civis, J., 1996. Late Neogene Depositional Sequences in the Foreland Basin of Guadalquivir (SW Spain). In: Tertiary Basins of Spain (P. Friend y C. Dabrio, eds.). Cambridge University Press, Cambridge, 329-334.
Sierro, F.J., Ledesma, S., Flores, J.A., 2008. Astrobiochronology of late neogene deposits near the strait of Gibraltar (SW Spain). implications for the tectonic control of the messinian salinity crisis. In: Biand, F. (Ed.), CIESM, 2008. The messinian salinity crisis from mega-deposits to microbiology. CIESM workshop monographs, pp. 45–48 Monaco.
Sierro, F.J., Ledesma, S., Flores, J.-A., Torrescusa, S., Martínez del Olmo, W., 2000. Sonic and gamma-ray astrochronology: cycle to cycle calibration of Atlantic climatic to Mediterranean sapropels and astronomical oscillations. Geology 28 (8), 695–698. http://dx.doi.org/10.1130/.
Slater, D.R., 2003. The transport of Mediterranean water in the North Atlantic Ocean (PhD Thesis), Univ. of Southampton (155 pp.).
Stein, R., Sarnthein, M., Suendermann, J., 1986. Late neogene submarine erosion events along the north-east Atlantic continental margin. In: Summerhayes, C.P., Shackleton, N.J. (Eds.), North Atlantic paleoceanography. Geological Sociey Special Publication 21, pp. 103–118.
Stoker, M.A., Praeg, D., Hjelstuen, B.O., Laberg, J.S., Nielsen, T., Shannon, P.M., 2005. Neogene stratigraphy and the sedimentary and oceanographic development of the NW European Atlantic margin. Mar. Pet. Geol. 22, 977–1005.
Stow, D.A.V., Faugères, J.C., Gonthier, E., Cremer, M., Llave, E., Hernández-Molina, F.J., Somoza, L., Díaz del Río, V., 2002b. Faro-Albufeira Drift Complex, Northern Gulf of Cadiz. In: Stow, D.A.V., Pudsey, C.J., Howe, J., Faugères, J.C. (Eds.), Deep-Water Contourite Systems: Modern Drifts and Ancient Series, Seismic and Sedimentary Characteristics. Geological Society London, Memoirs 22, pp. 137–154 Igcp 432.
Stow, D.A.V., Faugères, J.-C., Howe, J.A., Pudsey, C.J., Viana, A.R., 2002a. Bottom currents, contourites and deep-sea sediment drifts: current state-of-the-art. In: Stow, D.A.V., Pudsey, C.J., Howe, J.A., Faugères, J.-C., Viana, A.R. (Eds.), Deep-Water Contourite Systems: Modern Drifts and Ancient Series, Seismic and Sedimentary Characteristics. Geological Society, London, Memoirs. 22, pp. 7–20.
Stow, D.A.V., Hernández-Molina, F.J., Alvarez Zarikian, C.A., the Expedition 339 Scientists, 2013b. Proceedings IODP, 339. Integrated Ocean Drilling Program Management International, Tokyo http://dx.doi.org/10.2204/iodp.proc.339.2013.
Stow, D.A.V., Hernández-Molina, F.J., Llave, E., Bruno, M., García, M., Díaz del Río, V., Somoza, L., Brackenridge, R.E., 2013a. The Cadiz contourite channel: sandy contourites, bedforms and dynamic current interaction. Mar. Geol. 343, 99–114.
Terrinha, P., Matias, L., Vicente, J., Duarte, J., Luís, J., Pinheiro, L., Lourenço, N., Diez, S., Rosas, F., Magalhães, V., Valadares, V., Zitellini, N., Roque, C., Mendes Víctor, L., Team, M.A.T.E.S.P.R.O., 2009. Morphotectonics and strain partitioning at the Iberia–Africa plate boundary from multibeam and seismic reflection data. Mar. Geol. 267, 156–174.
Terrinha, P., Pinheiro, L.M., Henriet, J.-P., Matias, L., Ivanov, M.K., Monteiro, J.H., Akhmetzhanov, A., Volkonskaya, A., Cunha, T., Shaskin, P., Rovere, M., 2003. Tsunamigenic–seismogenic structures, neotectonics, sedimentary processes and slope instability on the southwest Portuguese margin. Mar. Geol. 195, 55–73.
Terrinha, P., Ribeiro, C., Kullberg, J.C., Rocha, R., Ribeiro, A., 2002. Compression episodes during rifting and faunal isolation in the Algarve basins, SW Iberia. J. Geol. 110, 101–113.
TGS, 2005. PD00: non-exclusive 2D Survey, TGS online data zone. (http://www.tgsnopec.com/specsheets/PD-00_Spec.pdf).
Thorpe, S.A., 1975. Variability of the Mediterranean in the gulf of Cadiz. Deep-Sea Res. 23, 711–727.
Torelli, L., Sartori, R., Zitellini, N., 1997. The giant chaotic body in the Atlantic ocean off Gibraltar: new results from a deep seismic reflection survey. Mar. Pet. Geol. 14, 125–138.
Toucanne, S., Mulder, T., Schönfeld, J., Hanquiez, V., Gonthier, E., Duprat, J., Cremer, M., Zaragosi, S., 2007. Contourites of the gulf of Cadiz: a high-resolution record of the paleocirculation of the Mediterranean outflow water during the last 50,000 years. Palaeogeogr. Palaeoclimatol. Palaeoecol. 246, 354–366.
Vail, P.R., Mitchum Jr., R.M., Thomson III, S., 1977. Global cycles of relative changes of sea level. In: Payton, C.E. (Ed.), seismic stratigraphy—applications to hydrocarbon exploration. American Association of Petroleum Geologists, Memoirs 26, pp. 83–98.
Van der Schee, M., Sierro, F.J., Flecker, R., Gutjahr, M., Jimenez-Espejo, F.J., Hernandez-Molina, F.J., Grunert, P., Garcia Gallardo, A., Flores, J.A., Hodell, D., Andersen, N., 2015. Discussion on identification of the Mio-Pliocene boundary and onset of the MOW recorded in IODP Site U1387C in the Gulf of Cádiz. RCMNS Interim Colloquium, Mediterranean – Atlantic Gateway (Neogene to present). Rabat (Morocco), 5–8 May, 2015. Abstract volume.
Van Rooij, D., De Mol, B., Huvenne, V., Ivanov, M., Henriet, J.P., 2003. Seismic evidence of current-controlled sedimentation in the belgica mound province, upper porcupine slope, southwest of Ireland. Mar. Geol. 195, 31–53.
Vannucchi, P., Sak, P.B., Morgan, J.P., Ohkushi, K., Ujiie, K. and the IODP Expedition 334 Shipboard Scientists, 2013. Rapid pulses of uplift, subsidence, and subduction erosion offshore central America: implications for building the rock record of convergent margins. Geology, 41, 995-998.
Vergés, J., Fernàndez, M., 2012. Tethys– Atlantic interaction along the Iberia– Africa plate boundary: the betic–Rif orogenic system. Tectonophysics 579, 144–172.
Viguier, C., 1974. Le Néogène de l'Andalousie Noroccidentale (Espagne) (Thesis), Univ. Bordeaux (449 pp.).
Villmoare, B., Kimbel, W.H., Seyoum, C., Campisano, C.J., DiMaggio, E., Rowan, J., Braun, D.R., Arrowsmith, J.R., Reed, K.E., 2015. Early Homo at 2.8 Ma from Ledi-Geraru, Afar, Ethiopia. Science http://dx.doi.org/10.1126/science.aaa1343.
Voelker, A.H.L., Lebreiro, S.M., Schönfeld, J., Cacho, I., Erlenkeuser, H., Abrantes, F., 2006. Mediterranean outflow strengthening during northern hemisphere coolings: a salt source for the glacial Atlantic? Earth Planet. Sci. Lett. 245 (1–2), 39–55.
White, R.S., McKenzie, D.P., 1989. Magmatism at rift zones: the generation of volcanic continental margins and flood basalts. J. Geophys. Res. 94, 7685–7729.
Whyte, N., Lovell, B., 1997. Measuring the pulse of a plume with the sedimentary record. Lett. Nat. 387, 888–891.
Wold, C.N., 1994. Cenozoic sediment accumulation on drifts in the northern north Atlantic. Paleoceanography 9, 917–941.
Wright, J.D., Miller, K.G., 1996. Control on north Atlantic deep water circulation by the Greenland-Scotland ridge. Paleoceanography 11, 157–170.
Zachos, J., Pagani, H., Sloan, L., Thomas, E. and Billups, K., 2001, Trends, rhythms, and aberrations in global climate 65 Ma to present: Science, v. 292, p. 686-693.
Zazo, C., Goy, J.L., Dabrio, C., Civis, J., Baena, J., 1985. Paleogeografia de la desembocadura del Guadalquivir al comienzo del cuaternario (provincia de C~idiz, espafia). Actas Reun. Cuat. Ibér. 1, 461472.
Zenk, W., 1975. On the Mediterranean outflow west of Gibraltar. "Meteor" Forsch.-Ergebnisse 16, 23–34.
Zitellini, N., Gràcia, E., Matias, L., Terrinha, P., Abreu, M.A., DeAlteriis, G., Henriet, J.P., Dañobetia, J.J., Masson, D.G., Mulder, T., Ramella, R., Somoza, L., Diez, S., 2009. The quest for the Africa-Eurasia plate boundary west of the strait of Gibraltar. Earth Planet. Sci. Lett. 280, 13–50.